



CONTRACT NO. A132-105
FINAL REPORT
SEPTEMBER 1994

Generation, Characterization and Transport of Owens (Dry) Lake Dusts

CALIFORNIA ENVIRONMENTAL PROTECTION AGENCY



AIR RESOURCES BOARD
Research Division

REPORT DOCUMENTATION PAGE

1. AGENCY USE ONLY (Leave Blank) PB95171799	2. REPORT DATE September 1994	3. REPORT TYPE AND DATES COVERED Final Report	
4. TITLE AND SUBTITLE Generation, Characterization and Transport of Owens, (Dry) Lake Dusts		5. FUNDING NUMBERS A132-105	
6. AUTHOR(S) Thomas A. Cahill, Thomas E. Gill, Dale A. Gillette, Elizabeth A. Gearhart, Jeffrey S. Reid, Mee-Ling Yau			
7. PERFORMING ORGANIZATION NAME(S) AND ADDRESS(ES) Air Quality Group Crocker Nuclear Laboratory University of California Davis, CA 95616-8569		8. PERFORMING ORGANIZATION REPORT NUMBER	
9. SPONSORING/MONITORING AGENCY NAME(S) AND ADDRESS(ES) California Air Resources Board Research Division 2020 L Street Sacramento, CA 95814		10. SPONSORING/MONITORING AGENCY REPORT NUMBER ARB/R- 95/557	
11. SUPPLEMENTARY NOTES			
12a. DISTRIBUTION/AVAILABILITY STATEMENT Release unlimited. Available from National Technical Information Service. 5285 Port Royal Road Springfield, VA 22161		12b. DISTRIBUTION CODE	
13. ABSTRACT (Maximum 200 Words) The concentrations of windblown PM ₁₀ dust generated from the surface of Owens Lake are among the highest found in the United States. The dust is generated by the grinding action of sand particles, broken crust, and other debris on the salt and silt components of the lake bed. Under certain meteorological conditions, the lake bed forms a hard crust that is initially resistant to abrasion by sand, but continued erosion eventually destroys it. The particle sizes in the windblown dust are finer than typical soil-based PM ₁₀ particles. The small particle size and the topographical constraints of the Owens Valley allows Owens Lake dust to be transported long distances to the north and south. Owens Lake dust impacts the Schulman Grove Ancient Bristlecone Pine forest and the Naval Air Weapons Center at China Lake, among other areas. The dust concentrations generated from Owens Lake could be reduced by limiting the movement of sand over the surface of the lake bed. This could be accomplished by wetting the surface, by stabilizing the surface with vegetation, or by trapping the sand in dune arrays. A combination of these methods may offer the best solution to the problem.			
14. SUBJECT TERMS Fugitive Dust, Particulate Matter, PM ₁₀ , Air Pollution, Dry Lakes		15. NUMBER OF PAGES 186	
		16. PRICE CODE	
17. SECURITY CLASSIFICATION OF REPORT Unclassified	18. SECURITY CLASSIFICATION OF THIS PAGE Unclassified	19. SECURITY CLASSIFICATION OF ABSTRACT Unclassified	20. LIMITATION OF ABSTRACT Unlimited



Generation, Characterization and Transport
of Owens (Dry) Lake Dusts

Final Report

Contract No. A132-105

Prepared for:

California Air Resources Board
Research Division
2020 L Street
Sacramento, California 95814

Prepared by:

Thomas A. Cahill
Thomas E. Gill
Dale A. Gillette
Elizabeth A. Gearhart
Jeffrey S. Reid
Mee-Ling Yau

Air Quality Group
Crocker Nuclear Laboratory
University of California
Davis, California 95616-8569

September 1994

DISCLAIMER

The statements and conclusions in this report are those of the contractor and not necessarily those of the California Air Resources Board and/or the California Environmental Protection Agency. The mention of commercial products, their sources, or their use in connection with material reported herein is not to be construed as actual or implied endorsement of such products.

ACKNOWLEDGMENTS

Work by Dale Gillette using Geomet data was carried out in collaboration with U.S. Geological Survey (USGS) researchers. USGS Desert Winds Project scientists (Flagstaff, Arizona) operate the Geomet station to support their geological research on wind erosion of desert surfaces. We acknowledge the assistance of Paula Helm and Carol Breed (USGS) for access to the Owens Lake Geomet site and data.

This study could not have been accomplished without the additional efforts of dozens of persons. We wish to thank Mike Patterson, Mike Brown, Trevor Ley, Steve Teague, Dave Campbell, Laurent Gomes, Tezz Johnson, Vladimir Smirnov, Jody Stewart and Lowell Ashbaugh for field assistance; Robert Flocchini, Robert Matsumura, Mark Van de Water, Tim Essert, Pete Beveridge, Michael Sisto, Scott Ruth, Mike Dunlap, Rolf Kihl, Paul Wakabayashi, Ken Bowers, Bruce Kusko, Bruce White, Greg Cho, Kent Wilkinson, Terry James and others for laboratory, shop and technical support; and Jeanette Martin, Donna McDaniel, Jennifer Geerts, Lori Hubbard and Andy Andersen for assistance in preparing this report. We also wish to acknowledge the cooperation of the following individuals and organizations in this study: Dan Salgado and Larry Mathews (Naval Air Weapons Station, China Lake); Paul Stockton (Sensit Labs Inc.); Gary Herbert (National Oceanic and Atmospheric Administration); Bill Fryrear (U.S. Department of Agriculture); Duane Ono, Bill Cox, Grace Holder, and Ellen Hardebeck (Great Basin Unified Air Pollution Control District); William Smith (COMARCO, China Lake); Bill McClung (Lake Minerals Co.); Marith Reheis (U.S. Geological Survey); and Luci McKee (U.S. Forest Service- Inyo National Forest).

This report was submitted in fulfillment of ARB Contract Number A132-105, "A Collaborative Owens Lake Aerosol Study," by the Air Quality Group, Crocker Nuclear Laboratory, University of California at Davis, under the sponsorship of the California Air Resources Board. Work was completed as of April 1994.

ABSTRACT

We investigated the sources of PM_{10} from the Owens Lake playa and its transport into both populated and wilderness areas. The levels of PM_{10} dust observed near the lake bed are among the highest ever seen in the United States. This study's results show that the dust is a consequence of the grinding of salt and silt components of the playa by wind-driven, saltating, coarse grains of sand, broken salt crust, and other debris. We ascertained that the lake bed forms saline crusts that, if not destroyed by sand or other causes, suppress or eliminate formation of PM_{10} . The "fetch effect," in which the mass of wind-eroded soil increases with distance downwind, is shown to exist at Owens (Dry) Lake. Data from our intensive field study in March 1993 lead us to a conditional acceptance of three mechanisms causing the wind-erosion fetch effect: avalanching, soil resistance, and aerodynamic feedback. Particle sizes in the dust are generally much finer than soil based PM_{10} . Due partly to the fine size and the topographically-confined transport paths, the dust is efficiently transported long distances north and south of the Owens Lake area, to sites including the Ancient Bristlecone Pine Forest and the Naval Air Weapons Station, China Lake. We also surveyed existing vegetation types at Owens (Dry) Lake and the conditions in which they survive, confirming the usefulness of native vegetation in dust suppression once sand motion has been controlled.

TABLE OF CONTENTS

DISCLAIMER.....	ii
ACKNOWLEDGMENTS.....	iii
ABSTRACT.....	iv
LIST OF FIGURES.....	viii
LIST OF TABLES.....	xiii
INTRODUCTION.....	1
Prior research at Owens Lake and related areas.....	7
The 1979 UC Davis/ARB Owens Lake Study.....	8
The 1984 UC Davis/ARB Mono Lake Study.....	11
The 1984 WESTEC/State Lands Commission Owens Lake Mitigation Study.....	14
The 1987 GBUAPCD/LADWP Owens Lake Mitigation (sand fence) Study.....	14
The 1991 GBUAPCD/LADWP Owens Lake Mitigation (sprinkler) Study.....	18
Summary of Earlier Work.....	18
OBJECTIVES.....	19
Mechanics of dust generation.....	19
Aerosol characterization and transport.....	19
Study of Owens playa vegetation.....	20
MECHANICS OF DUST GENERATION.....	21
Materials and Methods.....	21
Schedule.....	21
Work plan.....	21
Sources of Saltating Particles.....	22
Mechanisms of Initiating Saltation.....	22
Generation of PM ₁₀ Dusts.....	24
Detailed Characterization of Lake Bed Aerosols.....	26
PM ₁₀ Profiles of Particle Transport.....	30
Optical Diagnosis of Particle Transport (Remote Sensing).....	31
Detailed Size-Compositional Analyses of Dusts in Receptor Areas.....	32
RESULTS -- OVERVIEW.....	33
Meteorology during the March 1993 Intensive.....	33
Aerosols at Keeler during the March 1993 Intensive.....	34
Summary of Lake Bed Conditions during the March 1993 Intensive.....	41
RESULTS -- SOURCES OF SALTATING PARTICLES.....	42

Motion of Saltating Particles.....	45
Spatial Uniformity of Saltating Particles.....	48
Particle Size Classification of Saltating Grains	50
RESULTS -- MECHANISMS OF INITIATING SALTATION	51
Models for the Wind Erosion Fetch Effect	54
Tests of the Models.....	54
Experimental Procedures.....	55
Soil Flux measurements.....	57
Data processing and estimation of errors.....	57
Friction velocity and aerodynamic roughness height.....	57
Threshold velocity	58
Mass flux.....	60
Analysis of Results	60
Soil mass flux.....	60
Aerodynamic roughness heights.....	63
Friction velocities	64
Threshold velocity results	66
q vs. $u_* (u_*^2 - u_{*t}^2)$	71
Fetch effect discussion.....	72
Fetch effect conclusions.....	74
RESULTS -- GENERATION OF PM ₁₀ DUSTS.....	75
Discussion of the PM ₁₀ dust results	81
Conclusions of the PM ₁₀ Studies	87
RESULTS -- AEROSOL CHARACTERIZATION AND TRANSPORT	88
Meteorology of dust transport.....	88
Aerosol characterization.....	91
Optical Characterization of aerosols.....	99
Aerosol transport.....	102
Remote Sensing.....	111
CONCLUSIONS OF THE OWENS LAKE DUST STUDIES.....	113
RESULTS -- VEGETATION STUDY.....	114
Field Work.....	114
Conclusion of Vegetation Studies	119
SUMMARY AND CONCLUSIONS.....	120
Source mechanisms for PM ₁₀ dust generation.....	121
Nature of dusts, optical properties and transport.....	123
RECOMMENDATIONS	127

REFERENCES	130
LIST OF PUBLICATIONS AND PROFESSIONAL PRESENTATIONS RELATED TO THIS CONTRACT	138
GLOSSARY OF ACRONYMS.....	140
GLOSSARY OF TERMS.....	142
APPENDIX A -- Results of Test Plot Studies at Owens Dry Lake, Inyo County, CA	144
APPENDIX B -- Participants, affiliation (and specialty) in the Lake Owens Dust Experiment, March 1993	149
APPENDIX C -- Grain size analysis of playa materials	150
APPENDIX D -- Portable PM ₁₀ Filter Sampler Data.....	152
APPENDIX E -- Vegetation Inventory of Owens (Dry) Lake	154
APPENDIX F -- Saga of Inyo County.....	156
APPENDIX G -- The Ecology of Dune.....	158
APPENDIX H -- Instruments at Each Sampling Site, March 1993.....	160
APPENDIX I -- Control of PM ₁₀ Dust Episodes from Owens (Dry) Lake	161

LIST OF FIGURES

Figure 1.	(2 parts): Regional maps showing Owens (Dry) Lake and sites referred to in text (courtesy Marith Reheis, and after GBUAPCD, 1994)	2
Figure 2.	Owens Lake Bed, showing major dust-producing areas and study sites referred to in text.....	4
Figure 3.	Schematic of the on-lake bed experiments of March 1993, including the State Lands Commission test plot, April-June 1993.	5
Figure 4.	Example of TSP mass concentrations in Owens Valley during a south wind. (Barone <i>et al.</i> , 1979).....	9
Figure 5.	Mono-Owens Davis Dust Model run prediction for TSP at Owens (Dry) Lake, Keeler site (Kusko and Cahill, 1984)..	13
Figure 6a.	North to South Sand Movement, Owens (Dry) Lake, October, 1988. Dots represent sand motion monitors. (Aerovironment Corp., 1992)	15
Figure 6b.	South to North Sand Movement, Owens (Dry) Lake, October, 1988. Dots represent sand motion monitors. (Aerovironment Corp., 1992)	16
Figure 7.	Sand accumulation behind the fences throughout the Phase II project duration (Aerovironment Corp., 1992).	17
Figure 8.	Diagram of Weaver Sand Transport Sampler (Ono <i>et al.</i> , 1994)..	23
Figure 9.	Diagram of BSNE Sampler (after Fryrear, 1986)..	23
Figure 10.	Comparison of PM ₁₀ Mass: Average IMPROVE PM ₁₀ (24 hour) vs. PFS (48 hour) at Davis Field Site	26
Figure 11.	Average daily wind speeds at the Geomet site on the South Sand Sheet, our Olancha site, and the GBUAPCD Keeler site, March 1993..	33
Figure 12a.	Meteorology at Keeler, Geomet, and Olancha for storm of March 11, 1993.....	35
Figure 12b.	Meteorology at Keeler, Geomet, and Olancha for storm of March 17, 1993.....	36
Figure 12c.	Meteorology at Keeler, Geomet, and Olancha for storm of March 18, 1993.....	37

Figure 12d.	Meteorology at Keeler, Geomet, and Olancha for storm of March 24, 1993.....	38
Figure 13.	Soil particle motions during wind erosion. (After Gillette, 1981).....	46
Figure 14.	Comparison between sand motion and wind velocity, March 1993.....	47
Figure 15.	Comparison between the Sensit Sand Motion Monitor and the wind velocity at the Geomet site, March 1993.....	48
Figure 16a.	Mass of saltating particles blown by north winds and captured in Weaver Sand Motion Monitors, South Sand Sheet, Owens Lake Bed, Spring 1993.....	49
Figure 16b.	Mass of saltating particles blown by south winds and captured in Weaver Sand Motion Monitors, South Sand Sheet, Owens Lake Bed, Spring 1993.....	49
Figure 17.	Schematic diagram of the fetch effect (Owen, 1964).....	53
Figure 18.	Cumulative composition of surface sediments along a linear transect, South Sand Sheet, Owens Lake Bed, March 1993.....	56
Figure 19.	Geomet data for March 11, 1993.....	59
Figure 20.	Integrated soil mass fluxes (Q) along the linear transect, Owens Lake Bed fetch effect study, March 1993. N and S denote wind direction.....	62
Figure 21.	Estimated aerodynamic roughness heights up to 520 m downwind of zero point, Owens Lake Bed fetch effect experiment, March 11, 1993. Solid line indicates 90th percentile upper limit of confidence for the 150 m location.....	64
Figure 22.	Estimated aerodynamic roughness heights up to 150 m downwind of zero point, Owens Lake Bed fetch effect experiment, March 18, 1993. Solid line indicates 90th percentile upper limit of confidence for the 150 m location.....	65
Figure 23.	Friction velocities from zero point to 150 m downwind, Owens Lake Bed fetch effect experiment, March 11, 1993. Solid lines indicate the 90th percentile confidence interval for the 150 m location.....	65

Figure 24.	Friction velocities from zero point to 520 m downwind, Owens Lake Bed fetch effect experiment, March 18, 1993. Solid lines indicate the 90th percentile confidence interval for the 150 m location.....	67
Figure 25.	Friction velocities from zero point to 150 m downwind, Owens Lake Bed fetch effect experiment, March 23, 1993 (south wind). Solid lines indicate the 90th percentile confidence interval for the 150 m location.	67
Figure 26.	Relation of threshold friction velocity to percent of land surface as crust fragments, Owens Lake Bed fetch effect experiment, March 1993.....	68
Figure 27.	Relation of two-point friction velocity to two-minute Sensit response (saltating particle impact), 520 m downwind of initiation point, March 11, 1993 dust event, Owens Lake Bed South Sand Sheet.....	69
Figure 28.	Relation of two-point friction velocity to two-minute Sensit response (saltating particle impact), 1057 m downwind of initiation point, March 11, 1993 dust event, Owens Lake Bed South Sand Sheet.....	70
Figure 29.	Integrals in time of Q vs. G for March 1993 as well as preliminary data set obtained in 1991.....	71
Figure 30.	Diagram of NOAA/UCD sampling array by site code, March 1993. See Figure 3 for location and Appendix H for instrumentation at each site. Aerosol samplers at H sites only. Scale: .75 inch = 100 meters	77
Figure 31.	PM ₁₀ concentrations at two heights during six events, Owens Lake Bed South Sand Sheet. Wind directions are given in explanatory text on pages 76 and 78.....	79
Figure 32.	Dust vs. Time.....	80
Figure 33.	Intercomparison of average wind velocity at Geomet site (top), average percent of surface remaining as crust (center) and average friction velocity (bottom), Owens Lake Bed South Sand Sheet, March 1993.....	83
Figure 34.	PM ₁₀ Dust (top), Sand Flux (center), and ratio of PM ₁₀ dust to sand (bottom), Owens Lake Bed South Sand Sheet, March 1993.....	85
Figure 35.	Intercomparison of: Ratio of PM ₁₀ concentration (g/m ³) to saltating particle flux (gm/cm ²) vs. date (top) and percent of surface crust destroyed (bottom), Owens Lake Bed South Sand Sheet, March 1993.....	86

Figure 36.	Sand flux (g/cm^2) times wind run (km), representing both the mass of sand that cross an area and the total distance traveled across the surface.	87
Figure 37.	Typical air flow patterns around Owens (Dry) Lake.	88
Figure 38.	Intercomparison of hourly averaged wind speeds between Geomet site, Keeler and Olancha, March 1993.	90
Figure 39.	Owens (Dry) Lake Dust Aerosol Morphology.	92
Figure 40a.	Normalized size distributions from DRUM sampler, Owens (Dry) Lake aerosols, for four elements, Spring 1993.	96
Figure 40b.	Normalized size distributions from DRUM sampler, Owens (Dry) Lake aerosols, for four elements, Fall 1991.	97
Figure 41.	Mass size distributions for Owens (Dry) Lake dust aerosols, March 1993.	98
Figure 42.	Comparison of visibility derived from integrating nephelometer and laser aerosol counter, Owens Lake region, March 1993.	100
Figure 43.	Relation of ambient aerosol mass concentration to visibility, Owens Lake region, March 1993.	101
Figure 44.	Optical Characteristics of Source Dusts: Example of Sample from South Sand Sheet d_{0e} Derived Mass and Related Cross Section.	102
Figure 45.	Relation of Owens dust plume dilution to distance downwind, March 1993.	103
Figure 46.	Estimated TSP profiles from Owens dust transported on north wind, November 27, 1991.	104
Figure 47.	Probable dust transport patterns from Owens (Dry) Lake to Indian Wells Valley.	105
Figure 48.	Wind speed correlation, Olancha (near Owens Lake Bed) vs. Onion Valley (east slope Sierra Nevada), March 1993.	107
Figure 49.	Comparison of hourly wind speed, March 17, 1993, Olancha and Onion Valley.	108

Figure 50.	Elemental mass at Schulman Grove, March 1993, SMART Sampler, PM _{2.5} , for Si, S and Ca, showing impact of March 24 dust plume	109
Figure 51.	GOES Imagery- Owens Lake Dust Storm 16:00 March 17, 1993	112
Figure 52.	GOES Imagery- Owens Lake Dust Storm March 11, 1993	113
Figure 53.	Location of various springs and well sites at Owens (Dry) Lake. Refer to Table XV for the species composition of the sites which the numbers represent (after Yau, 1993).....	116
Figure 54.	Meteorology, sand motion, and dust production in the March 1993 intensive	124
Figure 55.	Example of the effect of sand fences on sand motion, Owens (Dry) Lake South Sand Sheet mitigation test, March 1994 (California State Lands Commission Contract No. C-9175, preliminary data).....	164

LIST OF TABLES

TABLE I.	Keeler: Monthly Maximum PM ₁₀ 1979-1992 (California Air Resources Board, 1979-1992).....	6
TABLE II.	China Lake: Monthly Maximum PM ₁₀ 1979-1992 (California Air Resources Board, 1979-1992).....	7
TABLE III.	Dust profiles in the Owens Valley, south winds, relative to Keeler. Profiles are derived from data on playa elements (sodium, chlorine, sulfur), silicon, which occurs in both playas and non-playa soils and mass (Barone <i>et al.</i> , 1979)..	10
TABLE IV.	Frequency and Severity of Occurrences of Dust Episodes near Mono and Owens (Dry) Lake 1979-1983 + March 1993 (1), with pre-1987 values PM ₁₀ converted (2). The values given are the average of all measurements within each category..	12
TABLE V.	Summary of stationary sites. "Location" lists distance and direction of site from the source regions. "To Monitor" lists the sensitive locations in which the dust flux is to be monitored.....	29
TABLE VI.	PM ₁₀ data at nearby sites during the March 1993 Owens Lake Intensive. Note how the one-day-in-six schedule missed the six dust events of March 11, 17, 18, 23, 24, and 25. The time mean and peak values were available from the new TEOM continuous PM ₁₀ monitor after March 11.....	39
TABLE VII.	Hourly PM ₁₀ Data From TEOM for Keeler, CA., March 1993 (GBUAPCD, 1993b).....	40
TABLE VIII.	Particle size classification of saltating grains, Owens Lake Bed South Sand Sheet, 1993.	50
TABLE IX.	Crust percentage and threshold friction velocities.	61
TABLE X.	Relationship Between Friction Velocity u^* and Aerodynamic Roughness Height Z_0 according to the theory of P. R. Owen.....	68
TABLE XI.	PM ₁₀ mass concentration in $\mu\text{g}/\text{m}^3$ at each site and sampling period, Owens Lake Bed South Sand Sheet aerosol experiment, March 1993.....	76
TABLE XII.	March, 1993 LODE Intensive Data Set.....	82

TABLE XIII. Elemental Composition of Owens Lake Dust detected by PIXE, selected elements, as % of total mass of detectable elements (Na and heavier). "ND" indicates that element was not detected above the minimum detectable level. Background averages and Northeast Sand Sheet data were compiled from samples taken during fall dust storms. Data from spring 1976 are from St. Amand <i>et al.</i> (1986) and include dust generated from both the Northeast and South Sand Sheets. Though elemental data were not taken for one dust event on the Northeast sand sheet, St. Amand <i>et al.</i> (1986) indicate little seasonal variation in composition.	93
TABLE XIV. Plant Cover Classes (CA. Department of Fish and Game, 1987).....	115
TABLE XVa. Major species found at various springs on the east side of the lake bed.....	117
TABLE XVb. Owens Valley Plant Community Classification (by Mary DeDecker). The communities are arranged in descending order of sensitivity to water withdrawal (Gaines and DeDecker, 1982).....	117

INTRODUCTION

The Los Angeles Department of Water and Power (LADWP) began diverting Owens River water to Los Angeles County in 1913. Since 1926, there has been near-continuous diversion of surface and ground water from the Owens River basin into the Los Angeles Aqueduct (Nadeau, 1950), leaving Owens Lake without its primary source of water. Within a few years the desert climate forced the evaporation of the 280 km² saline lake leaving a dry alkaline lake bed (playa). Despite the dry surface, the depth to moisture underneath the lake bed is very close to the surface, typically from a few centimeters to a meter, due to recharge by aquifers derived from the remaining untapped watersheds of the Sierra Nevada and the White-Inyo mountain ranges, as well as the deep brine pool beneath the playa. This feature, coupled with frequent surface flooding during the winter and spring, has allowed the formation of efflorescent and salt crusts on the eastern and southern sides of the lake bed that are extremely vulnerable to wind blown saltating particles (Barone *et al.*, 1981; St. Amand *et al.*, 1986; Cochran *et al.*, 1988). The frequent high winds in the Owens Valley and subsequent erosion of the salt crust and other lake bed sediments has made Owens (Dry) Lake one of the largest single PM₁₀ sources in the United States, with production estimates ranging from 900,000 to 8,000,000 metric tons annually (Gill and Gillette, 1991).

Owens (Dry) Lake is located approximately 100 km south of Bishop in the southern portion of the Owens Valley (Figure 1). Small towns along Highways 395, 136, and 190 are frequently impacted by dust. Nearby are numerous areas sensitive to visibility degradation and deposition by dust, including Sequoia and Kings Canyon National Parks, Death Valley National Monument, Naval Air Weapons Station, China Lake (NAWS, CL), and numerous wilderness areas.

An intensive study by WESTEC (1984) for the State Lands Commission (SLC), reproduced in part here as Appendix A, identified four major dust producing regions on the eastern and southern ends of the lake bed (Figure 2). When the lake bed is not saturated, these regions generate dusts when wind speeds exceed approximately 7 m/s. Because of topographic forcing by the Sierra Nevada and White-Inyo ranges, winds over the lake bed during major events tend to stay roughly north/south (Appendix A). Saltation during wind erosion is accepted as the primary mechanism for generation of PM₁₀ dusts in desert regions (Gillette and Walker, 1977). Lake bed sediment and sand from near shoreline deposits provide sufficient saltating particles in erodible regions to sandblast the crust and generate extensive PM₁₀.

The largest and most frequent storms tend to occur in the spring and fall, though large events have been documented all year around. Extensive research has been performed for dust plumes transported to the north and south of the lake, respectively (Barone *et al.*, 1979, 1981; St. Amand *et al.*, 1986). St. Amand *et al.* have shown that atmospheric loading during major dust events has reached 1.5 metric tons per square kilometer and plumes have had concentrations as high as 2,600 µg/m³ one hundred kilometers to the south at the NAWS, CL, only 10 kilometers north of the city of Ridgecrest (pop. 40,000).

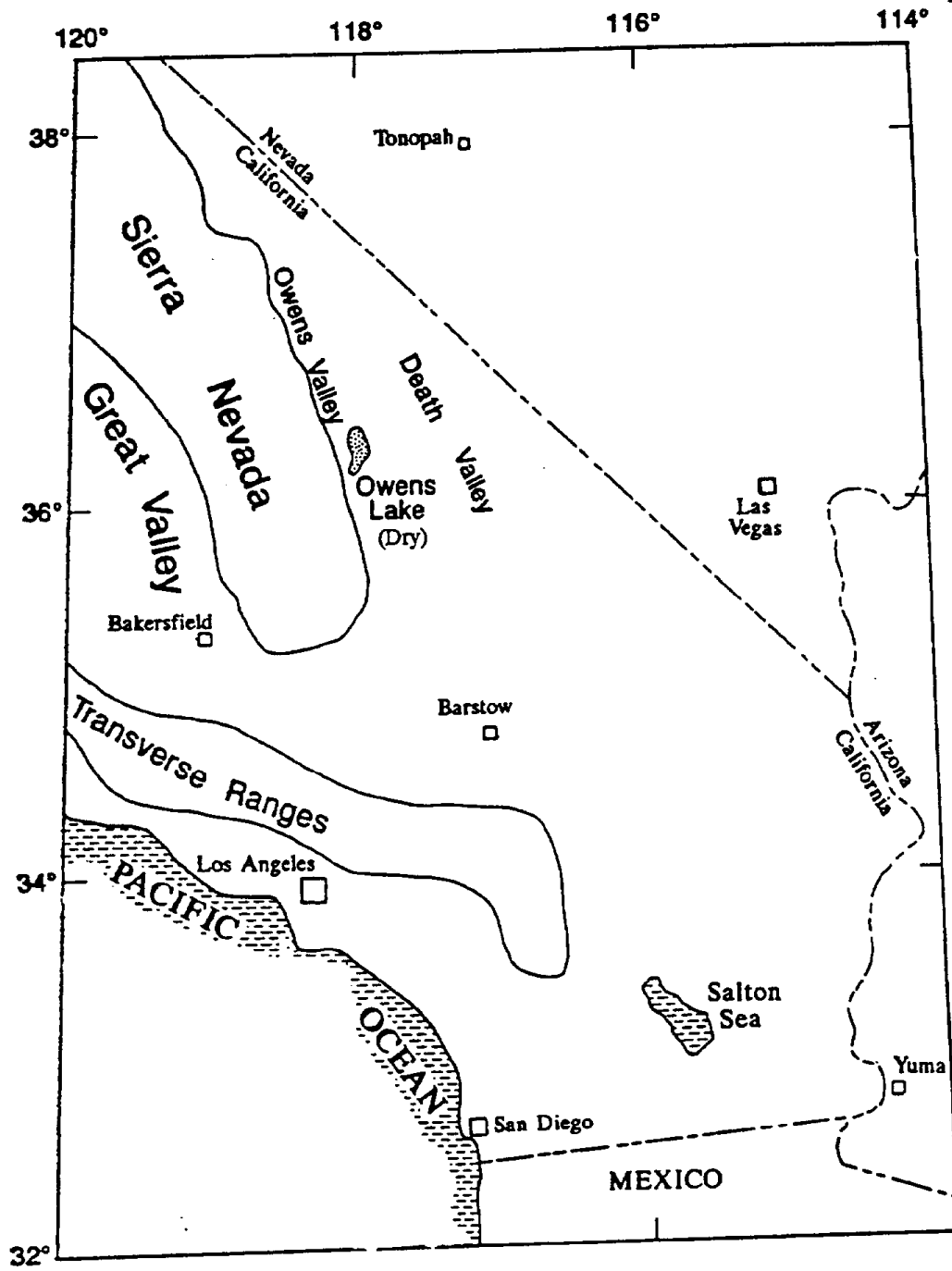


Figure 1 (in part). Regional map showing Owens (Dry) Lake.
(courtesy Marith Reheis)

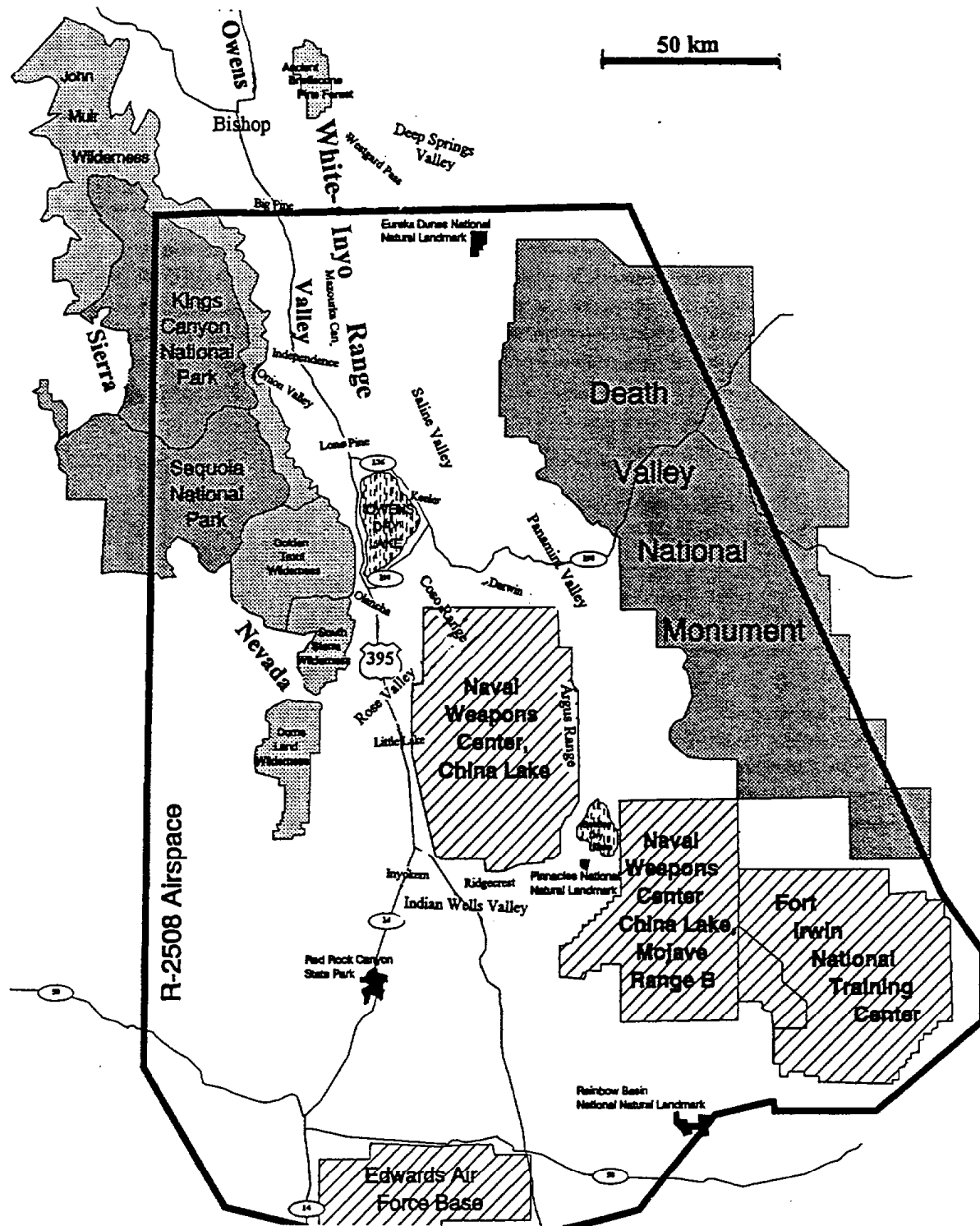


Figure 1 (in part). Regional map, showing sites referred to in text (Modified from GBUAPCD, 1994).

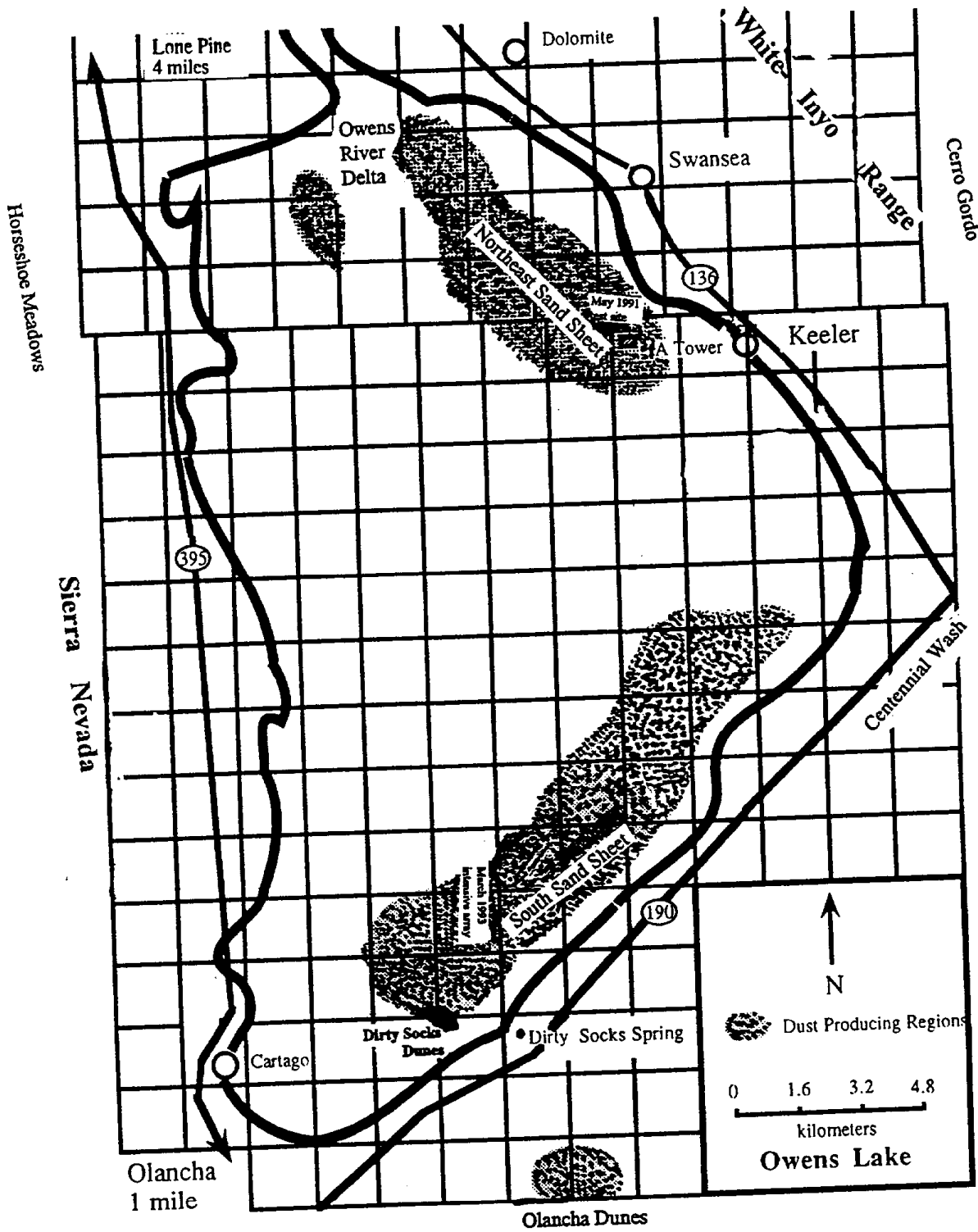


Figure 2. Owens Lake Bed, showing major dust-producing areas and study sites referred to in text.

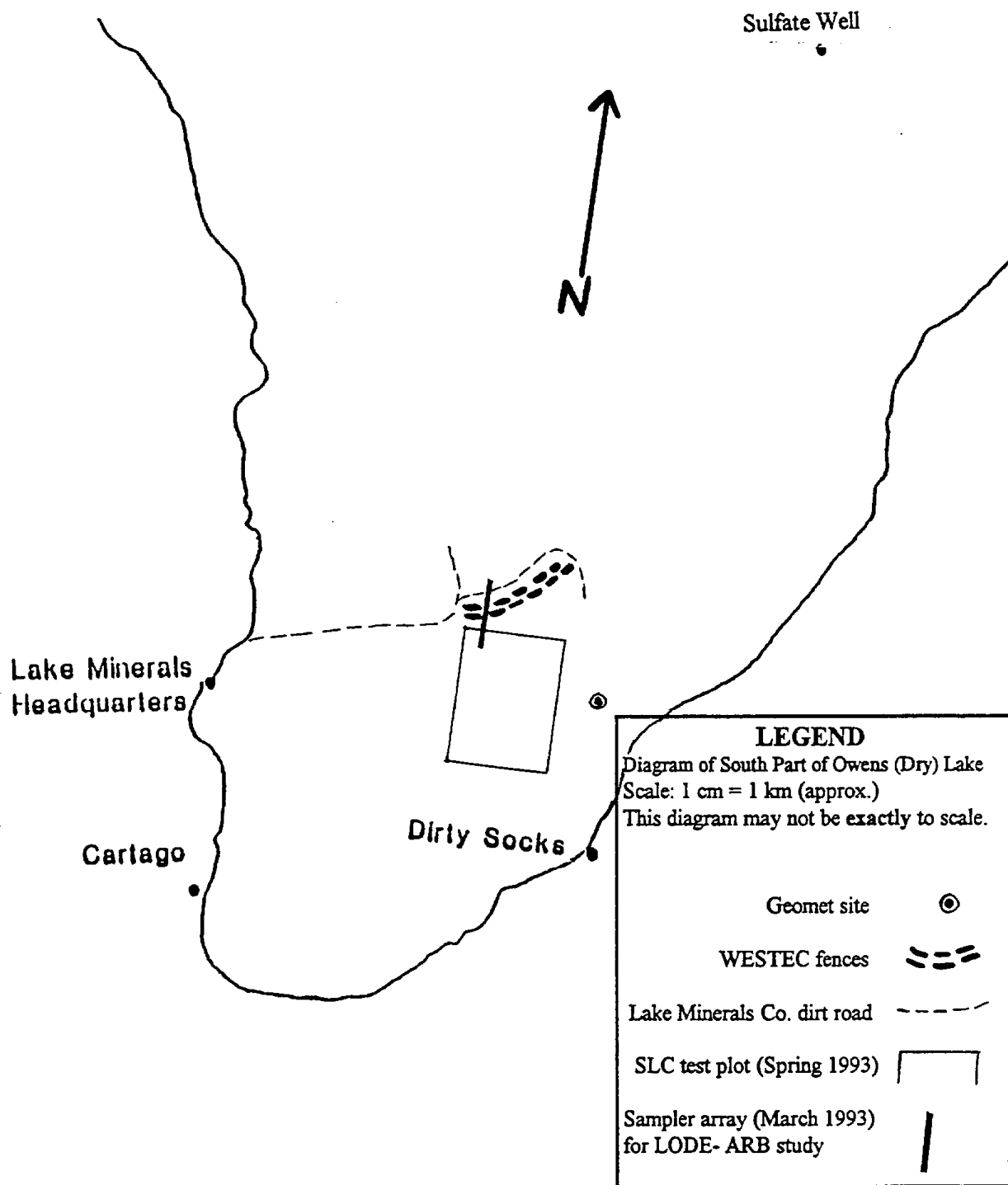


Figure 3. Schematic of the on-lake bed experiments of March 1993 including the State Lands Commission test plot, April-June 1993.

Because of their small size and the extreme turbulence in the boundary layer, Owens Lake dust particles can be transported long distances. This has been confirmed by St. Amand's use of satellite imagery in which plumes have been observed to be transported 250 kilometers to the south, covering over 90,000 square kilometers.

Though Owens (Dry) Lake produces large quantities of fugitive dust, its remote location in the desert region of southern California limits the impact from the majority of storms to the residents of local towns and travelers on Highways 395, 136, and 190. The most frequently affected township is Keeler (population 100), located 1 km from the northeastern shoreline of the lake bed. Review of the monthly 24 hour PM_{10} maxima for the last 12 years (one day in six) at Keeler, shows levels as high as $4,184 \mu\text{g}/\text{m}^3$, approximately 28 times the federal standard (Table I).

Table I. Keeler: Monthly Maximum PM_{10} , 1979-1992* (California Air Resources Board, 1979-1992)

Year	JAN	FEB	MAR	APR	MAY	JUN	JUL	AUG	SEP	OCT	NOV	DEC
1979	N/A	N/A	N/A	N/A	N/A	N/A	27	26	52	668	474	1008
1980	349	304	152	65	28	25	12	6	N/A	N/A	N/A	N/A
1981	7	4	17	195	187	14	16	23	7	242	461	135
1982	775	432	1182	97	121	9	13	35	513	7	48	1796
1983	10	232	487	30	N/A	N/A	N/A	N/A	N/A	N/A	N/A	10
1984	159	112	580	453	85	28	288	91	527	1013	704	10
1985	63	96	4184	650	279	50	18	32	33	33	357	10
1986	29	268	88	29	165	278	10	4	30	23	23	22
1987	764	273	230	33	24	91	40	30	49	65	71	111
1988	394	14	115	21	56	30	21	70	19	324	11	N/A
1989	98	1861	44	326	567	104	43	115	59	23	18	120
1990	11	533	49	95	181	22	15	23	16	13	858	125
1991	40	35	144	181	335	32	N/A	16	28	N/A	N/A	N/A
1992	19	10	20	350	22	526	19	19	242	35	100	N/A

* Data from 1979 through 1986 are converted from TSP, using the formula utilized by Great Basin Unified Air Pollution Control District ($PM_{10} = \text{TSP} \times 0.545$)

A moderately populated region affected by Owens (Dry) Lake is the combined cities of Ridge-crest and Inyokern, and the personnel at the NAWS, CL, located 90 km south of the lake bed (Table II). The total population of these cities is approximately 50,000. While the impact of dust episodes on PM_{10} in the populated portions of this region is sporadic (severe dust episodes occurring only 3-5 times per year), there is a more pronounced effect on visibility on the NAWS, CL weapons range, shutting down range operations up to eight times per year, resulting in an economic impact of many millions of dollars.

Table II. China Lake: Monthly Maximum PM₁₀ 1979-1992* (California Air Resources Board, 1979-1992)

Year	JAN	FEB	MAR	APR	MAY	JUN	JUL	AUG	SEP	OCT	NOV	DEC
1979	30	42	20	70	43	56	51	41	44	137	54	50
1980	25	28	316	66	91	74	64	61	95	46	53	56
1981	41	26	27	35	34	31	47	40	43	26	24	23
1982	16	16	10	35	34	33	25	28	30	23	19	18
1983	18	21	N/A	3	26	42	30	26	20	23	136	20
1984	26	80	51	71	34	32	26	26	32	36	61	31
1985	15	83	1094	99	25	33	28	29	26	17	56	16
1986	10	8	14	694	32	35	22	23	31	38	15	23
1987	14	66	24	28	19	43	27	31	32	17	14	13
1988	29	121	19	32	24	19	29	31	38	16	40	13
1989	14	26	14	N/A	N/A	N/A	N/A	28	34	18	32	33
1990	25	65	15	13	41	40	27	53	18	28	31	26
1991	N/A	26	166	411	534	31	29	27	31	N/A	N/A	N/A
1992	19	9	19	23	45	40	24	39	30	22	27	31

* Data from 1979 through 1986 are converted from TSP, using the formula utilized by Great Basin Unified Air Pollution Control District ($PM_{10} = TSP \times 0.545$)

While research has been performed on dust impact on populated locations, the lack of infrastructure (i.e. inadequate 110 V power, poor roads etc.) in most of the surrounding regions and on the lake bed has prevented extensive study of the aerosol's characteristics, transport patterns, and impact on the region's air quality.

Prior research at Owens Lake and related areas

The present research program was designed to complement and extend earlier air quality research at Owens (Dry) Lake, answering unresolved questions from earlier work, relating problems at Owens (Dry) Lake to similar situations such as Mono Lake (a saline lake approximately 200 km northwest of Owens (Dry) Lake, also experiencing dust storms), and laying the scientific ground work for the dust mitigation efforts of Great Basin Unified APCD, the State Lands Commission, and others. In this section, we will summarize some of the most pertinent research done at Owens (Dry) Lake and Mono Lake.

There have been comments on the airborne dust from Owens (Dry) Lake since the lake was desiccated in the 1920s, to the point that the term "Keeler Fog" was coined for the dry dust events at the small town of Keeler northeast of the lake. It is very instructive to recall that the parameters of the "Keeler Fog," namely that it did not scratch paint but could penetrate the smallest crevice and contaminate dwellings, are in full accord with later measurements showing that the particles are much finer than those produced by virtually any other natural dust storm. Reinking *et al.* (1979) reported that dust events at Owens (Dry) Lake have been known since the 1930's.

The recent investigations were triggered by complaints from the Naval Air Weapons Station, China Lake (California) in the 1970s. In response to loss of range visibility at the site, a proposal was crafted in the late 1970's by Dr. Pierre St. Amand to the California Air Resources Board (ARB) for an extensive study of the problem. A small contract was solicited from the UC Davis Air Quality Group (ARB Contract #A7-178-30) to lay the ground work for more extensive future efforts, to find the sources of the dust, to characterize its composition, and to evaluate transport (Barone *et al.*, 1979, 1981).

The 1979 UC Davis/ARB Owens Lake study

This study featured measurements of particles in two size modes (about 11 to 2.5 micrometers, and less than 2.5 micrometer diameter) in both single storms or events, and in weekly average samples. The samplers were placed both north and south of Owens (Dry) Lake, upwind and downwind of the prevailing N-S winds, from Little Lake to Bishop. Figure 4 shows the results of three 24 hour storm events on winds from the south.

Clearly, the dust levels upwind of Owens (Dry) Lake are small compared to those downwind of the lake, which then fall off for the roughly 100 km to Bishop. The source of the dust must be the lake bed itself, and not the surrounding desert soil as had been argued prior to this study.

This study also showed that the aerosol mass achieved levels far in excess of any state and federal ambient air standards, or even some industrial standards for dust. The residents indeed had a reason to complain.

An analysis of the composition of the dust showed interesting patterns. As one moved downwind of Owens (Dry) Lake, there was a consistent change in the relative fraction of soluble salts such as sulfates, chlorides, carbonates etc., versus fine soils or silt. Table III shows this pattern for all the spring 1979 storms.

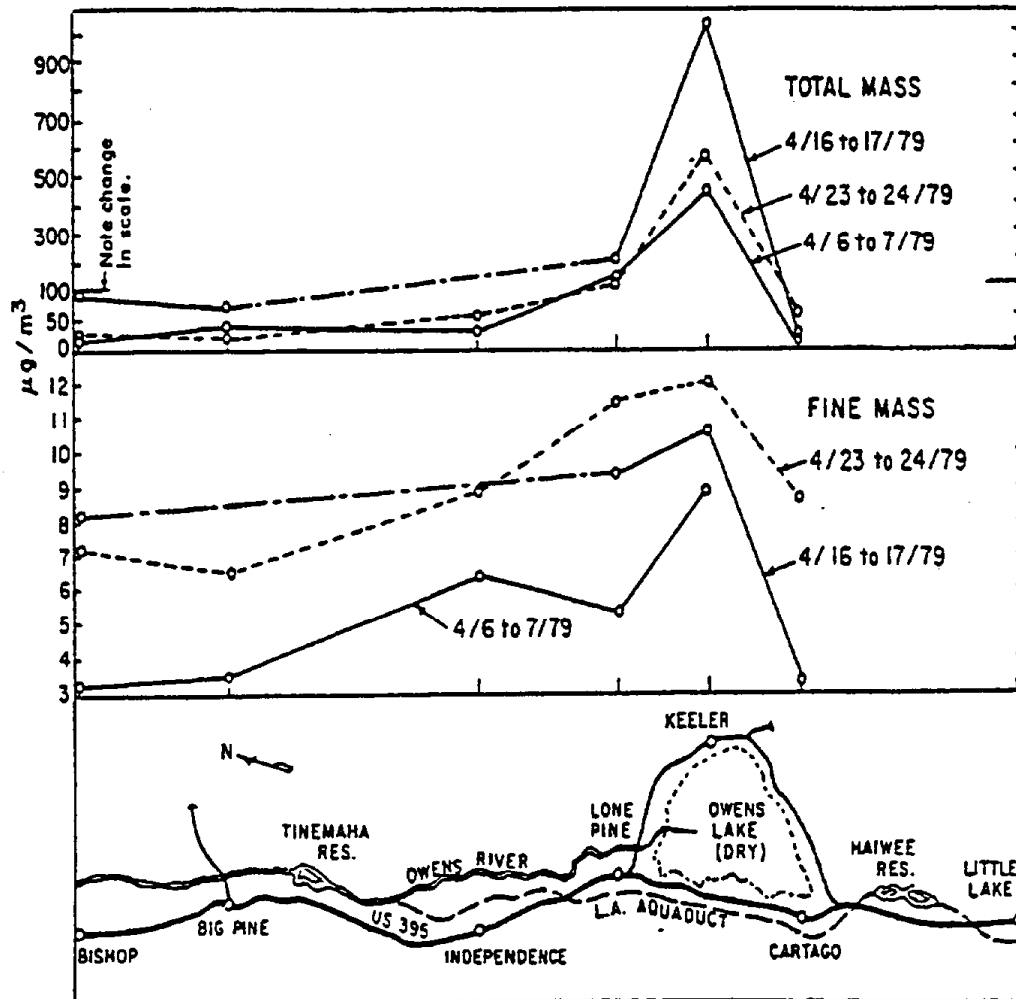


Figure 4. Example of TSP mass concentrations in Owens Valley during a south wind. (Barone *et al.*, 1979)

TABLE III. Dust profiles in the Owens Valley, south winds, relative to Keeler. Profiles are derived from data on playa elements (sodium, chlorine, sulfur), silicon, which occurs in both playas and non-playa soils, and mass (Barone *et al.*, 1979).

Three Episodes, April 1979 (UCD SFU's)				Episode 12/20 to 12/21/82 (GBUAPCD HiVols)
Site	Na, Cl, S	Silicon	Mass	Mass
Upwind (far)				
Little Lake	2.5%	1.5%	0.7%	N/A
Upwind (close)				
Cartago	5.3%	9.3%	4.4%	N/A
Owens Lake				
Keeler	= 100%	= 100%	= 100%	= 100%
Lone Pine	26%	43%	27%	30%
Independence	8%	16%	10%	18%
Big Pine	1%	14%	5.6%	N/A
Bishop	< 1%	19%	6.4%	7%

As can be seen, the characteristic lake bed materials didn't penetrate much farther than Big Pine, and the dust in Bishop was not predominantly from the Owens Lake Bed. These data were the basis for the semi-empirical computer model MODDM (the Mono-Owens Davis Dust Model) (Kusko and Cahill, 1984). This model used a linear fetch hypothesis for the dust source, but calibrated the concentration to the levels at the nearest site (Keeler). The fall off versus distance was then fit to the characteristic lake bed components. No attempt was made to produce a deterministic aerosol model since it was realized that extensive lake bed information (in space, over the entire lake bed and in time, on a day by day basis) would have had to be included in the model to have any chance in generating reliable source strengths.

Finally, the analyses were able to give some idea of the chemicals that made the erodible crust, and identified relatively high levels of arsenic (roughly 50 ppm) in the surface materials.

Shortly after completion of the ARB Owens Lake study, the Great Basin Unified Air Pollution Control District (GBUAPCD) under its Air Pollution Control Officer, Chuck

Fryxell, greatly expanded its TSP monitoring in the Owens Valley, including a site at Keeler. The value of these data became more and more apparent in establishing the exact level and frequency of the dust events.

The 1984 UC Davis/ARB Mono Lake Study

After the Owens Study, UC Davis performed two studies at Mono Lake for ARB, (Kusko *et al.*, 1981; Kusko and Cahill, 1984), and a study funded by Senate Bill 270 funds (under the auspices of the Community and Organization Research Institute, UC Santa Barbara; Cahill and Gill, 1987). Not only did these studies elucidate the mechanisms of dust formation on playas, they demonstrated the great similarities between the Owens and Mono Lake data. Table IV compares air quality at Owens and Mono Lakes in the period 1979-1983 at sites immediately downwind of the lake bed. Note that in this period, Mono Lake was at its recent low point, roughly 6373 +/- 2 feet elevation MSL.

The two lakes are statistically very similar, with Mono Lake being generally about 30% cleaner than Owens (Dry) Lake. Also note how clean the majority of the days were when there was no dust. On these days, both sites are among the cleanest in California. We have included data taken at Keeler during the March 1993 intensive field study, showing similar concentrations as those seen 1979-1983.

With confidence gained from the similarities between Owens and Mono Lakes, and the research of Dale Gillette (below) on dust generation mechanisms, conceptual studies of mitigation measures were performed. The requirements dominating the generation of most dust storms are summarized below (Kusko and Cahill, 1984).

"Findings from this and earlier studies indicate that once the wind threshold is reached, a saltation process is begun that rapidly escalates into a general dust event generated from all locations downwind of the point of initiation. Five conditions must occur simultaneously to generate the alkaline/saline storms typical at Owens and Mono Lakes:

- a. Threshold wind velocity about 10 m/sec at Owens, perhaps somewhat higher at Mono Lake.
- b. High wind shear at the flat surface due to lack of obstructions (small Z_0 parameter).
- c. Adequate fetch across the playas, at least one mile (from photographs at Mono).
- d. Coarse sand particles ($D_p > 100 \mu\text{m}$) to initiate saltation process.
- e. Efflorescent alkaline/saline crust, to generate fine particles, $D_p \leq 10 \mu\text{m}$."

Later data show that the threshold wind velocity needed to initiate erosion of the surface may be as low as 7 m/sec (measured at 2 meters), depending on surface conditions, and that the necessary fetch length may be less.

Table IV. Frequency and Severity of Occurrences of Dust Episodes near Mono and Owens (Dry) Lake 1979-1983 + March 1993 (1), with pre-1987 values PM₁₀ converted (2). The values given are the average of all measurements within each category.

	MonoLake		Owens (Dry) Lake	
	Lee Vining (upwind)	Binderup/Simis (downwind)	Keeler (downwind)	Keeler (3) (downwind) March 1993
Worst day measured 1979 to 1983	71 $\mu\text{g}/\text{m}^3$	1683 $\mu\text{g}/\text{m}^3$ *	1796 $\mu\text{g}/\text{m}^3$	N/A
Worst 1.3% of all days 1979-1983	55 $\mu\text{g}/\text{m}^3$	931 $\mu\text{g}/\text{m}^3$	1197 $\mu\text{g}/\text{m}^3$	N/A
Worst 5% of all days 1979-1983	38 $\mu\text{g}/\text{m}^3$	425 $\mu\text{g}/\text{m}^3$	653 $\mu\text{g}/\text{m}^3$	512 $\mu\text{g}/\text{m}^3$
Worst 11% of all days 1979-1983	30 $\mu\text{g}/\text{m}^3$	270 $\mu\text{g}/\text{m}^3$	343 $\mu\text{g}/\text{m}^3$	394 $\mu\text{g}/\text{m}^3$
Remaining 89% of all days 1979-1983	11 $\mu\text{g}/\text{m}^3$	9 $\mu\text{g}/\text{m}^3$	14 $\mu\text{g}/\text{m}^3$	34 $\mu\text{g}/\text{m}^3$
Sampling days	197	78	327	18

- (1) Based upon all 24-Hour days measured by GBUAPCD Hi-volume samplers, generally operated on a one-day-in six pattern.
- * Measured by Davis Sampler and corrected to equivalent Hi-Volume value. Estimated uncertainty, +/- 400 $\mu\text{g}/\text{m}^3$. Not included in statistical summaries since it was not taken randomly.
- (2) PM₁₀ conversion, TSP x 0.545 at Owens Lake, TSP x 0.51 at Mono Lake (Formula from GBUAPCD)
- (3) Preliminary TEOM data, 3/11- 3/31/93.

For the case of Mono Lake, "An obvious mitigation measure is to place the playa areas under water" (Kusko and Cahill, 1984).

For the case of Owens (Dry) Lake, the situation was more difficult since there was no significant lake remaining to modulate, the effect on Los Angeles' water supply was

potentially far greater than at Mono Lake, and a mining operation with long term leases would be flooded out at the first addition of water to Owens Lake. Further, the first 1/3 of the lake area that would be flooded is not a significant source of dust in almost all occasions, since the area is already wet, possesses a sturdy salt crust in the dry areas, and lacks movable sand to erode the crust.

Nevertheless, the MODDM model was run simulating a 2 mile band of water southwest of Keeler, ponded using the laser techniques of Sacramento Valley rice fields to make low berms. Under the prediction of a uniform source strength (now known to be unrealistic), a 30% decrease of TSP was predicted at Keeler (Kusko and Cahill, 1984) (Figure 5).

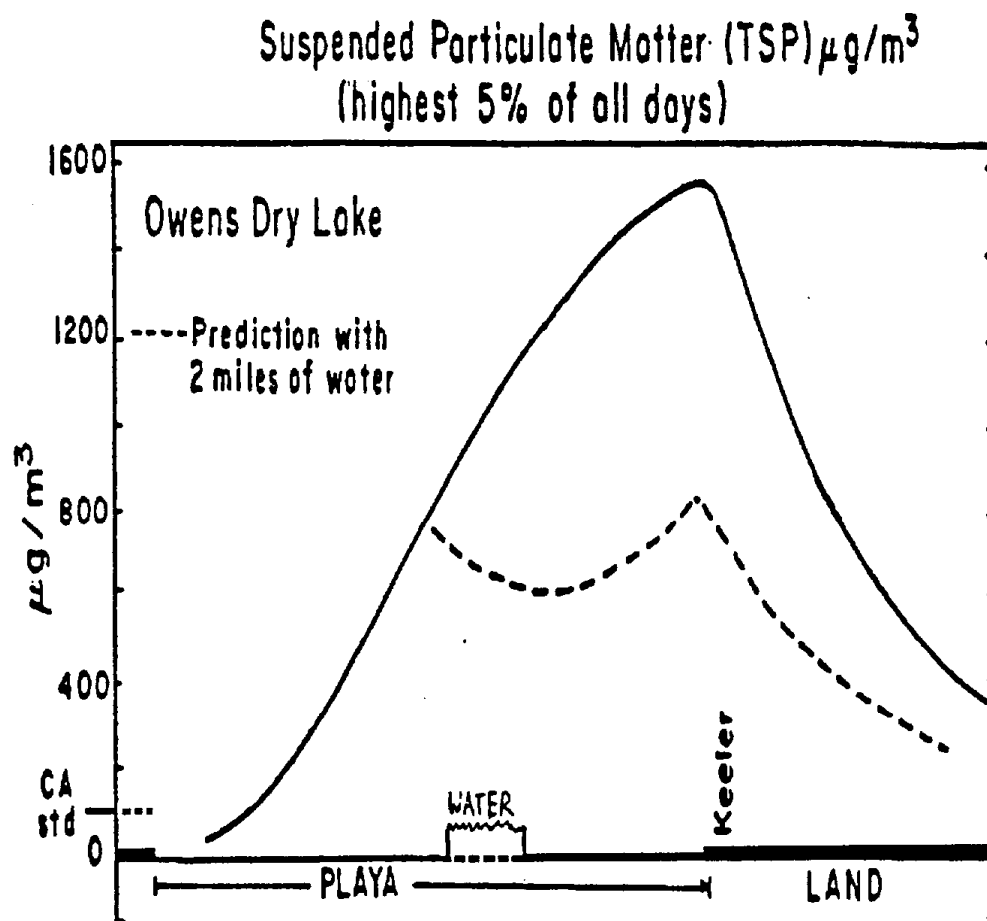


Figure 5. Mono-Owens Davis Dust Model run prediction for TSP at Owens (Dry) Lake, Keeler site (Kusko and Cahill, 1984).

It is interesting to note that such ponds would have to be about 10 mi² (6400 acres) in extent and use somewhere between 30,000 and 70,000 acre feet of water each year to maintain.

The 1984 WESTEC/ State Lands Commission Owens Lake Mitigation Study (GBUAPCD Phase I)

Most of the bed of Owens Lake is owned by the State of California, and thus managed by the State Lands Commission (SLC). Following the proof that it was the lake bed itself that caused the dust, the SLC initiated the first efforts of on-lake bed mitigation, together with additional research on the causes of the dust. This study (WESTEC, 1984) tested a variety of methods, including lake bed covers (railroad ties, cementing agents, gravel etc.) sand fences, and vegetation to mitigate the dust. The UC Davis Air Quality Group and NOAA (Gillette, 1984) were sub-contractors on a small lake bed air quality component.

The NOAA studies of Gillette showed that the lake bed crust was not easy to resuspend, requiring extremely high winds across the surface. This accorded very well with the WESTEC measurements of sand motion across the lake bed. Large dunes built up in a short time behind the sand fences, showing that the motion of sand across the surface crust was a major, if not dominant, mechanism in the generation of fine dusts.

Our work showed dust levels at 2 meters above the ground reached 5,000 $\mu\text{g}/\text{m}^3$, and identified the range of 2 to 5 μm D_{ae} where the arsenic reached its maximum concentration. Due to the importance of this work, the WESTEC Executive Summary is reproduced as Appendix A.

The 1987 GBUAPCD/LADWP Owens Lake Mitigation (sand fence) Study (GBUAPCD Phase II)

In response to the documented dust levels in Keeler, research studies and mitigation tests were performed in 1986-1987 largely based on WESTEC suggestions. Additional fences were built using plastic fencing, sand motion plots were measured across the lake bed, vegetation studies were started, and a limited set of TSP measurements were made near a sand fence near Keeler. Other than the engineering success of the taller fences (WESTEC had to cut their fences down to 3 feet high due to wind stresses), the most important results involved the relative localization of sand motion.

Figures 6a and 6b (Aerovironment Corp., 1992) show plots of sand motion across the lake bed during this study taken at a height of 10 cm above the surface. As can be seen, the sand motion is not uniform, but maximizes in two "hot spots," the North Sand Sheet near Keeler, and the South Sand Sheet near Olancho. The sand motion measured in the sand collection buckets accords well with the sand collection data from the fences.

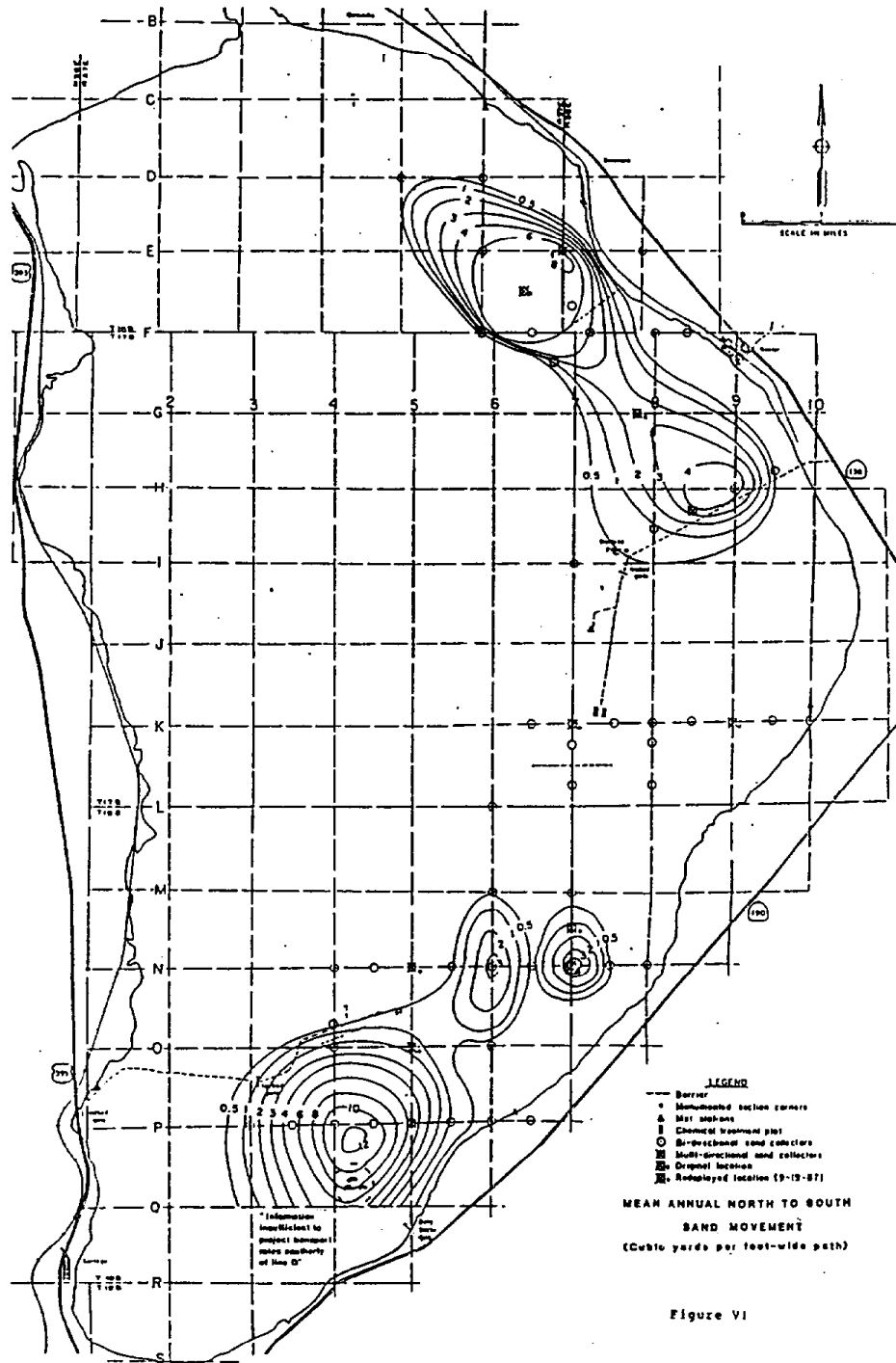


Figure 6a. North to South Sand Movement, Owens (Dry) Lake, October, 1988. Dots represent sand motion monitors. (Aerovironment Corp., 1992).

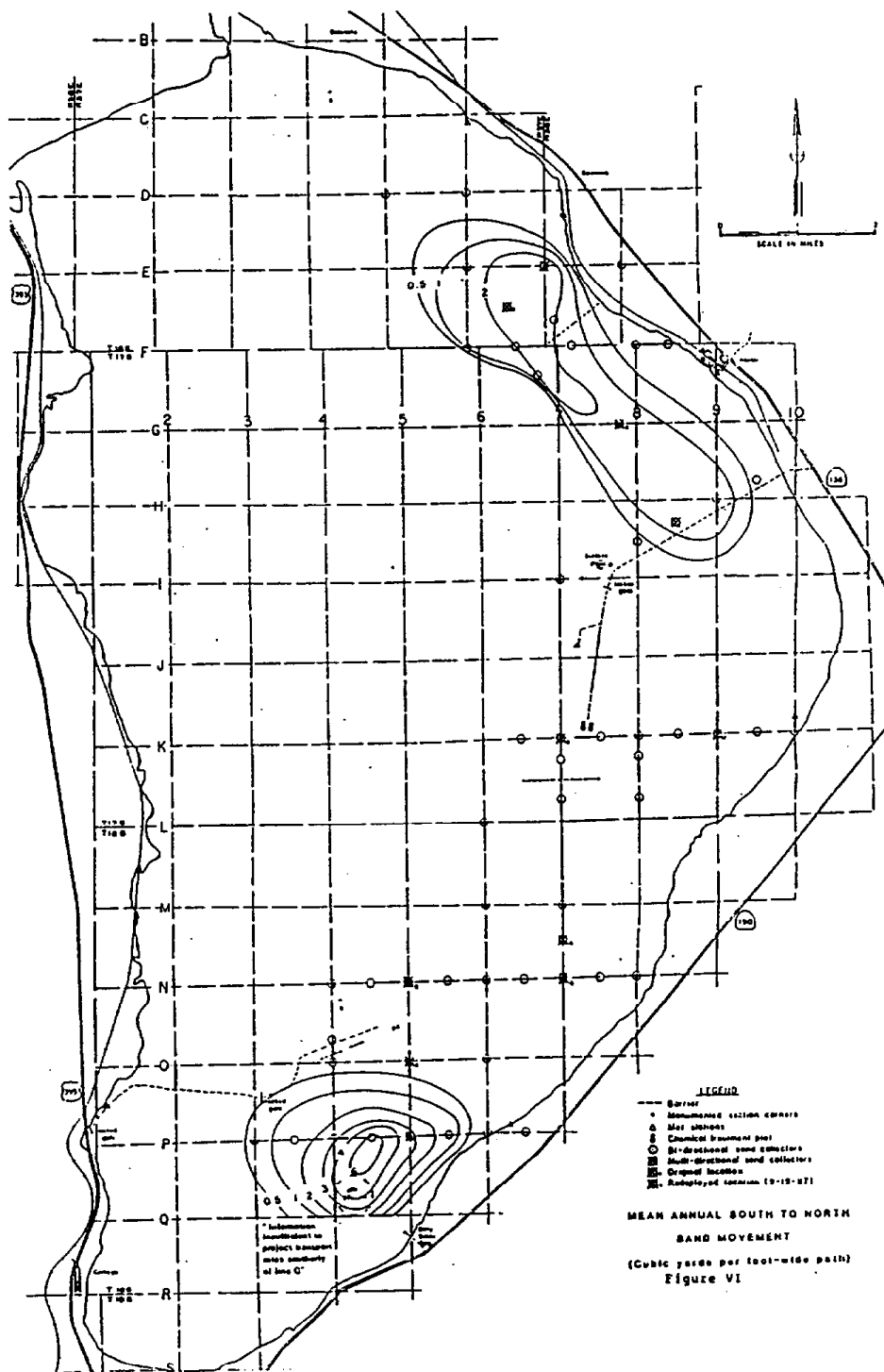


Figure 6b. South to North Sand Movement, Owens Lake, October 1988. Dots represent sand motion monitors. (Aerovironment Corp., 1992)

Figure 7 shows the collection of sand behind the sand fences shown on Figures 6a and 6b. Note that the south fence, in the area of little sand motion, collected little sand over a two year period, while those on the sand sheets filled up in about 2 years. The collected sand is in semi-quantitative agreement with the sand motion data of Figure 6. Sand motion data from Spring 1994, taken as part of a study of dust mitigation at Owens (Dry) Lake (State Lands Commission Contract C-9175 to UC. Davis) confirmed this earlier work, resulting in a quantitative relationship between sand transport and sand fence capture.

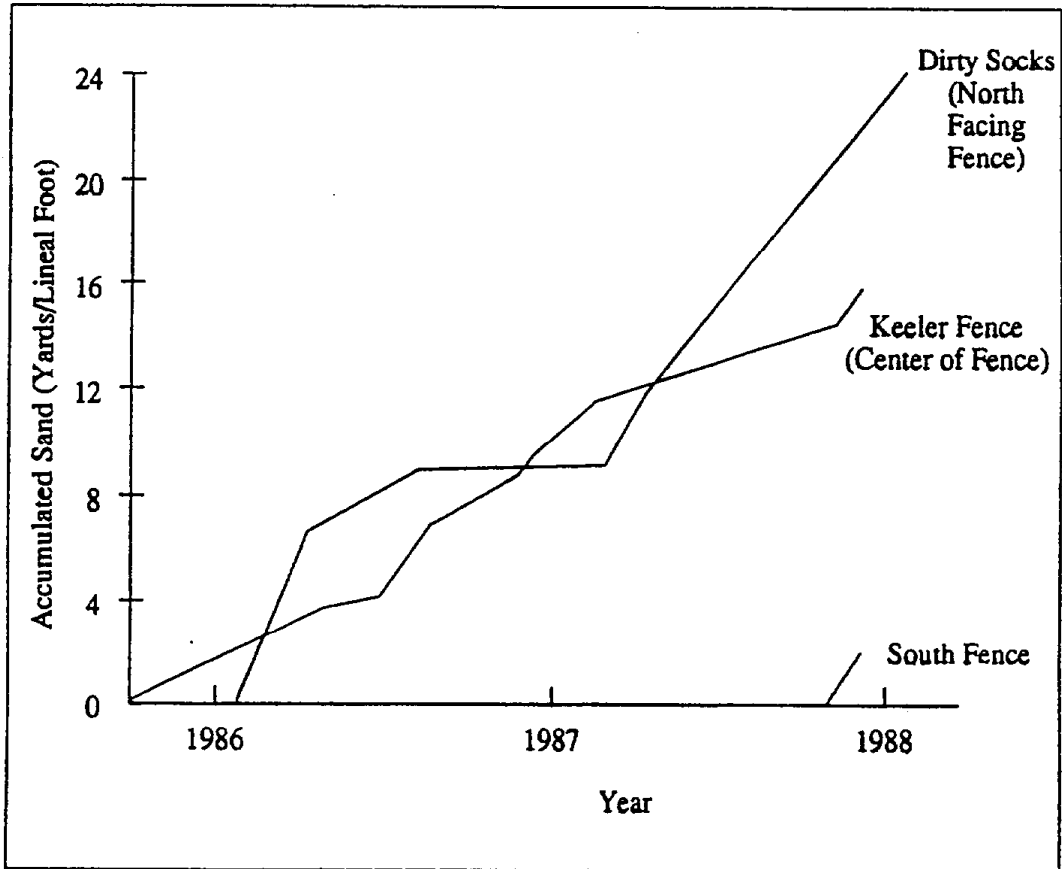


Figure 7. Sand accumulation behind the fences throughout the Phase II project duration. (Aerovironment Corp., 1992).

The point of these data are that the amount of sand motion is limited, both in the amount that moves in one year, and in those locations on the lake bed that have significant sand motion. These data do not say what other factors may cause dust, such as a fluffy crust in spring that needs no abrasion to blow away, but they do correlate to the highest observed dust production localities.

The 1991 GBUAPCD/LADWP/SLC Mitigation (sprinkler) Study (GBUAPCD Phase III)

Extensive tests were conducted in spring 1991 in order to test if a competent, dust-suppressing salt crust, could be formed at the time of occurrence of high winds by wetting the surface with an array of sprinklers. While the final report is still not available, encouragement of crust formation by surface wetting during strong winds was found to be an unreliable method in the sand areas (Ono, 1991, Ono *et al.*, 1994).

Summary of Earlier Work

The early work clearly identified that it was broken efflorescent salt/alkaline crust plus fine silt that caused the "Keeler Fog." The particulate mass levels were extremely high on those days (roughly 11%) that showed any dust, and sand motion across the crust was a major factor in dust generation. Finally, the presence of arsenic was confirmed and quantified.

However, serious questions remained unanswered about the exact mechanisms that converted sand motion to respirable dust, the size distribution of dusts in the respirable range, and the efficiency of dust transport, especially to the China Lake area. Resolution of these questions would be vital for any attempt to quantify the costs and effectiveness of dust suppression schemes at Owens (Dry) Lake.

OBJECTIVES

Mechanics of dust generation

The objectives were addressed in the intensive study of March 1993, on the South Sand Sheet, with continuing work on changing lake bed conditions both before and after the intensive study.

1. Identify factors that result in the motion of coarse particles across the lake bed. The objectives of this section are to identify the types of particles seen on the lake bed and establish the sources of such particles. The objectives also include isolating those factors, including meteorology and the state of the lake bed, that either enhance or suppress motion of coarse particles across the lake bed.

2. Identify the causes of PM_{10} dust generation in the presence of or absence of coarse or saltating particle motion.

The objectives of this section are to identify those factors that operate to enhance or suppress the generation of PM_{10} dust in the presence or absence of the motion of coarse particles across the lake bed. One component of this effort is to examine the "fetch effect," in which dust production rates increase as one moves downwind along a fetch during a single dust storm. Another objective is to examine how changes in the lake bed correlated with dust production, storm by storm.

3. Quantify the rate of PM_{10} generation.

The objective of this section is to derive a quantitative relationship between meteorological and lake bed parameters in objectives 1 and 2, above, and the generation of PM_{10} dusts. The ultimate goal of this effort is to produce an improved source emission term to aid in modeling future behavior of the lake bed in both the presence of, and absence of, dust mitigation efforts.

Aerosol characterization and transport

The goals of this portion of the study were to observe and evaluate the impact of Owens (Dry) Lake dust events on the air quality of the eastern Sierra Nevada and White-Inyo ranges as well as the populated and remote regions of the Owens, Panamint, Saline, Rose, and Indian Wells Valleys. This was to be done by running a short term intensive study of transport during the March 1993 intensive, and applying its findings to previous long term studies from November 1991 to June 1993. The objectives of this study included:

1. Determine the dust particles' characteristics as a function of time and downwind distance.

The objective of this component was to understand the physical and chemical nature of the PM₁₀ dusts from the Owens Lake bed. Information on particle size was necessary for prediction of transport phenomena downwind of Owens (Dry) Lake. The changes in size would establish the relationship between visibility (laterally and vertically) and dust concentration.

2. Determine the deposition velocities/dilution rates of the dust, and ascertain the distance at which the impact of the dust on air quality is negligible.

From information on meteorology and particle size, this objective established removal and dilution rates downwind of Owens (Dry) Lake. Particle removal rates from the transported plumes allow predictions of concentrations downwind, which are the basis for health, welfare, and optical impacts.

3. Identify intrusion of and impact of deposited and airborne dust on the visibility and plant and animal populations in the numerous Class I and II airsheds near the lake bed.

The objective of this section was to examine intrusion of Owens (Dry) Lake dusts into Death Valley National Monument, Sequoia National Park, South Sierra Wilderness, John Muir Wilderness, Schulman Grove (Ancient Bristlecone Pine Forest), and Golden Trout Wilderness. In this case, emphasis was to be on deposition of salts and other components in ecologically sensitive areas, such as the Ancient Bristlecone Pine Forest, and degradation of visibility.

Study of Owens playa vegetation

The vegetative component had as its objective an understanding of what types of plants grow in what types of conditions on the Owens Lake playa, with an eye to vegetatively-enhanced mitigation of dust formation.

1. Quantitatively describe and compare the species composition, abundance, zonation, and soil characteristics of the three spring and well sites.

In this component, the objective was to determine the correlation, if any, between the soil and the vegetation parameters of existing habitats. This would involve a comparison between the two natural sites (Keeler Spring and Tamarix Spring) to the artificial site (Sulfate Well) based on the plant and soil data obtained.

2. Identify possible factors for plant establishment on the playa.

In this objective, an evaluation was to be made of the suitability of local plants to aid in revegetation of the lake bed and eventual suppression of dust formation. This included both irrigated plants as well as those that have been proven to be able to survive on rainfall alone.

MECHANICS OF DUST GENERATION

Materials and Methods

The techniques, methods, and instrumentation used in this study rank it among the most intensive primary aerosol studies ever performed. The conditions in which the study was performed were formidable, with wind gusts above 90 mph, blasting tons of sand across the playa, generating PM_{10} levels as high as 47,400 micrograms/ m^3 (during the 1 to 2 hour sampling periods). New instruments had to be developed and tested to handle these conditions, while other types were modified and adapted to the study plan. Almost unique to this study was the use of satellite data to clarify surface crust conditions for direct comparisons to on-site samples. This section will summarize these techniques, while the actual experimental operations will directly precede the results of each study component.

Schedule

The Owens (Dry) Lake Studies can be grouped into four periods:

- a. fall 1991 study
- b. fall 1991- spring 1993
- c. spring 1993 intensive
- d. spring 1993 post-intensive

The fall 1991 study was the primary source of detailed size-compositional analyses of aerosols and the behavior during successive dust storms. On the other hand, the spring 1993 intensive was the source of almost all data on the saltation/ PM_{10} connection and in fact represented over 75% of the effort of the program.

Work plan

The original work plan from the proposal was (using the numbering of the proposal):

- D.1.a. Sources of Saltating Particles
- D.1.b. Mechanisms of Initiating Saltation
- D.1.c. Generation of PM_{10} Dusts

The work in this component was largely accomplished during the spring 1993 intensive, and our description will follow this order. In the section on "Generation...", we have broken the topic into the study of the "fetch effect," which looks at sand motion and meteorology, and "direct PM_{10} generation," which measures PM_{10} levels.

D.1.d. Cost-effective Control of Saltating Particles

This section will directly follow the section on the vegetation studies, at the end of the report in "Conclusions."

D.2.a. Optical Diagnosis of Particle Transport

D.2.b. PM₁₀ Profiles of Particle Transport

D.2.c. Detailed Size-Compositional Analyses of Dusts in Receptor Areas

The work in these sections was accomplished throughout the study. We will follow the same nomenclature and ordering, but add a section, "Detailed characterization of lake bed aerosols," before we discuss transport. A list of personnel and cooperating agencies is included in Appendix B.

1. Sources of Saltating Particles

Saltating particles were collected for study with several different passive sand motion monitoring devices. Temporal flux of sand motion and physical characteristics of saltating particles were determined using a sand motion monitor (Figure 8) of modified Weaver design (Ono *et al.*, 1994). This design has been field tested at Owens (Dry) Lake by the GBUAPCD and found to provide the most precise results in an inter comparison of sand trap designs (Ono, 1992). The sand motion monitors were loaned to UCD by GBUAPCD. Vertical flux of sand motion was determined using BSNE samplers (Fryrear, 1986) (Figure 9) utilized in the NOAA fetch effect study array and/or loaned by the USDA. BSNE samplers were mounted on a vertical stand at 10, 20, 30, 50, 60 and 100 cm above ground level: the Weaver sand catchers have inlets at 10 cm above ground level. The Weaver design sand motion monitors were also deployed in April 1993 in a 1.3 km² grid on the South Sand Sheet of Owens (Dry) Lake, centered between Dirty Socks Dunes and the WESTEC sand fences and approximately 1 kilometer west of the Geomet site.

2. Mechanisms of Initiating Saltation

a. Sensit sand motion sensors

Sensit is the trade name of a wind erosion measurement system manufactured by the Sensit Company, Mayville, ND. Sensit towers consist of four anemometers mounted on a

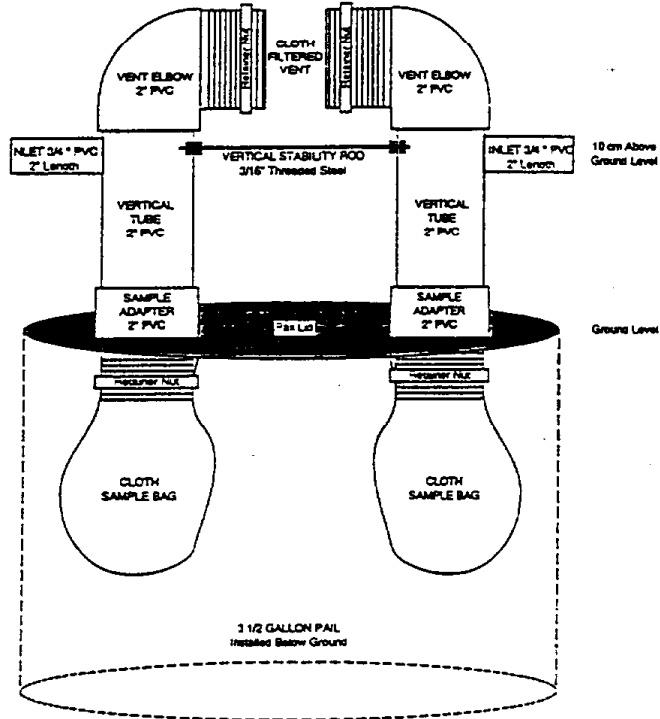


Figure 8. Diagram of Weaver Sand Transport Sampler (Ono *et al.*, 1994).

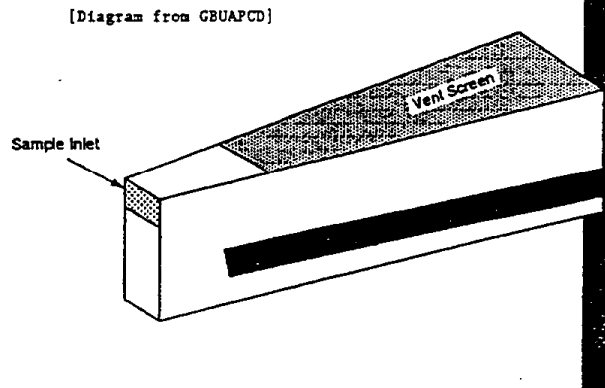


Figure 9. Diagram of BSNE Sampler (after Fryrear, 1986).

portable tower at 20 cm, 50 cm, 1 m and 2 m heights. Horizontal mass flux of soil material is measured continuously using a five level flux sensor and a pair of 3-level BSNE passive soil flux collectors. Wind direction, soil and air temperature, and precipitation are also measured. Data are logged on portable computers housed at each tower. The system is powered by solar panels. The anemometers used in the Sensit tower are manufactured by the R.M. Young Co. and are calibrated by wind tunnel. A more complete description of the Sensit instrument is given in Stockton and Gillette (1990).

b. Geomet-HANDAR meteorological monitoring system (McCauley *et al.*, 1994)

The Geomet meteorological tower located on the South Sand Sheet of the Owens Lake Bed is a self-contained monitoring instrumentation package that transmits meteorological and soil flux data to a satellite. The data are collected routinely by the Astrogeology Branch of the USGS. The Owens Lake Geomet station was built largely by funding from the NOAA Air Resources Laboratory as part of a cooperative project with the USGS. The tower is part of a network of monitoring stations known as the Desert Winds Project. It uses a HANDAR meteorological measurement system with anemometry at three levels (1.22, 2.68 and 6.10 meters -i.e., 4', 8.8' and 20' respectively) to measure wind profiles, temperature profile, soil temperature, precipitation, and airborne soil flux using the Sensit instrument and a BSNE flux collector (Fryrear, 1986). It is solar powered.

c. Other Meteorology Towers

A variety of other standard meteorology towers from various manufacturers were employed in this study. All meteorology towers employed contained wind speed/direction sensors and temperature/humidity probes. Wind speed and direction sensors were at least 3 meters above the ground.

3. Generation of PM₁₀ Dusts

Direct measurement of PM₁₀ dusts in the presence of high winds and moving sand required design and construction of an entirely new portable PM₁₀ sampler by UC Davis for the intensive study of March 1993. The inlet was designed to provide a PM₁₀ size cut at wind velocities up to 24 km/hr. At Owens (Dry) Lake, measured wind speeds have exceeded 100 km/hr, so our inlet required modifications to retain its effectiveness. We added a wind baffle to reduce the wind velocity to a level at which the inlet can provide a PM₁₀ cut point (velocity times 0.11).

The cassettes containing the 47 mm Teflon filters were installed in the sampler just prior to sampling to reduce the possibility of contamination by fugitive dust. Care was taken to avoid exposing the filters in the cassettes to contamination, and the cassettes were stored in sealed bags prior to and after sampling. Despite these precautions, artifact levels were higher than we expected due to the invasive nature of the dusts and the conditions on the lake bed.

The pump, battery, and programmable controller were located in a sealed sampler module. Unfortunately, the Owens (Dry) Lake dust was more invasive than we had expected. This, and errors on the operator's part, resulted in dust contamination of the electronics and pumps in the modules. This contamination manifested itself as instability in the air flow provided by the pumps. This was noted following the third sampling period, after which the pumps were thoroughly cleaned and the modules returned to the lake bed for further use in the study.

Two aerosol measurements at each meteorological station site were taken in this study. One sampler inlet was located at 60 cm above the lake bed, and the other at 3 m. These samplers were affixed to the met towers and run for sample periods from 1-3 hours. The resulting data were meant to give the flux of particles with elevation, and to be correlated with saltating particle flux and wind data. A total of forty-two samples were taken during the study, all of which were analyzed for mass concentration.

After the study was concluded, we thoroughly cleaned and documented the condition of the samplers and inlets and performed quality assurance studies. The instability of the pump flows proved related to dust contamination of the diaphragms and valves inside the pumps, and the crankshafts and tubing outside the pumps. This contamination, since it was in line after the cassette and filter, could not adversely affect the artifact levels. Visual inspection of the PM₁₀ inlets, observation of the contents of the particle traps, and distribution of particles in the inlet head indicated that the inlets functioned as designed. The quality assurance studies included bench top flow vs. time and temperature documentation, and field comparisons of the PM₁₀ Portable Filter Samplers with IMPROVE PM₁₀ samplers at the Davis evapotranspiration field site. The results of these tests can be seen in Figure 10, showing agreement better than +/- 10%.

Aerosol mass was then determined gravimetrically using Cahn microbalances and the quality assurance protocols of the Interagency Monitoring of Protected Visual Environment (IMPROVE) program, a joint program of the U.S. National Park Service, Environmental Protection Agency, Forest Service, Bureau of Land Management, and Fish and Wildlife Service, together with the state agencies.

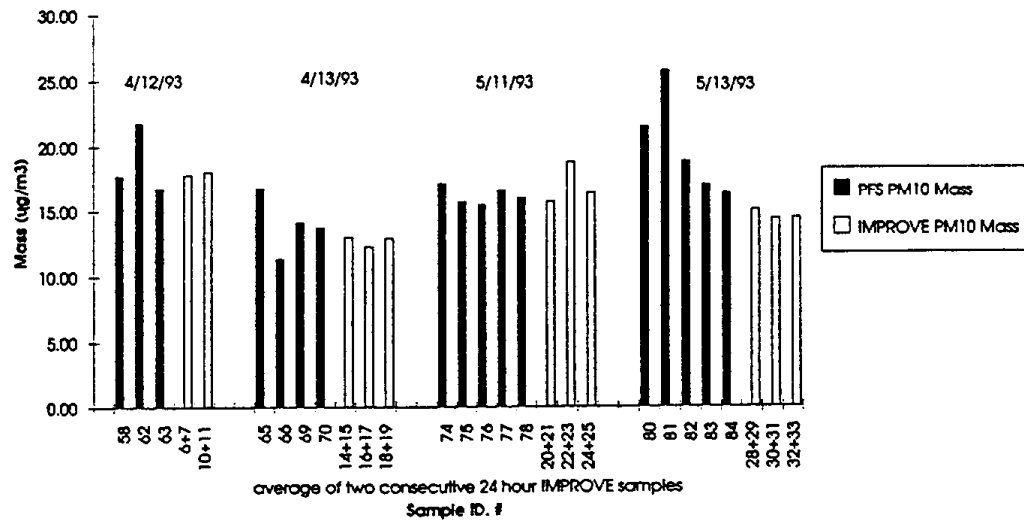


Figure 10. Comparison of PM₁₀ Mass: Average IMPROVE PM₁₀ (24 hour) vs. PFS (48 hour) at Davis Field Site

4. Detailed Characterization of Lake Bed Aerosols

a. The Fall 1991 Study

The lake bed was continually monitored for the three weeks from November 15 through December 6, 1991, at the height of the fall dust season. In order to observe multiple aspects of dust storms in the northeastern lake bed, aerosol sampling, meteorological monitoring, and time lapse photography were all employed in this portion of the study.

Aerosols were collected less than one kilometer from Owens (Dry) Lake's eastern shoreline on the southwestern edge of the township of Keeler. The surface conditions between the sampler and the lake bed consisted of coarse sand and gravel with intermittent scrub grasses and brush (vegetation cover about 5%). Keeler has no current industrial activity and vehicular traffic through the desert community was low during the study.

For this study two types of aerosol samplers were used. The primary sampler was a Davis Rotating-drum Unit for Monitoring (DRUM) impactor (Cahill *et al.*, 1987; Raabe *et al.*, 1988). A secondary stacked filter unit (SFU) sampler (Cahill *et al.*, 1990) was run side by side with the DRUM as a direct measure of gravimetric mass and for quality assurance purposes. Elemental analysis was done by PIXE (Cahill *et al.*, 1984; Cahill, 1986).

The DRUM impactor is an eight stage plus after-filter Lundgren-type impactor. At a flow rate of 1.1 l/min., the DRUM sampler has an aerodynamic equivalent diameter inlet cut point of 15 μm , and stage sizes of 15-10, 10-5, 5-2.5, 2.5-1.15, 1.15-0.56, 0.56-0.34, 0.34-0.24, 0.24-0.07 μm . On each stage, aerosols impact on an Apiezon grease coated Mylar strip on the exterior of a continuously rotating drum, with analysis in pre-determined size bites.

One stacked filter unit (SFU) was in operation at all times, taking 48 or 72 hour time integrated samples with flow rates at 5 liters per minute. The SFU system consists of two stages; the first stage contains a 47 mm Apiezon grease coated Nuclepore filter (8 micron pore size) for collecting all aerosols with diameters greater than 2.5 μm , and the second stage contains a 25 mm Teflon filter to collect the remaining aerosols. The inlet has been found to have a size cut of 14 μm at this flow rate.

Selected DRUM and SFU samples of dust episodes were analyzed by scanning and transmission electron microscopy (SEM/TEM). Each sample was mounted on an aluminum Cambridge-type mount and was sputter coated with gold to 300 angstroms with a Poloron E5 100 sputter coater. Samples were then viewed in a ISI DS 130 SEM at energies of 10 to 20 keV.

Hourly horizontal wind speed and direction, temperature, and humidity data were collected at 4 meteorological towers maintained by the Great Basin Unified Air Pollution Control District (GBUAPCD). These towers are located around and on the lake bed at Lone Pine, A-Tower, Keeler, and Olancha. Data from one additional GBUAPCD tower located 90 kilometers to the north of Lone Pine in Bishop were also collected.

Two additional meteorological towers, Baker and G1, were located at and maintained by, the Naval Air Weapons Station, China Lake (NAWS, CL), approximately 75 km south of Olancha. The Baker site is approximately 24 kilometers east of the base of the Sierra Nevada, while G-1 is approximately 7 kilometers further east. Light scattering (b_{scat}) was measured at each of these sites by an integrating nephelometer.

A single automatic camera site was located at an elevation of 1400 m above the lake bed in the White-Inyo Range 5 kilometers east of Keeler. An intervalometer was set to trigger every half hour from 10:00 to 18:00 during storm periods. The camera was activated into its daily cycle by field technicians when the National Weather Service's 36 hour forecasts predicted moderate to strong winds in the Owens Valley. The field of view covered 70% of the total lake bed (including the entire northern region).

b. Intermediate study (summer, fall 1992 camera)

SFUs were placed at the Baker and G-1 sites at NAWS, CL throughout this period. These SFUs were triggered to operate by integrating nephelometers at the sites when

visibility dropped below 10 km. After each dust event, the samples were collected and replaced by NAWS, CL personnel.

Automatic camera sites were installed at Horseshoe Meadows (on the east slope of the Sierra Nevada, overlooking the Owens Lake playa) from May 21 to July 15 1992 to observe late spring dust activity on the South Sand Sheet. Photographs were taken twice daily at 12:00 and 16:00. The camera site was reactivated for the month of October with photographs taken at 13:00 and 17:00. This site was shut down for the remainder of the study period due to snow.

Automatic cameras, SFUs, and DRUM samplers were placed in the Owens and Indian Wells Valleys for four weeks in October and November 1992. Two DRUM samplers were employed: The first DRUM was placed 1 km east of Highway 395 and 3 km south of the lake bed in order to monitor size distribution of dust in the fall from the South Sand Sheet (to complement data taken the previous fall in Keeler). A camera site was placed on Cerro Gordo Peak (in the White-Inyo Range, overlooking the Owens Lake playa) to monitor dust production. The second DRUM was placed along with an automatic camera at Inyokern Airport to monitor dust intrusion into Indian Wells Valley.

c. The Spring 1993 Intensive

Our intensive study during March 1993 was a key part of a major international collaboration known as LODE (the Lake Owens Dust Experiment), involving dozens of researchers from a number of agencies in the United States, France, and Russia. A complete list of the participants in LODE is given in Appendix B.

An overview of the stationary sites and their associated instrumentation is presented in Table V. One primary meteorology tower was placed on the lake bed to constantly monitor the source region. Under the lake bed conditions during the March intensive study, wind speeds in excess of 8 m/sec at 6.1 m height were indicative of dust production.

Two SMART samplers were placed north of the lake bed. The first was located 0.5 kilometer east of the base of the Sierra Nevada (30 km north of the lake bed), just outside Onion Valley. This sampler plus a meteorological tower monitored the dust flux into the John Muir Wilderness. The second SMART sampler was located just outside Schulman Grove in the White-Inyo mountain range (approximately 100 km north of the lake bed) to monitor the flux of dust into the regions supporting the Ancient Bristlecone Pine Forest Area of Critical Ecological Concern, Inyo National Forest.

The SMART is a split flow sampler (one stage rotating drum impactor and integration filter) designed for operation in remote sites. The sampler consists of a PM₁₀ inlet and pre-filter (2.5 μ m size cut) followed by the impactor (2.5 to 0.3 μ m) plus after-filter.

Aerosols are collected on an Apiezon coated Mylar strip on the exterior of a continuously rotating drum, with analysis in pre-determined sized bites.

Table V. Summary of stationary sites. "Location" lists distance and direction of site from the source regions. "To Monitor:" lists the sensitive locations in which the dust flux is to be monitored.

Site	Location	Instrumentation	To Monitor:
Schulman Grove	100 km N	SMART	Ancient Bristlecone Pine Forest, Inyo NF
Onion Valley	40 km N	SMART, Met Tower	John Muir Wilderness
Owens (Dry) Lake	South Sand Sheet	Met Tower	Immediate Dust Production Zone
Olancha A	3 km SW	Met Tower	S. Sierra Wilderness, Sequoia Natl. Park
Olancha B	3 km S	DRUM	Dust Production Zone
Baker	90 km S	DRUM, SFU, Integrating Nephelometer	Ridgecrest
G-1, east side, NAWS, CL	90 km S	Met Tower, SFU	Ridgecrest
Inyokern Airport	90 km S	Auto-Camera	Ridgecrest

Three kilometers southwest of the lake bed, one additional meteorological tower was placed to monitor winds and transport of dust into the southern Sierra Nevada. Two additional aerosol and meteorology monitor stations, (Baker and G-1) were located at and maintained by NAWS, CL, about 75 kilometers to the south of Olancha. Each site had a meteorological tower, an integrating nephelometer, and an SFU. The SFU was triggered by the nephelometer when visibility decreased below 15 km. The Baker site was also equipped with a DRUM sampler with 8 hour time resolution.

Automatic camera sites were placed in three locations: The first was located in the White-Inyo Range at an elevation 1000 m above that of the lake bed, 6 kilometers northeast of the township of Keeler. The field of view covered 85% of the lake bed. A similar site was placed at the Inyokern Airport, 80 kilometers to the south of Olancha, to monitor dust impact on Indian Wells Valley. These cameras were equipped with an intervalometer that was set to trigger at 9:00, 11:00, 13:00, 14:00, 15:00, and 16:00. The final site was placed alongside the south side of the lake bed to aid in measuring plume rise and thickness. This camera was triggered every half hour during daylight storm periods.

5. PM₁₀ Profiles of Particle Transport, March 1993

a. The Mobile Unit

A small motor home was outfitted for aerosol characterization with aerodynamic, optical, and sampling instrumentation. Dust aerosols were sampled from two stacks at a height of 5 meters above the surface (1.5 meters from the roof of the vehicle). Vehicular instrumentation included an aerodynamic particle sizer (APS 3300), laser aerosol counter, integrating nephelometer, DRUM sampler (see above), and a Stacked Filter Unit (SFU).

When dust events occurred, calibration and background reading for the APS 3300, LAC, and integrating nephelometer were taken just outside of the plume. Once completed, the vehicle was taken into the main plume, and proceeded to sample the source aerosol for at least 10 minutes. Existing roadways allowed for sampling within 1 km of the lake bed.

After several source samples were taken, the vehicle proceeded to track the plume. Stopping along the road side every 3-10 km, 5 to 10 minute samples of the plume were taken by all instrumentation. A hand-held anemometer gave a rough estimate of wind speed and direction. Once the vehicle repeated this operation and reached its far point, roughly 60 to 120 km downwind, sampling was repeated on the return trip at the same locations. Finally, if time permitted, further source samples were taken.

b. Aerodynamic Particle Counter (APS 3300)

An APS 3310 (manufactured by TSI, Inc.) was employed to yield real time aerodynamic size distributions (Baron *et al.*, 1986). This is accomplished by measuring particle velocity relative to a known air flow in an acceleration nozzle, and comparing this to a calibration curve. Unfortunately, the APS 3310 measures particles outside the Stokes regime and therefore errors are introduced. Corrections for gas density (altitude), and particle density were made. Furthermore, errors due to large dynamic shape factors (k) can be as large as 25% for particles with $k=1.19$ (Marshall *et al.*, 1991). Therefore, further corrections were made using particle morphology estimates from electron microscopy and aerosol chemistry. In some cases the particle morphology corrections were so extreme that we used the device as a simple particle counter.

c. Laser Aerosol Counter

An Oriel model 256 Laser Aerosol Counter (LAC) was employed to yield real time optical size distributions. Particles are counted and sized by their forward scattering properties. Data are output in the form of an optical equivalent diameter (D_{oe}); that is, particles recorded by the LAC are related to a sphere of index of refraction of 1.33. The LAC has sizes in 15 channels from 0.1 μm to 6.0 μm . All particles greater than 6 μm D_{oe} are placed in channel 16.

d. Integrating Nephelometer

MRI 1240 integrating nephelometers were employed in this study to give base line point visibility measurements on both stationary and mobile units. These integrating nephelometers have roughly a 160 degree scattering detection and can measure visibility degradation down to 2 km. A large portion of the scattering of particles larger than 6 μm will not be detected due to truncation error. This is not a problem for the NAWS, CL sites due to their distance downwind and subsequent fallout of the aerosols. However, scattering estimates taken by the nephelometer on the mobile unit within 10 km of the lake bed are under estimated.

e. Automatic Camera

Three automatic cameras were employed in this study to monitor dust production locations and transport of plumes. These systems used a Canon EOS 650 body with a 28 mm lens. A battery-operated intervalometer allowed for as many as 20 photographs per day. Both Kodachrome 64 and Fujichrome 100 films were used. All sites were serviced by UCD or UCD trained personnel at least once a week.

6. Optical Diagnosis of Particle Transport (Remote Sensing)

Because of the large area of impact by Owens (Dry) Lake dust plumes in regions with poor infrastructure it became necessary to employ remote sensing techniques. While automatic cameras provide excellent temporal and spatial resolution, the large areas affected by dust make it impossible to obtain total coverage. In this study a feasibility test of employing satellites to regularly monitor plume transport was conducted. Furthermore, satellite data were employed to monitor crust erosion on the lake bed. Other participants in LODE conducted additional remote sensing investigations of the destruction of crusts and transport of dust plumes from Owens (Dry) Lake; they used different platforms from those we utilized in this study. Their results (e.g., MacKinnon and Chavez, 1993; Chavez and MacKinnon, 1994; MacKinnon *et al.* 1994), while complementary to this project, were funded by other sources and are beyond the scope of this report.

Currently, there are three satellite systems available with acceptable sensor resolution to perform the test: LANDSAT, AVHRR (NOAA satellites), and GOES. While LANDSAT has excellent spatial resolution (up to 30 meter) and spectral resolution, it has extremely poor temporal resolution. Furthermore, LANDSAT is prohibitively expensive for routine monitoring. AVHRR has adequate spatial resolution (1.1 km nadir) as well as excellent spectral resolution (5 bands). AVHRR data are also available, no charge, at several data node (ftp) sites on the Internet. But, poor temporal resolution (twice daily) again makes it inappropriate for plume monitoring (but is still viable for crust erosion studies). The GOES visible channel has 1.1 km nadir resolution and downloads every half hour, allowing monitoring of plume transport. Furthermore, GOES data are relatively

inexpensive to obtain. GOES visible data has poor sensitivity, however, making plume detection difficult. This is caused by the necessity of high temporal resolution required by the short duration of most dust storms.

GOES 7 visible channel data were acquired during the spring intensive from March 8 to March 25, 1993. 650X450 pixel images were obtained hourly from 8 a.m. through 5 p.m. PST, on the hour. Data were cropped to 300X300 pixel data files. Images were generated and analyzed for the day before and on all storm days without preventive cloud cover. Furthermore, a 90X90 pixel data file was generated of the lake bed to monitor crust erosion. The 12:00 p.m. PST image was used each day to ensure comparability. On days with appreciable cloud cover the nearest usable hour was used.

The GOES visible sensor relies on external calibration to determine true albedo. Therefore, GOES data were calibrated using snow from the Sierra Nevada and White-Inyo ranges as well as Mono Lake and the Pacific Ocean. Due to poor sensor resolution (6 bit per pixel visible) as well as fairly crude albedo calibration methods the error of true albedo listed is estimated to be as large as 10%, absolute (i.e. albedo of (40% +/- 10%). However, selected geographic test points were used to ensure the relative comparability between images is within 3%.

Dust plumes were detected and enhanced by monitoring the change in albedo. Data from days with known dust activity had the closest usable previous day image (same zenith angle) subtracted. This method allows for detection with a change of absolute albedo of 5-10%. The change in albedo method is generally applied when the surface reflectance is low (i.e. lakes, ocean, forest etc.); the desert environment has a fairly large albedo. Further complications exist for the detection of plume transport into the snow covered Sierra Nevada (Under these cases the plume can reduce the overall albedo). Thus, in these regions we were only able to detect intrusion and not necessarily the extent of transport.

7. Detailed Size-Compositional Analyses of Dusts in Receptor Areas

The techniques applied to collection sites near China Lake were identical to those used near Keeler in the "Detailed Characterization of Lake Bed Aerosols," above. Basically, a DRUM sampler was operated continuously during the March 1993 study, with time resolution set to match that at Keeler, 4 hours. All 8 size ranges were utilized, including the important cuts at 10 and 2.5 μm . The purpose was to see if there was a shift in particle size during transport.

RESULTS - OVERVIEW

The results described in the following five sections were mostly obtained during the March 1993 intensive on the South Sand Sheet, Owens Lake playa.

The March intensive of the ARB/LODE programs exceeded our expectations in many ways. We were extremely fortunate in the meteorology, with the first "normal" spring after 6 years of drought. Statistically, as shown in Table IV, spring 1993 at Keeler was very similar to the non-drought period of 1979-1983. Further, the timing of the program in March was as close to optimum as one could hope, largely due to the extensive planning and preparation of Dale Gillette. The study began with an intact salt crust, which then degraded through several major storms, only to be reestablished after the last storm by the rains of March 25. Even the equipment, much of which was destroyed in the course of the study, remained operational through the key period of March 23. Only the mammoth storm of March 24 escaped our scrutiny, and that was largely due to intolerable conditions on the lake bed for both personnel and equipment.

Before beginning these discussions, we will summarize the meteorology and local aerosols as measured by the existing instrumentation operated continuously at sites on and around the lake bed.

1. Meteorology during the March 1993 Intensive

The average daily wind speeds for March 1993 at the Geomet site on the South Sand Sheet, and the GBUAPCD sites at Olancha and Keeler, are shown in Figure 11.

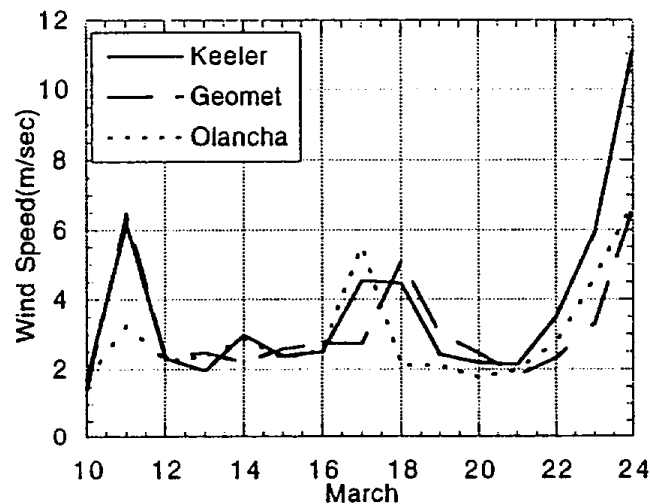


Figure 11. Average daily wind speeds at the Geomet site on the South Sand Sheet, our Olancha site, and the GBUAPCD Keeler site, March 1993.

Four distinct types of storms were observed during the study period. The meteorology at Keeler, Geomet, and Olancha for the storms of March 11, 17, 18, and 24 demonstrates four of these and is presented in Figure 12 a-d. The synoptic waves inducing these events can be complex, making prediction of the length and nature of a dust storm very difficult. The stalling or rapid passage of fronts and ridges as well as the placement of highs and lows in the Pacific Northwest and US southwest dramatically changes the initiation, length, and nature of high winds in the Owens Valley. The steep descent of the slopes of the Sierra Nevada coupled with the steep increase in the White-Inyo Range increases the complexity of the synoptically induced wind storms in the Owens Valley.

The March 11 storm shown in Figure 12a is typical of a "post frontal passage" storm. With the passage of a weak cold front, ridge building formed moderate to high northerly winds on a time scale of about 6 to 12 hours.

The March 17 storm(s) shown in Figure 12b demonstrates the classic example of a rapid cold front passage. Strong morning southerly winds formed and transported large amounts of dust northward. The field investigators at Owens (Dry) Lake observed a rapid shift in wind direction in late morning; a strong northerly wind developed, "backwashing" dust from the Owens Valley to the south into Lone Pine, Keeler and Olancha. By afternoon the ridge was already forming. The ridge was uncharacteristically further south, creating a rare straight westerly flow across the lake bed. High winds at the Olancha station show the rapid descent of cold air down the Sierra Nevada into the relatively warm valley.

Mesoscale afternoon winds developed frequently, producing minor dust events. These plumes tend to disperse within 10 km of the lake bed. The dust event of March 18, 1993 shown in Figure 12c is typical of these events. Automatic camera data coupled with meteorological data taken on the lake bed showed extremely complicated flow patterns over the playa. However, automatic camera data indicates that the dust production was intense and but extremely localized.

The March 24 storm shown in Figure 12d demonstrates the stalled and strengthening low which extends southerly winds for days at a time. The largest dust storm observed was produced by this flow pattern. Significant dust was generated with the induced southerly wind on March 23, 24, and 25. On March 25, dust was being generated on the South Sand Sheet during moderate precipitation.

2. Aerosols at Keeler during the March 1993 Intensive

During the March 1993 intensive, aerosols were monitored by the GBUAPCD PM₁₀ samplers near Owens (Dry) Lake on the regulatory one-day-in-six schedule. These data are given below in Table VI, and may be compared with the data in Table IV for historical perspective. The dust levels at all these sites were very low, indicating that these sites possessed some of the cleanest air in California during the month of March 1993.

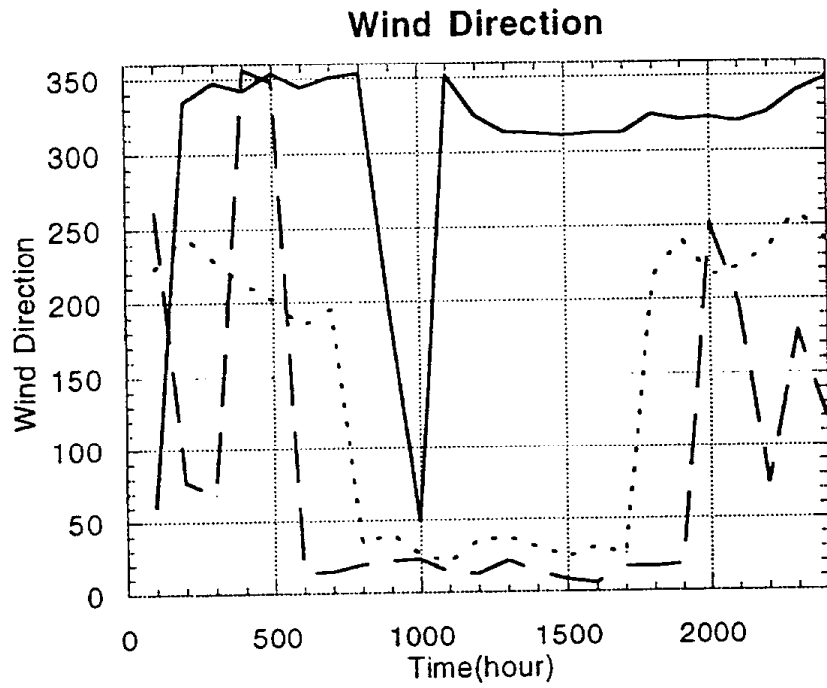
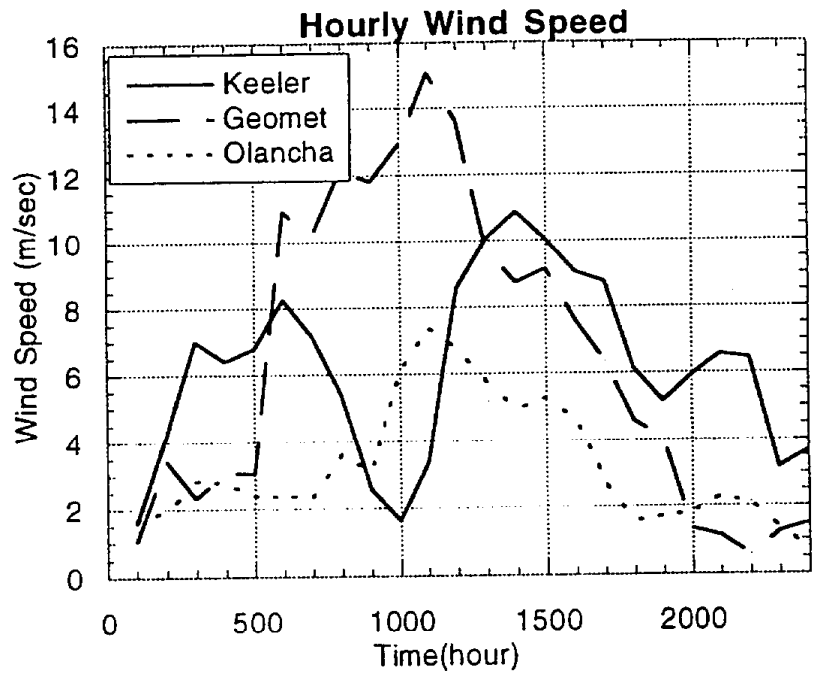


Figure 12a. Meteorology at Keeler, Geomet, and Olancha for storm of March 11, 1993.

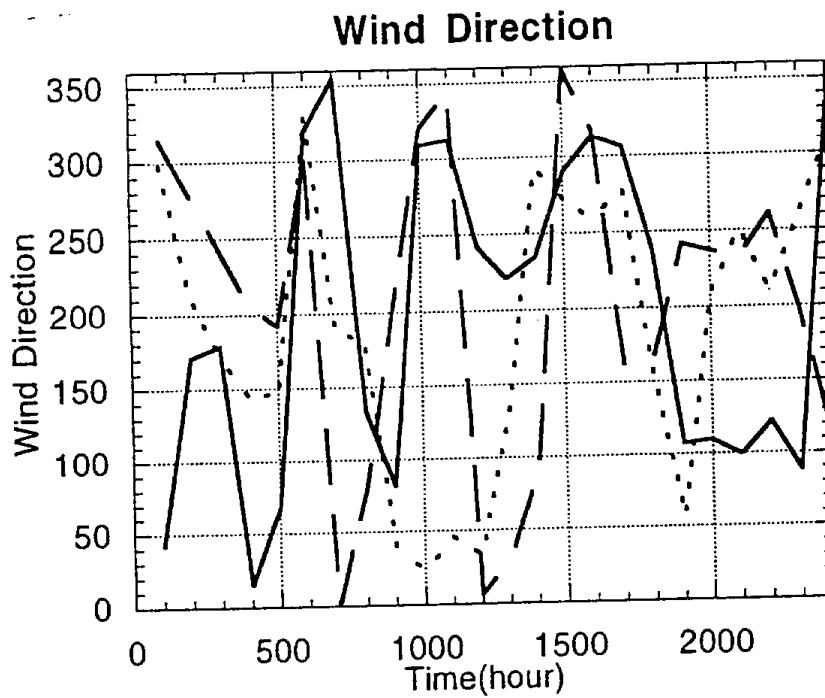
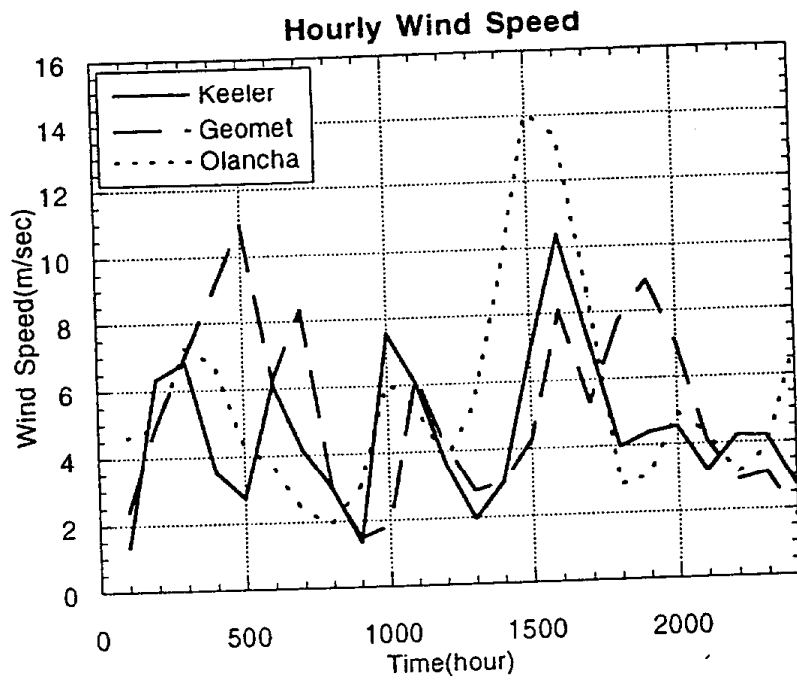


Figure 12b. Meteorology at Keeler, Geomet, and Olancha for storm of March 17, 1993.

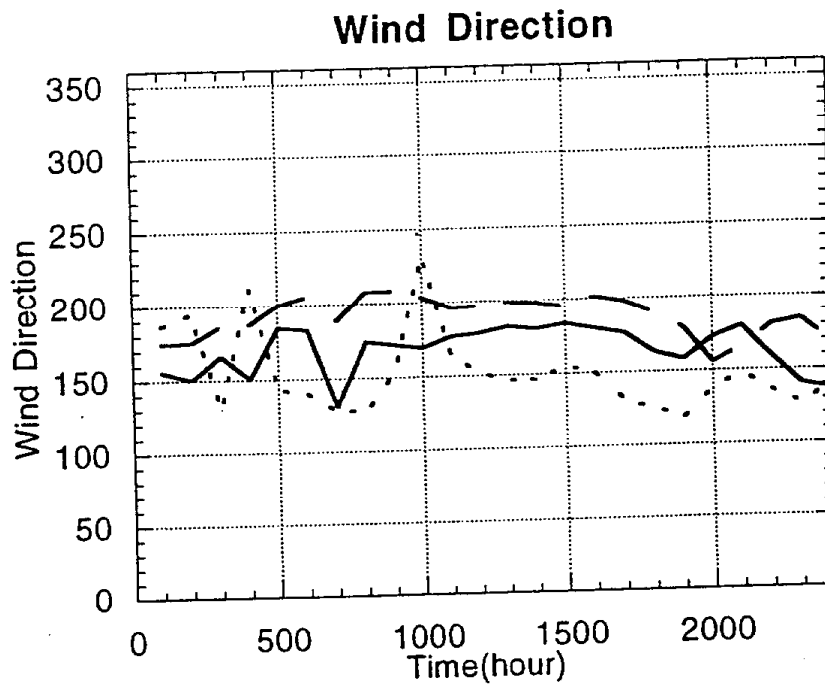
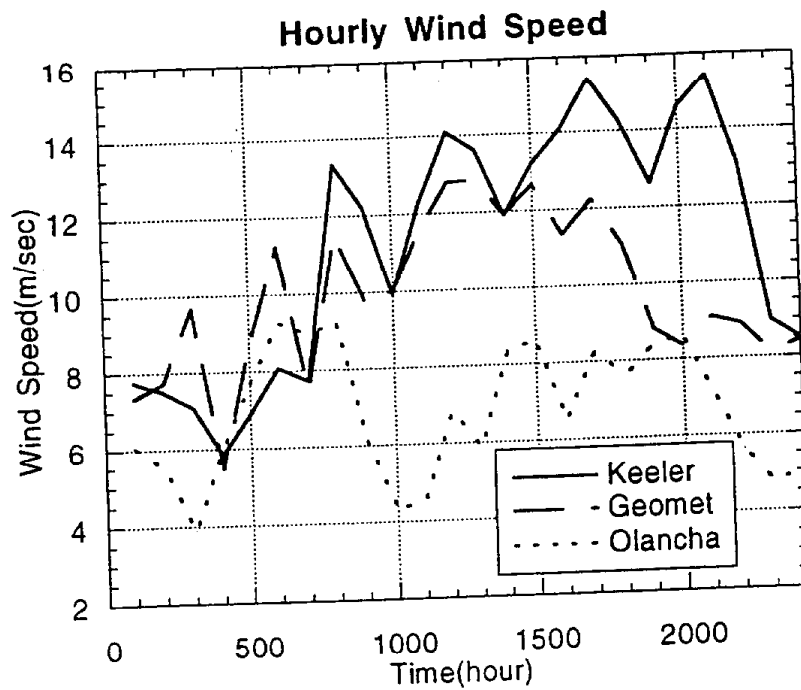


Figure 12d. Meteorology at Keeler, Geomet, and Olancha for storm of March 24, 1993.

The reality was much different, and it was fortunate that continuous PM₁₀ monitoring was initiated at Keeler on March 11, 1993 for this study. Preliminary data from the measurements made by the TEOM sampler newly purchased by GBUAPCD are available throughout the test period (GBUAPCD, 1993b). The data are presented as 1 hour PM₁₀ average values, as well as daily average values (Table VII). With the TEOM data, it can be seen that the one-day-in-six pattern of the PM₁₀ monitors missed all major dust events during the month of March. The maximum concentration by the one-day-in-six PM₁₀ samplers was 10 µg/m³ (March 14), with a mean during the study of 6 µg/m³, while the TEOM showed a maximum of 512.6 µg/m³ (March 17) with a mean value during the study period of 66.5 µg/m³. In fact, March 1993 was very similar statistically to the entire period 1979-1983 at Keeler shown in Table III.

It can also be seen from the TEOM data that one hour peak values of the aerosols were as high as 2,614 µg/m³ at 4 a.m. on March 17 (Table VIII). On the other hand, the massive dust storms on the South Sand Sheet of March 11 and March 25 were not seen on either the TEOM or standard PM₁₀ samplers at Keeler.

PARTICULATE MATTER - 10 MICRON
MARCH 1993
24-HOUR SAMPLING PERIOD CONCENTRATIONS
MICROGRAMS PER CUBIC METER

DATE: March	2	8	14	20	26	Monthly Mean	Highest Value
CHINA LAKE	9	10	-	-	-	9.5	10
COSO JUNCTION (10 miles East)	9	9	10	16	1	9.0	16
COSO JUNCTION	5	11	8	-	1	7.2	11
LONE PINE	11	9	11	10	7	9.6	11
KEELER	5	9	10	5	3	6.4	10
KEELER*						45.3**	512.6***

* Continuous PM₁₀ for TEOM, March 11-31, 1993.

** March 11 through 31, and using standard PM₁₀ values March 1-10.

*** March 17, 24 hour average.

Table VI. PM₁₀ data at nearby sites during the March 1993 Owens Lake Intensive. Note how the one-day-in-six schedule missed the six dust events of March 11, 17, 18, 23, 24, and 25. The times, 24 hour average values, and peak values were available from the new TEOM continuous PM₁₀ monitor after March 11.

PM₁₀ DATA FROM TEOM FOR KEELER, CA - March 1993

Date	11	12	13	14	15	16	17	18	19	20	21	22	23	24	25	26	27	28	29	30	31
1	6.2	10.7	14.3	5.7	9.9	5.8	2419.2	-7.2	6.2	9.8	9.8	11.8	8.4	14.2	17.9	11.3	6.9	18.7	5.3	6.7	11.1
2	7.0	10.3	14.6	4.0	8.6	8.6	2047.3	-12.3	5.0	23.2	9.0	13.9	6.1	14.1	10.3	12.2	5.6	12.9	5.0	4.8	8.9
3	8.0	8.5	11.2	31.4	8.4	2614.2	-5.7	7.6	9.3	8.4	11.5	9.3	9.3	32.0	11.2	0.0	4.2	3.4	5.9	7.0	7.3
4	6.4	9.2	15.4	19.9	9.0	753.3	-9.2	7.5	10.1	9.1	12.3	8.1	8.1	549.3	45.2	0.9	6.7	3.5	5.1	7.7	9.7
5	7.4	9.8	11.0	10.9	7.5	241.9	-3.5	8.2	10.4	13.5	12.6	10.3	10.3	557.7	14.0	1.9	7.6	2.9	4.2	5.4	9.2
6	6.6	10.6	15.0	9.4	10.4	260.1	-0.9	9.2	7.2	10.7	15.0	20.2	20.2	51.9	2.7	8.4	11.4	4.8	14.7	7.6	10.7
7	7.6	11.6	18.6	7.4	9.7	225.4	-3.8	5.8	8.1	10.4	13.5	33.4	33.4	599.3	36.2	2.8	3.2	5.9	-0.6	11.8	7.0
8	6.7	10.6	20.2	6.6	25.2	8.5	520.9	-9.9	3.2	9.7	7.9	11.4	16.2	51.6	22.6	3.1	2.0	4.5	4.5	7.2	11.9
9	6.3	10.3	15.4	16.6	8.5	432.5	-13.5	1.3	5.3	6.3	8.9	20.6	20.6	24.6	58.0	5.2	-2.7	5.0	4.1	2.3	6.6
10	3.7	8.8	13.1	4.7	6.2	334.9	-6.6	-0.3	3.6	5.1	5.2	40.7	40.7	133.4	23.3	3.7	-4.0	5.5	0.8	-0.1	0.8
11	6.4	8.2	15.5	2.7	1.7	201.1	112.7	0.7	0.2	3.2	4.1	322.4	322.4	494.7	31.9	-2.0	3.6	2.8	-8.7	0.4	7.0
12	3.0	5.3	13.0	2.6	0.2	155.9	75.9	-1.5	0.2	2.6	4.3	538.0	538.0	341.2	51.7	3.3	16.1	0.8	1.3	-1.5	15.0
13	0.1	5.2	14.3	1.3	0.8	114.3	38.4	0.7	1.9	1.8	7.5	1079.4	1079.4	247.6	41.8	-0.3	4.3	-0.5	-4.0	-1.5	34.2
14	2.5	8.1	9.9	3.3	5.9	249.4	0.0	4.1	2.8	4.2	4.0	1120.3	1120.3	438.7	32.0	2.7	3.1	0.4	7.0	8.8	13.6
15	3.3	8.6	15.9	6.8	345.0	211.4	0.0	111.2	1.8	4.0	4.3	245.5	245.5	438.7	19.9	2.3	10.9	-0.5	4.1	5.0	33.4
16	3.4	10.5	-2.2	81.9	334.6	30.9	0.8	773.0	3.0	3.0	4.3	419.6	2002.8	1121.4	50.8	7.0	6.4	-1.1	9.5	3.0	22.1
17	11.6	3.4	10.5	3.7	130.0	185.3	457.1	7.5	446.4	11.0	12.1	199.2	689.1	308.6	14.0	5.1	7.2	3.3	12.2	13.7	12.3
18	9.2	20.0	35.2	3.7	130.0	185.3	457.1	7.5	446.4	11.0	12.1	199.2	689.1	308.6	14.0	5.1	7.2	3.3	12.2	13.7	12.3
19	9.6	10.8	23.6	8.8	12.1	21.2	784.4	7.4	10.7	11.5	12.5	19.4	361.2	19.8	4.1	7.2	9.0	9.2	10.3	14.3	13.4
20	5.6	8.2	18.4	17.3	14.3	12.0	171.9	7.1	14.2	19.7	21.0	10.7	30.7	186.5	20.7	6.8	7.5	6.7	11.5	13.2	13.5
21	7.4	15.3	17.0	16.0	23.9	10.4	60.6	6.9	9.0	13.6	19.9	8.8	12.5	124.8	17.1	9.0	8.7	6.7	12.9	17.2	11.7
22	6.7	16.4	17.0	11.7	9.1	11.1	-0.3	5.0	12.2	15.6	15.6	10.7	13.0	0.0	15.1	8.8	18.5	2.2	11.0	9.7	15.0
23	6.9	11.9	15.5	6.9	9.7	8.3	-0.8	3.3	8.3	14.0	0.0	10.8	16.9	-4.2	11.8	7.7	19.4	7.1	8.2	5.9	14.2
24	7.1	12.3	14.8	8.7	10.4	5.8	10.7	5.4	7.8	15.6	0.0	7.9	19.3	14.8	20.3	10.6	20.5	5.3	8.4	5.3	9.6
Date	11	12	13	14	15	16	17	18	19	20	21	22	23	24	25	26	27	28	29	30	31
TEOM Avg	7.5	12.3	12.6	17.7	45.8	512.6	8.4	60.7	9.1	8.6	35.1	276.3	257.2	24.2	4.8	7.4	5.0	5.7	6.5	12.9	
PM ₁₀ Hi-Vol			10.0						5.0						3.0						
Ratio-TEOM/PM ₁₀			1.3						1.8						1.6						

Average Ratio, March, 1993 1.55
 Sigma 0.23

Average Ratio, Spring, 1993 1.21
 Sigma 0.3

Table VII. Hourly PM₁₀ Data From TEOM for Keeler, CA, March 1993. (GBUAPCD, 1993b)

3. Summary of Lake Bed Conditions during the March 1993 Intensive

On the lake bed itself, over the 26 day spring 1993 study period a total of 8 dust events were monitored. The four largest of these occurred on March 11, 17, 23, and 24, 1993. Furthermore, four other moderate to minor dust events were recorded over the lake bed, where the plumes dissipated within 30 km of the shoreline. Except for the afternoon of March 24, almost all of the dust was generated on the two main dust producing areas on the South Sand Sheet (Figure 6). Plumes from the South Sand Sheet had near-surface PM_{10} loadings at the shoreline ranging from 500 to 10,000 $\mu\text{g}/\text{m}^3$.

On the afternoon of March 24, the Northeast Sand Sheet began to blow. Instantaneous PM_{10} measurements from the mobile unit on the shoreline exceeded 27,000 $\mu\text{g}/\text{m}^3$, and the total concentration of suspended particles $<15 \mu\text{m}$ - i.e. PM_{15} - was greater than 47,000 $\mu\text{g}/\text{m}^3$. For perspective, the NIOSH industrial recommendations suggest dust mask usage when TSP levels exceed 5,000 $\mu\text{g}/\text{m}^3$. Unfortunately, all of the SFU cassettes prepared for that day were used in that morning's dust storm on the South Sand Sheet. Therefore, we did not have any samples from this area suitable for elemental analysis. However, aerodynamic and optical information was obtained.

Various storms were tracked as far as 140 km north past Bishop, 120 km south to Ridgecrest, and 70 km east into Panamint Valley. Reports from citizens, with partial confirmation from GOES 7 data, described significant dust impact as far as 250 km south at Mojave.

Of the 25 days of visible GOES 7 monitoring, cloud cover allowed only 2 major storms (March 11 and 17) to be adequately monitored. However, images acquired between storms showed the dynamic state of surface crust on the lake bed. The white crust's high albedo allowed easy distinction from the exposed grayish-beige sediment underneath. By early March a roughly 3 mm thick efflorescent salt layer had formed over most of the South Sand Sheet. Pooled surface water from the winter rains on the southwestern side of the lake bed evaporated throughout the study period and was replaced by salt crust with a powdery, efflorescent surface.

Similarly, at the beginning of the study, the still moist Northeast Sand Sheet was almost devoid of crust. As the study period progressed, salt crystals started to form and be deposited on the surface as the surface dried. Until the wind storm of March 24 no significant dust production was observed in this region. Days before the storm small patches of salt crystals (not a full salt crust) formed over the surface, generally in the form of 5 mm diameter patches spaced about 2 to 5 cm apart.

Analysis of these albedo data, coupled with location estimates of plume production regions found by the automatic camera site, showed that specific sub-regions of dust production existed on the South Sand Sheet. These sub-regions correspond to the

portions of the lake bed eroded on March 11. It should be further noted that these locations correspond exceedingly well with measurements of sand motion produced by the Phase II study (Figure 6) as well as dust production areas identified in the WESTEC report. Locations where crust completely eroded on the first major storm (March 11) were the predominant locations of dust production for three subsequent northerly wind storms and produced over 95% of the visible dust during camera monitoring hours. The dust producing area of the South Sand Sheet (eroded portion) was slightly enlarged with a strong easterly wind that formed on March 17 and a minor event on March 18. This can be observed by comparing albedo from March 14 and 21. We also see a slight erosion of the efflorescent salts on the eastern lake bed. Camera data were inconclusive in determining plume fraction (if any) that was produced in this region by the "direct lofting" theory.

RESULTS - SOURCES OF SALTATING PARTICLES

The surface of Owens (Dry) Lake is soft in winter, when it is wetted by winter rains and becomes muddy or covered by a thin sheet of water. Under these conditions, dust storms are generally reported to be small and infrequent, as shown by the statistical record of PM₁₀ at Keeler. During dry periods in winter and into very early spring, an efflorescent crust typically rich in mirabilite (St. Amand *et al.*, 1987) covers the surface. In early spring, the efflorescent salts covering the lake bed crust give it a snow-covered appearance until they are blown away. Subsequently, and through most of the spring, the dust-producing areas of the lake bed are covered by the remaining salt-silt-clay crust. Additional wetting of these crusts will provide little or no subsequent efflorescent salt particles, as the Soret effect promotes movement of the salts below the surface by osmosis (St. Amand *et al.*, 1986). The crust is broken up and degraded into a rough surface by the effects of desiccation, and abraded by saltating particles. Large areas of the lake bed are covered by a thin layer of rippled sand, generally several centimeters deep.

The playa surface is generally quite hard in summer and into autumn, in areas not covered by loose mobile sands. A few summer thunderstorms often drift away from the surrounding mountains and drop significant rains on the lake bed, wetting the silt-clay surface which dries into a hard crust, which we call the "cemented crust" in order to distinguish it from the "efflorescent crust" of spring and the "salt crust," which is in reality a mixture of salt, silt, and sand. When the surface temperature of the lake bed reaches 40 degrees Celsius in midsummer, some of the hydrated salts admixed in the surface layer lose their water of hydration and wet the surface (St. Amand *et al.*, 1987), which also promotes the formation of a hard crust upon drying. Although the lake bed may be very moist several centimeters below the surface throughout the year, the surface layer is dry. As the autumn months are typically free of precipitation, but often characterized by strong winds, the crust again becomes degraded by moving sand. PM₁₀ episodes become more frequent in this period.

As long as the surface of the dry lake is stabilized by a non-efflorescent crust and the integrity of the crust is maintained, the formation of dust is discouraged, as shown by studies using wind tunnels (Gillette *et al.*, 1982). When the crusted surface is disturbed by moving sand, aerosols are generated. The areas north and west of Keeler (the North Sand Sheet) and north of Dirty Socks dunes (the South Sand Sheet) are both primary aerosol production zones and possess an abundance of loose sand. The center of the lake bed keeps its hard undisturbed crust of sediment or salt intact during the dry season because there is little or no sand moving across it. "Mature" playas such as Panamint Valley are not sources of PM₁₀ because the sand deposits are stabilized by vegetation and the water table is too deep to allow brine to migrate to the surface and deposit efflorescent salts (Gill and Cahill, 1992).

Therefore, we characterize the crusts as follows:

1. Efflorescent, fragile crust that grows from complete wetting of the surface in late winter. On the South Sand Sheet, this crust was destroyed in about 2 to 3 hours on March 11, 1993. Its impact on PM₁₀ dusts was not documented, but many fragments appeared to be too large to directly loft into PM₁₀ dusts. After the rains of March 25, 1993, a cemented crust was formed. Soon thereafter, a new efflorescent crust began to form by early April, only to be destroyed by the sand abrasion in April and May.
2. A relatively hard, salt-silt-clay crust that underlies the fragile efflorescence above. This crust slowly eroded, from March 11 to March 24 at our sites, on a storm by storm basis. In areas in which the crust was intact, little PM₁₀ dust was generated. As the crust was eroded, large "gray-beige" areas of broken crust with loose sand appeared. These areas were easily resuspended by winds, and formed the major PM₁₀ sources during the intense March storms, with a saltation-erosion mechanism generating particles as fine as 0.3 μm diameter.
3. A cemented crust that forms after rain storms and/or release of water of hydration in spring, summer, or fall. This is a very sturdy crust that forms on dry sand/salt mixtures, cemented by salt and clay, that will even support vehicles (in extreme cases) and is highly resistant to dust formation. Until this crust was, in turn, eroded by saltation abrasion, dust production was sharply curtailed even in high winds. We were able to document the erosion of this crust on the South Sand Sheet through the generation of new loose sands, starting near the Dirty Socks Spring dunes, and spreading northward, during summer 1993.

There are doubtless other types of crusting around the lake, such as the silty crusts observed at outwash streams and the Owens River, and the rock-like salt crust of the central area of the lake and the Sulfate Well. Neither were common at or near the study site.

For convenience in this report, we will call all coarse, saltating particles "sand," although in fact they are a complicated mixture of sand, silt, and salt. Figure 13 shows a schematic of such motion.

Therefore:

- No Sand Motion + Crust = No Dust
- No Sand Motion + No Crust = Rare Dust
- Sand Motion + Crust = Some Dust
- Sand Motion + No Crust = Most Dust

We believe that the causative mechanism for well over 95% of the Owens (Dry) Lake dust events observed during the period of this study is the release of fine (PM_{10}) particles from the lake bed surface upon impact by saltating coarse particles (Figure 13). This phenomenon was supported by the data documented in previous ARB-funded Air Quality Group projects at Owens and Mono Lakes more than 10 years ago (Barone *et al.*, 1979; Kusko and Cahill, 1984; Cahill *et al.*, 1986).

Saltating particles on the lake bed are formed by a number of processes. The saltation process itself creates new sand-sized particles out of the crust as it breaks up the surface. Disturbance of the playa surface by human activity (vehicles, construction) breaks crust down into grains. Wind tunnel tests by Gillette (1984) indicated that rare, extreme wind events (sustained winds of 25 to 50 m/sec) over the lake bed can eventually break down the crust into constituent particles. However, most saltating particles are derived directly from existing major sand deposits in the vicinity of the sand motion maxima.

Several areas have been identified as primary source regions of saltating sand particles on the Owens Lake Bed by WESTEC (1984) and the GBUAPCD Phase II project (1988) (Figure 6). Field observations during this study confirmed these areas as the significant zones of moving sand and thus, not surprisingly, major dust storm genesis areas.

The South Sand Sheet, located on the southeastern part of the lake bed north of Dirty Socks Spring, is one such area. The sand is supplied to this area primarily by the unstabilized Dirty Socks Dunes. Some sand is derived from the Braley, Cartago and Ash Creek alluvial fans draining the Sierra Nevada. On-site observations by the investigators since 1991 have shown that during periods of sustained strong southerly wind (velocity at 2 m height on the order of 15 m/sec), waves of sand stream off the very large and old Olancha Dune complex - located several kilometers south of the lake bed across State Route 190 - and onto the South Sand Sheet of Owens (Dry) Lake, intensifying the

probably on the order of 10% to 15% cover - is such that a significant amount of sand (approximately 25% to 50%) should be able to pass through the vegetated zone (Buckley, 1987). The Olancha Dunes have been identified previously as a major source of saltating particles for the Owens Lake playa (WESTEC, 1984), and this dune complex has been

designated by the Bureau of Land Management as an off-road vehicle (ORV) recreation area. Wilshire (1980) has described the role of disturbance by ORVs in accelerating the wind erosion potential of dunes in the Mojave Desert region; it is distinctly possible that ORV use on the Olancha Dunes may be facilitating PM_{10} generation on the playa by increasing the transport of sand out of the dune field.

The second area identified as a high sand motion area is located north and west of Keeler and south of Swansea on the Northeast Sand Sheet. This area obtains its sand supply primarily from a field of young, partially vegetated, sand drifts and dunes along the lake shore generally referred to as the Swansea Dunes, as well as from lacustrine sediments deposited by longshore drift and flowing in through the Owens River Delta. Some sediments are also shed off alluvial fans draining the White-Inyo Range to the northeast.

Motion of Saltating Particles

During the March 1993 intensive study period, BSNE sand samplers were arranged in vertical arrays called sand towers. There is a significant concentration of saltating particles near the surface: approximately 50% of the total mass was collected at 10 cm, 80% below 20 cm height, and 90% within the first 30 cm. Only a few percent of the total mass of saltating particles was captured at 1 meter above the surface. This effect was more pronounced during the smaller storms. Over 80% of the total saltating particle capture took place in the two major events of March 11 and 24.

Sand motion on the South Sand Sheet correlates extremely well with high wind speed events. Figure 14 shows the sand motion and wind speed plotted on the same time scales. The sand flux was high only when the average wind velocity of the three anemometers on the Geomet exceeded approximately 4 m/s.

The Geomet site recorded both sand motion and wind speed for the same period with high time resolution. Figure 15 shows this comparison during the March 1993 Intensive. The relationship between wind velocity and sand motion is complex. Note the times when sand motion was high relative to wind velocity (3/11), moderate (3/17), or low (3/19).

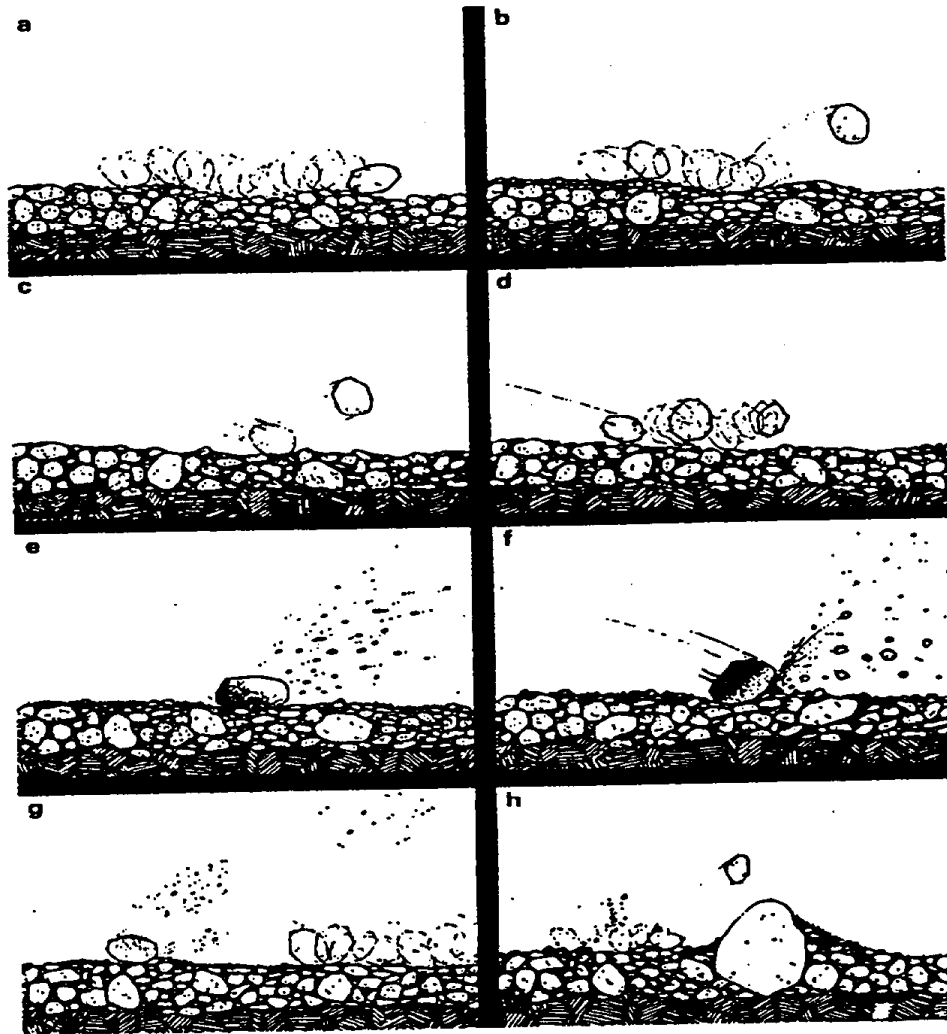


Figure 13. Soil particle motions during wind erosion. (a) Creeping motion of a particle moving with wind speed slightly greater than threshold. (b) A coarse particle lifted into the air by turbulent air fluctuations. (c) An airborne particle collides with the surface and bounces (saltation motion). (d) An airborne particle collides with the surface, rolls, and is then relifted by air fluctuations. (e) A particle collision followed by breaking off of smaller particles that were encrusted on the surface of the colliding particle. (f) A particle collision followed by "splashing" of the soil. (g) A combination of c, d, e, and f. (h) A nonerodible element giving protection to the soil downwind (After Gillette, 1981).

Owens Lake Intensive

March, 1993

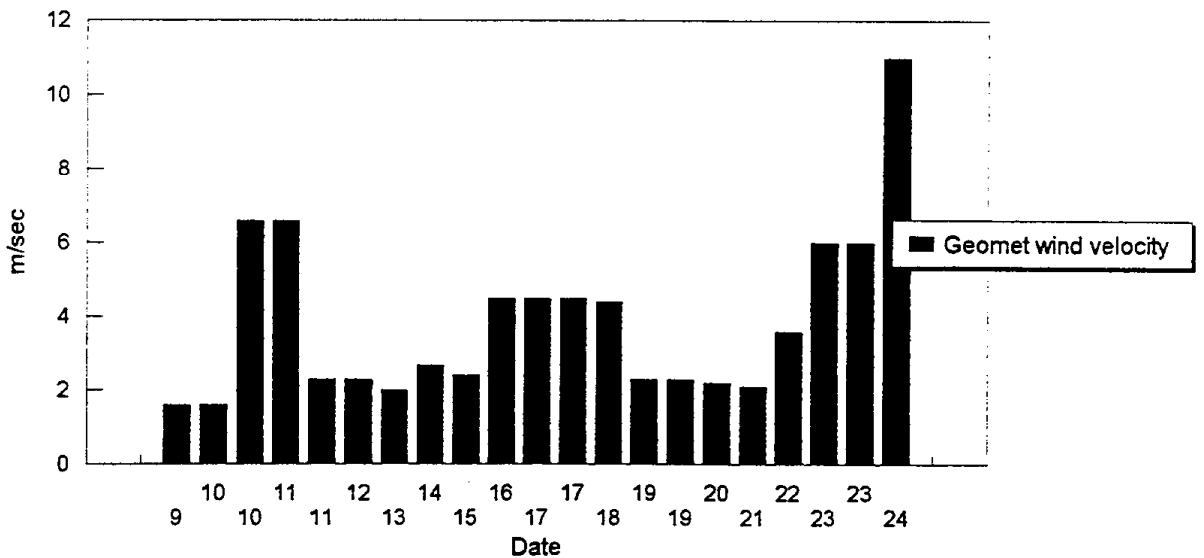
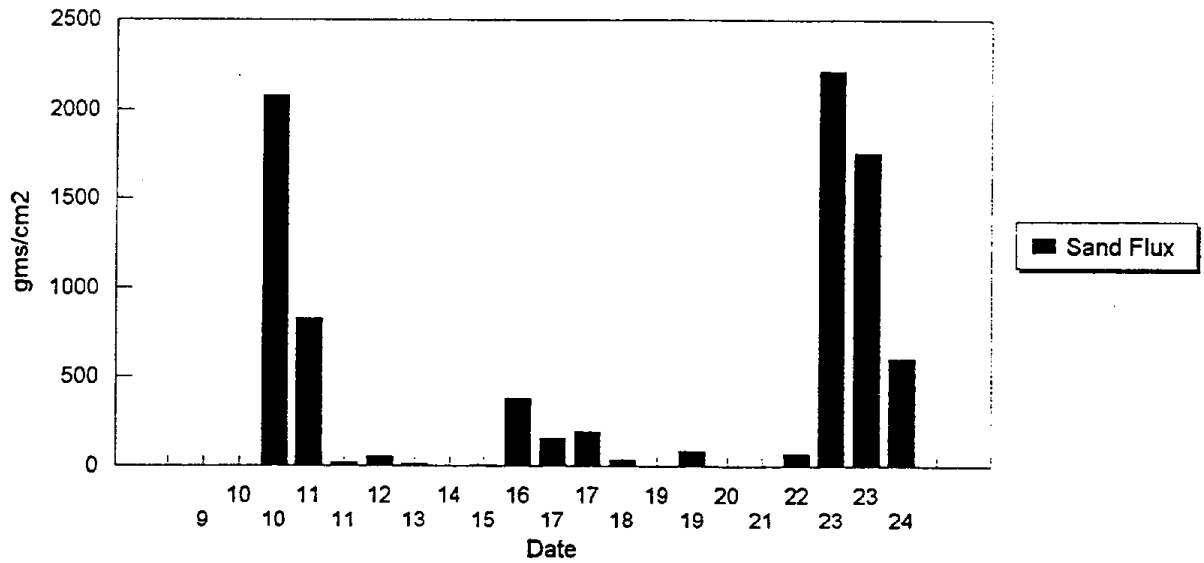


Figure 14. Comparison between sand motion and wind velocity, March 1993.

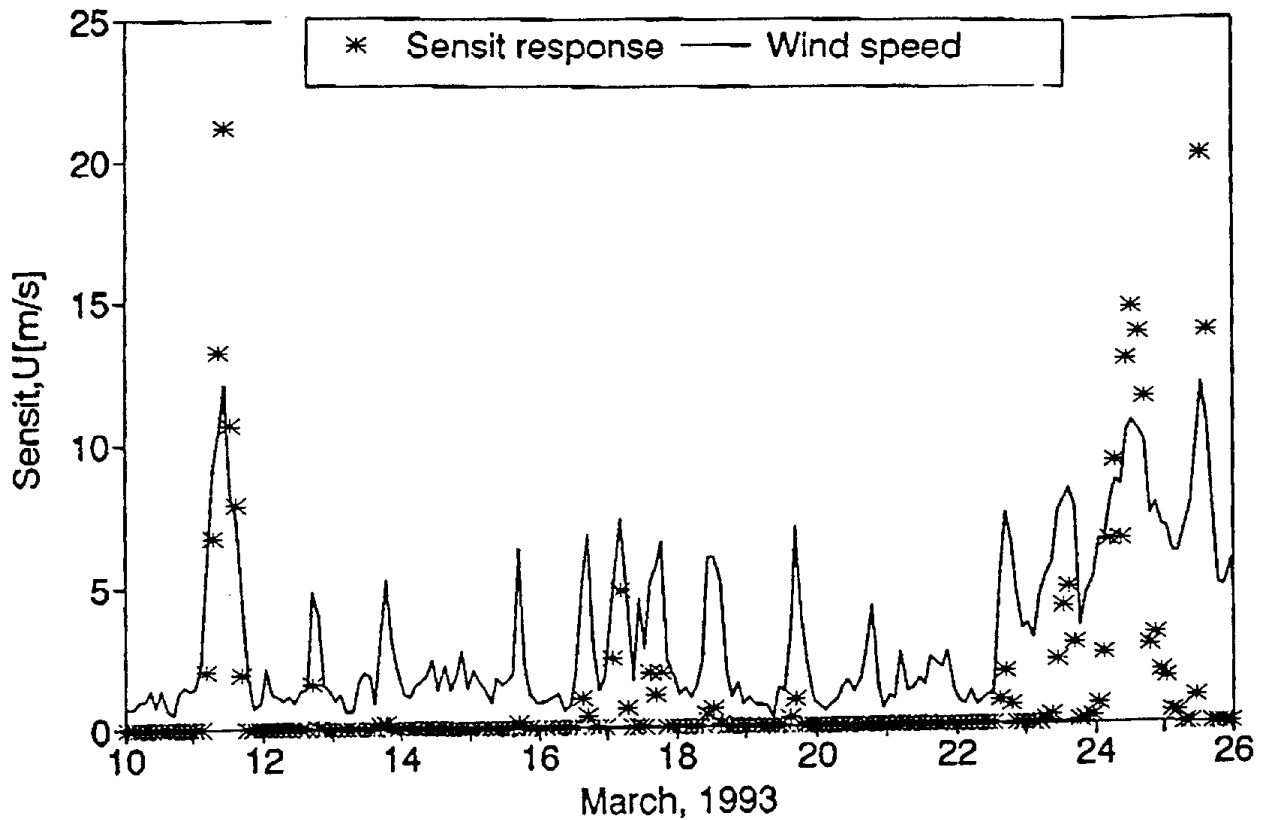


Figure 15. Comparison between the Sensit Sand Motion Monitor and the wind velocity at the Geomet site, March 1993.

Spatial Uniformity of Saltating Particles

No spatial profiles were made of sand motion during the March intensive, but measurements were made in April and May in a large area (1.2 by 2.2 km) south of the March intensive test plot. This area overlapped the southernmost meteorological tower. The sand motion data from the Weaver samplers from spring 1993, as summarized in Figures 16a and 16b, represent a time period when the South Sand Sheet was uniformly covered by broken salt-silt-clay crust containing loose sand. There was only a small variation in the amount of sand captured from one end of the test area to the other. Note how the amount of sand moving from south to north or north to south is similar (Cahill *et al.*, 1993).

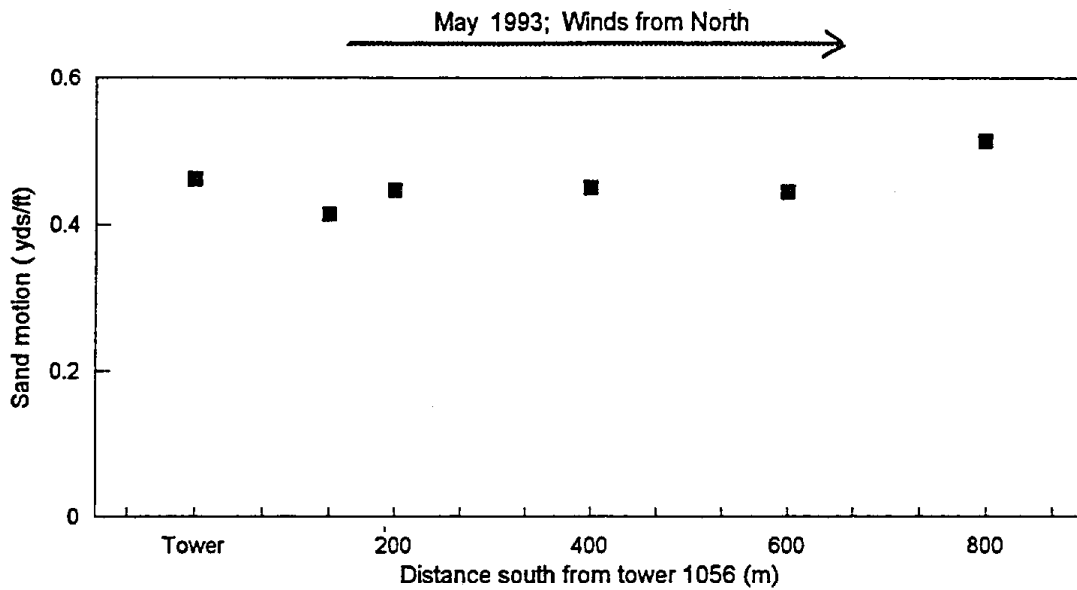


Figure 16a. Mass of saltating particles blown by north winds and captured in Weaver Sand Motion Monitors, South Sand Sheet, Owens Lake Bed, Spring 1993.

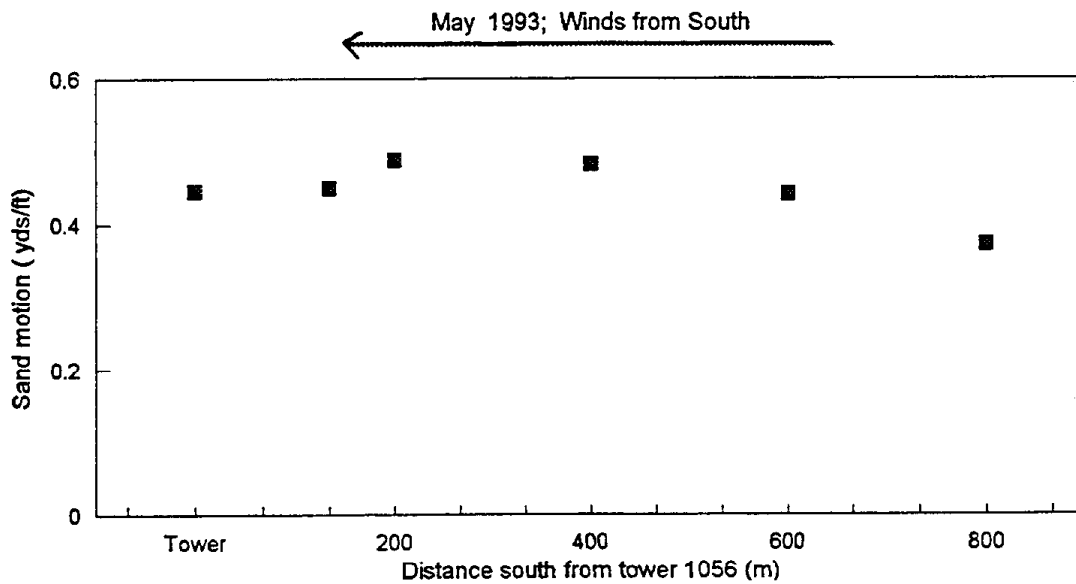


Figure 16b. Mass of saltating particles blown by south winds and captured in Weaver Sand Motion Monitors, South Sand Sheet, Owens Lake Bed, Spring 1993.

Particle Size Classification of Saltating Grains

Samples for particle size analysis were taken from a spot on the South Sand Sheet in an area of high sand activity just south of the southernmost sampling tower.

Samples were analyzed for particle size by dry sieving at UC Davis. Standard techniques were used; approximately 500 grams of material was poured into a nested set of Tyler USA standard sieves and shaken and tapped for nine minutes (Goudie *et al.*, 1981; Allen, 1975). The material trapped in each sieve was weighed on an Ohaus 700 series mechanical triple beam balance. Table VIII summarizes the results.

PERCENT OF TOTAL MASS IN EACH PARTICLE SIZE CLASS (+/- 0.02%)

Particle Size Range	Sand Dune, Lee Side	Sand Dune, Crest	Weaver Sand Motion Monitor, N wind	Weaver Sand Motion Monitor, S wind
> 2 mm	0	< 0.1*	< 0.1**	< 0.1***
1 to 2 mm	0.04	0.02	0.14	0.95
500 µm to 1 mm	1.03	3.00	1.37	20.07
250 to 500 µm	27.90	64.34	22.66	32.03
125 to 250 µm	59.30	27.73	63.67	34.46
63 to 125 µm	10.82	4.41	9.59	11.12
< 63 µm	0.91	0.50	2.58	1.37

COMPOSITION OF COARSEST GRAINS:

- * Rock fragments.
- ** Rock fragments and pieces of broken crust.

Table VIII. Particle size classification of saltating grains, Owens Lake Bed South Sand Sheet, 1993.

The large clasts found in the sand motion monitor described as "pieces of broken crust" are very thin, soft, platy, readily pliable light brown sheets with the look and feel of small strips of "tree bark," but made of cemented crust. These particles are on the order of 3 to 5 mm long by 2 to 3 mm wide, perhaps several hundred microns thick. The large rock fragments appear to be from fine-grained igneous rocks, most probably transported onto the lake bed from alluvial fans draining off the east slope of the Sierra Nevada.

The sediments blown into the sand motion monitor by the south wind are poorly sorted in the coarse, medium, and fine sand modes. Both of the dune sands and the north wind sample from the sand trap appear to be well sorted, having (89 +/- 3)% of their mass in the fine and medium sand mode, and are positively skewed as is typical of most wind-transported sediments. This is to be expected on a dune built as the result of a north wind,

on the south side of the fence. The poor sorting and lesser skewness of the south wind samples shows they have not traveled far, and indicates that these saltating, dust-generating particles are themselves generated very nearby. This tends to confirm that sand-sized grains originating in the Dirty Socks Dunes and transported onto and across the South Sand Sheet are a dominant component of the saltating coarse particles.

RESULTS - MECHANISMS OF INITIATING SALTATION

Abundant coarse sand particles are available to initiate erosion of the three major crust types on the lake bed that inhibit the generation of dust. The second part of this study was directed to understand how erosion occurs, so that the PM_{10} source function can be modeled for Owens Lake playas. Dust mitigation methods then can be evaluated quantitatively to discover the most cost effective method(s) of mitigation. This component of the study involved a detailed analysis of the so-called "fetch effect" or "field length effect," wherein the generation of dust increases as one moves downwind.

The increase of soil movement with distance downwind from the leading edge of erodible material, after the threshold for wind erosion is exceeded, was observed by Chepil and Milne (1939). Soil flux q is measured as mass of soil particles moving through an area of unit width perpendicular to the ground, normal to the wind, and of unit width extending to the top of the atmosphere. Chepil (1957) explained the effect as "avalanching" in which the saltation (hopping) motion of a sand particle sets more than one sand particle into motion after traveling a hop distance. Chepil visualized a chain of such events resembling the avalanching of snow. For constant wind stress and a constant number of particles dislodged by one impact such an explanation predicts an exponential growth in sand movement measured downwind. That is, the horizontal flux q of soil increases exponentially until it comes to a "saturation" where sand movement near the ground carries all the vertical momentum flux from the wind. With regard to snow, the fetch effect has been observed as an increase of the quantity of snow transported with distance (fetch) from stable snow up to fetches of 300 m for low wind speeds and 1000 m for high wind speeds, after which the effect of sublimation of snow particles decreases the transported snow (Pomeroy *et al.*, 1993). Gregory and Borrelli (1986) expressed the increase of flux as an exponential increase using dimensional analysis to predict soil mass detached by airflow. Stout (1990) derived a similar semi-empirical expression for exponential increase of soil flux,

$$f(x,z) = f_{\max}[1 - \exp\{-x/b(z)\}] \quad (1a)$$

where f is mass flux of soil particles at a given height z and downwind distance x , f_{\max} is the maximum of that flux, and b is a function only of z . The relationship between $f(x,z)$ and $q(x)$ is

$$q(x) = \int_0^H f(x,z)dz \quad (1b)$$

Stout derived an expression for b by rewriting the equation of mass conservation for sand by assuming that the first derivative divided by the second derivative of horizontal sand flux with respect to fetch distance is a function only of height. This variable $b(z)$ was interpreted by Stout (1990) as an entrainment coefficient for loose saltation-size material. Since b has the units of length, it is also interpretable as the distance at which the flux reaches 63% ($1-e^{-1}$) of its maximum. The exponential form fitted extensive data rather well for increase of sand flux with fetch at a circular sandy farm field in Big Spring, Texas, however, the values of b changed with height and with individual storms. The value of b was typically of tens of meters to a hundred meters for homogeneous sand at Big Spring (Stout, personal communication, 1993). Shao and Raupach (1992) also found variation of q with downwind distance in a wind tunnel and successfully modeled it using the model of Anderson and Haff (1991). This model showed that a fetch of several meters was required for q to come to an equilibrium value. The scale of this effect for the wind tunnel work of Shao and Raupach was of the order of meters for homogeneous sand deposits. The scale of the above observations suggests that avalanching may explain wind erosion for distances of a few tens of meters from the edge of the erodible material but that other mechanisms may perhaps be required for a larger scale fetch effect.

The experimental data of Bradley (1968) on adjustment of shear stress to an abrupt change of roughness for the transition from a rough surface to a smooth surface showed that the friction velocity adjusted rapidly so that an equilibrium value was reached within 2 to 4 meters after the change. This very small adjustment distance precludes this mechanism as a cause of the large scale fetch effects described above.

Owen (1964) suggested that the cause of the fetch effect was an aerodynamic feedback effect with respect to distance downwind. Saltating sand grains could increase the apparent aerodynamic roughness height; this increase of roughness height leads to an internal boundary layer in which more momentum is transferred to the surface. In Owen's theory, the increased momentum flux to the soil leads to an increased particle flux that further increases the aerodynamic roughness height. These interactions constitute a positive feedback of increasing momentum flux with fetch. Since the square of friction velocity times air density is equal to momentum flux, aerodynamic feedback implies an increase of friction velocity with fetch distance. Owen finished a short manuscript before his death that indeed showed a fetch effect caused by adjustment of an internal boundary layer to erodible material having u_{*c} for an aerodynamically smooth upwind surface and a rough upwind surface. A sketch of the physical scenario modeled by Owen is given in Figure 17. The key concept is that the feedback from the growing mass of saltating particles to the meteorology that increases sand motion versus distance. Unfortunately, Owen left no other supporting material or data for the aerodynamic fetch effect before his demise.

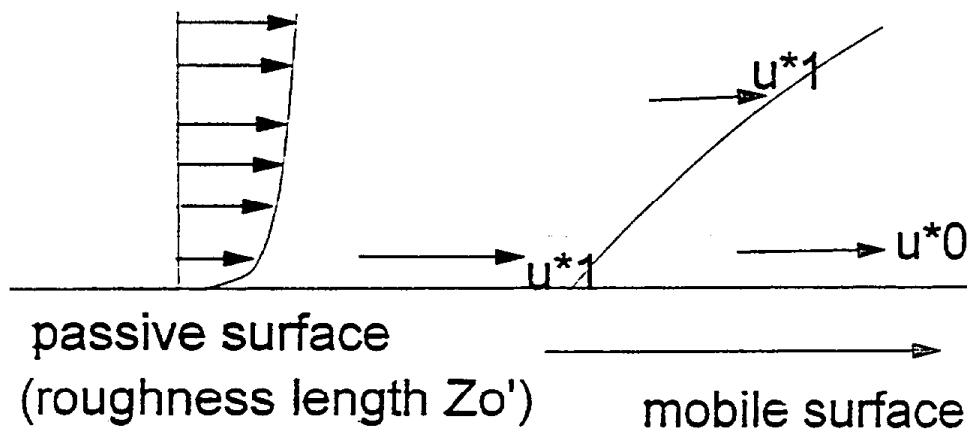


Figure 17. Schematic diagram of the fetch effect (Owen, 1964)

Gillette suggested that a mechanism for the fetch effect is change of the soil's resistance to erosion with distance. This effect followed from observations of Gillette and Stockton (1989) that showed more of the wind momentum flux went to transporting soil through the air as the frontal area fraction of non-erodible particles decreased. Because soil aggregates (including soil crusts) are destroyed by sandblasting, which increases as a function of distance from the leading edge, a given wind stress could transport more airborne soil mass as distance increased from the leading edge. The change of soil resistance to wind erosion with distance is observable as a change in the percentage of the surface as crust. Because Gillette and Stockton (1989) showed that threshold friction velocity also decreased with destruction of surface crusting, this effect could also be detected as a decrease of threshold friction velocities with distance downwind.

One purpose of this study is to find the relative importance of the three mechanisms of wind erosion fetch effect described above. The mechanisms must explain both small-scale and large-scale (greater than tens of meters) fetch effect and increase or decrease of q with downwind distance. We suggest that three mechanisms work together to bring about the wind erosion fetch effect (field length effect). These mechanisms are avalanching, aerodynamic feedback, and soil resistance. We tested a (conceptual) model incorporating the three mechanisms versus a model which invokes only the avalanching mechanism. Since the avalanching mechanism is widely accepted to be the sole cause of the wind erosion fetch effect, we would like to point out the importance of the aerodynamic feedback and soil resistance mechanisms. The two models were tested for scales of hundreds of meters in the natural outdoor setting of Owens (Dry) Lake.

Models for the Wind Erosion Fetch Effect

We may write equations of the Avalanching Model and the Avalanching/Aerodynamic Feedback/Soil Resistance Model as follows.

The pure avalanching model (Model 1) may be written as

$$q(x) = F(x)q_{\max} \quad (2)$$

where q_{\max} is not a function of x . $F(x)$ is a positive number between 0 and 1, and is similar to Stout's $f(x)$ term above.

The quantity q_{\max} may be written as Owen's (1964) solution of the equations of mass and momentum conservation for an air/particle system:

$$q = A \frac{\rho}{g} u_* (u_*^2 - u_{*t}^2) \quad (3)$$

where u_{*t} is the threshold friction velocity, ρ and g are density of the air and gravitational acceleration, respectively, and A is a constant. Using this equation, equation (2) becomes:

$$q(x) = F(x) A \frac{\rho}{g} u_* (u_*^2 - u_{*t}^2) \quad (4)$$

The pure avalanching model (Model 1) requires u_{*t} and u_* to be constant with x . Model 2, an avalanching/aerodynamic feedback/soil resistance model allows change of u_{*t} with x and change of u_* and Z_0 with x as effected by airborne sand-sized grains.

Tests of the Models

The following tests were made for the two models for conditions when the erosion threshold was exceeded for all locations and where there was a measurable change of soil flux q with distance downwind.

The Avalanching model: (model 1)

1. The direction of q increase is always downwind. That is, $F(x)$ must lie between 0 and 1 and must increase with distance downwind.
2. Friction velocity and threshold friction velocities are constant.

Avalanching/aerodynamic feedback/soil resistance model (model 2).

1. For some range of u_{*c} , aerodynamic roughness height increases with friction velocity (and saltation flux). For this range of u_{*c} , u_{*c} should increase downwind.
2. Disaggregation of the soil (alternately u_{*t}) decreases in the direction that q increases.
3. An avalanching effect is identified from the data $q/[u_{*c}(u_{*c}^2 - u_{*t}^2)] = AF(x)$ where A' is a constant equal to $A\rho/g$. $F(x)$ must be non-random and increase with x . In a case where u_{*t} increases with fetch, transport of sand will modify the decrease of q such that q decreases less rapidly with distance (the overshoot of q).

Experimental Procedures

The above tests require measurement of soil flux, wind friction velocity, aerodynamic roughness height, and threshold friction velocity. Because the severely abrasive atmosphere in a dust storm is extremely damaging to sensitive instrumentation, we chose instruments for ruggedness as well as precision. Based on many years of experience in outdoor wind erosion measurements, we decided to measure friction velocity and aerodynamic roughness height by the wind profile method with sensitive anemometers that we thought would withstand the sandblasting of the wind erosion episodes. Soil flux was measured with instrumentation developed for agricultural wind erosion measurements. We located the experiment at a site on the Owens Lake Bed having frequent high winds and erodible soils.

The site of the experiment conducted in March 1993 was on an erodible part of the South Sand Sheet of the Owens Lake playa, latitude approximately $36^{\circ} 20'$ N by longitude approximately $118^{\circ} 0'$ W, approximately 5 km northeast of Olancho. A site on another part of the erodible (dry) lake floor near the town of Keeler on the Northeast Sand Sheet was used for feasibility tests in May 1991. The area chosen for the March 1993 experiment was a loose, sandy, flat area immediately downwind of a crusted flat area on the South Sand Sheet. Both the upwind and sandy areas were totally unvegetated and very flat. Visually, the upwind crusted area was about the same flatness as the loose area.

An analysis of the surface material is shown in Figure 18 and Appendix C. The soil at the secondary site consisted of (by mass) 0.54% organic material, 10% carbonate, and 9.13% soluble salts. A size analysis of the surface material for the primary experiment and the feasibility study in 1991 is given in Appendix C. Soil pH values were 9.6 at the secondary site and 10.0 ± 0.1 at the 11 sites of the north-south line of the primary site. Figure 18 shows a gradient of sand content from north to south. Such a gradient in composition can give rise to a gradient in crust strength (Gillette *et al.*, 1982) with crust strength increasing to the north.

Instrumented meteorological towers were located on a line predicted to be in the direction of the wind. The towers were set on a north-south line at locations predicted to show the fetch effect, based on the 1991 preliminary experiment and repeated examination of the surface from May 1991 until early March 1993. Four instrumented towers were set at the points 0, 50, 100, and 150 m on the line, starting from the north. Two instrumented Sensit towers were set at measured distances of 520 m and 1057 m. For the 1991 feasibility test, the two Sensit towers were set at distances of 77 m and 442 m downwind of the leading edge of the erodible sandy material (Figure 30, Appendix H).

Wind measurements were taken by Climet light chopping cup anemometers. The threshold was 0.33 m/s and accuracy was $\pm 1\%$ for the range 0-40 m/s. The distance constant of the anemometers was 1.5 meters. The heights of measurements were 20, 50, 100 and 300 cm. The instruments were carefully chosen from a pool of 67 units matched to have identical response to the wind. Testing allowed the selected anemometers to be matched to within $\pm 3\%$. The instruments were chosen from a pool of 67 anemometers to have identical response to the wind. Testing of the anemometers took place on Table Mountain, Colorado (a flat, elevated mesa north of Boulder) in October and November 1992. The anemometers were calibrated in the National Center for Atmospheric Research calibration wind tunnel in Boulder, Colorado. One minute average speeds were recorded for all four towers using a laptop computer-based data logging system. The system was contained in a dust-proof case and was powered by sealed batteries.

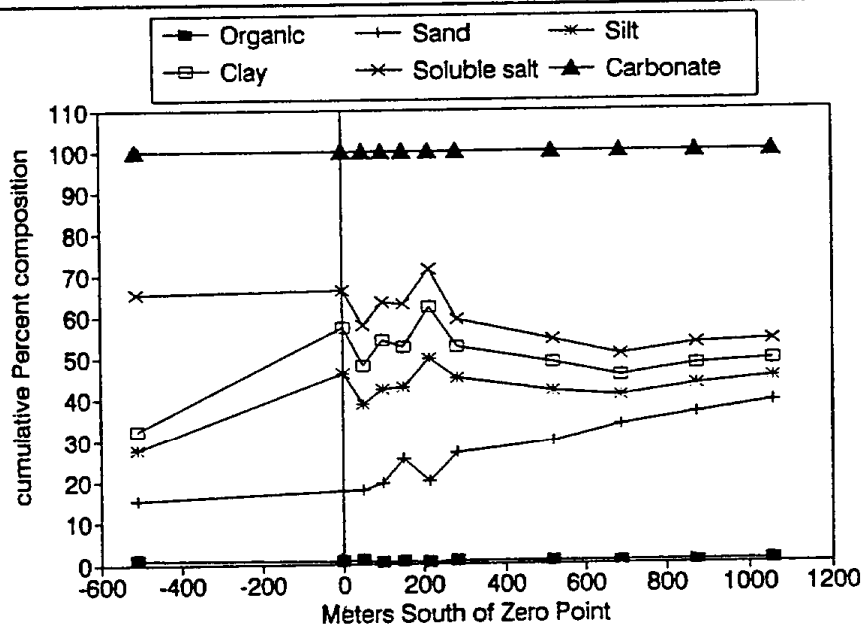


Figure 18. Cumulative composition of surface sediments along a linear transect, South Sand Sheet, Owens Lake Bed, March 1993.

The towers located at 520 and 1057 m south of the zero point had the following instruments: four anemometers at 20, 50, 100, and 200 cm height, an external system thermometer, and a wind direction sensor. The anemometers were calibrated as above. The instruments were controlled and data were stored using a computer controlled data system capable of storing 1 megabyte of digital data. Each tower was powered by a 45 W solar panel that used a 36 amp-hour sealed storage battery.

Soil Flux measurements

Soil flux measurements were taken using six BSNE collectors at each measurement location. These collectors and their calibration were described by Fryrear (1986). The collectors are passive devices that maintain 90% efficiency for all winds (Shao *et al.*, 1993) because of top-venting and the large Stokes numbers of the soil particles being collected. Soil flux was collected at six heights: 10, 20, 30, 50, 60, and 100 cm above the surface for sampling times of from one to five hours.

At the 520 m and 1057 m locations, erosion kinetic energy sensors (Sensit™) were placed at heights of 5, 10, 30, and 50 cm from the ground surface. These sensors were previously used by Stockton and Gillette (1990) to sense airborne sand movement. The output of the devices is proportional to the airborne particle mass flux times the square of the particle speed plus a background. An example of the data is included in Figure 19, covering the major dust event of March 11, 1993.

Data processing and estimation of errors

We obtained data sets of friction velocity, aerodynamic roughness height, and integrated mass flux Q (defined below in equation 9).

Friction velocity and aerodynamic roughness height

Friction velocity was calculated for each 20-minute period by finding the 20-minute-average wind speed at the four heights ($z = 20, 50, 100, 300$ cm or 200 cm for the Sensit tower). The least-squares fit of mean wind speed to the natural logarithm of height z was used with

$$U(z) = 2.5 u_* \ln(z/Z_0) \quad (5)$$

to compute friction velocity, where Z_0 is aerodynamic roughness height (Panofsky and Dutton, 1984). The 90 percent confidence interval (CI) for the estimate of friction velocity was related to the standard error of the regression, S_{err} , (Miller and Freund, 1977) as

$$CI = \pm t_{\alpha/2, S_{err}} \sqrt{(n/S_{xx})} \quad (6)$$

$$\text{where } S_{xx} = \sum_1^n x_i^2 - \left(\sum_1^n x_i \right)^2 \quad (7)$$

where x_i is the independent value of the regression (in our case the natural logarithm of height), n is the number of observations and $t_{\alpha/2}$ is the t statistic for the $\alpha / 2$ level. The 90% confidence interval for aerodynamic roughness height (the height at which the extrapolated value of mean wind speed goes to zero) was calculated as

$$CI = \frac{+}{-} \exp \left(t_{\alpha/2} S_{err} \left(\left(\frac{1}{n} - \frac{n + (a/b) + \bar{x}}{S_{xx}} \right)^{1/2} - a \right) \right) / b \quad (8)$$

where a and b are the constant and coefficient of the linear regression and \bar{x} is the mean of the x_i and n is as above.

Threshold velocity

Threshold friction velocities are the friction velocities above which soil eroded steadily (not intermittently) during the sampling period. We estimated threshold friction velocities by carefully noting when threshold for erosion was reached or when it stopped. Since the surface was disaggregated by the several wind erosion episodes between March 11 and 25, threshold velocity decreased during that time. From March 12 to March 15 several small episodes took place slightly above or slightly below threshold, too short in duration and too weak to break down the surface aggregation. These events allowed us to make more than one estimation of when threshold was reached. We estimated the error for threshold friction velocity as above for the estimates of error of the friction velocity.

OWENS LAKE GEOMET

MARCH 11, 1993

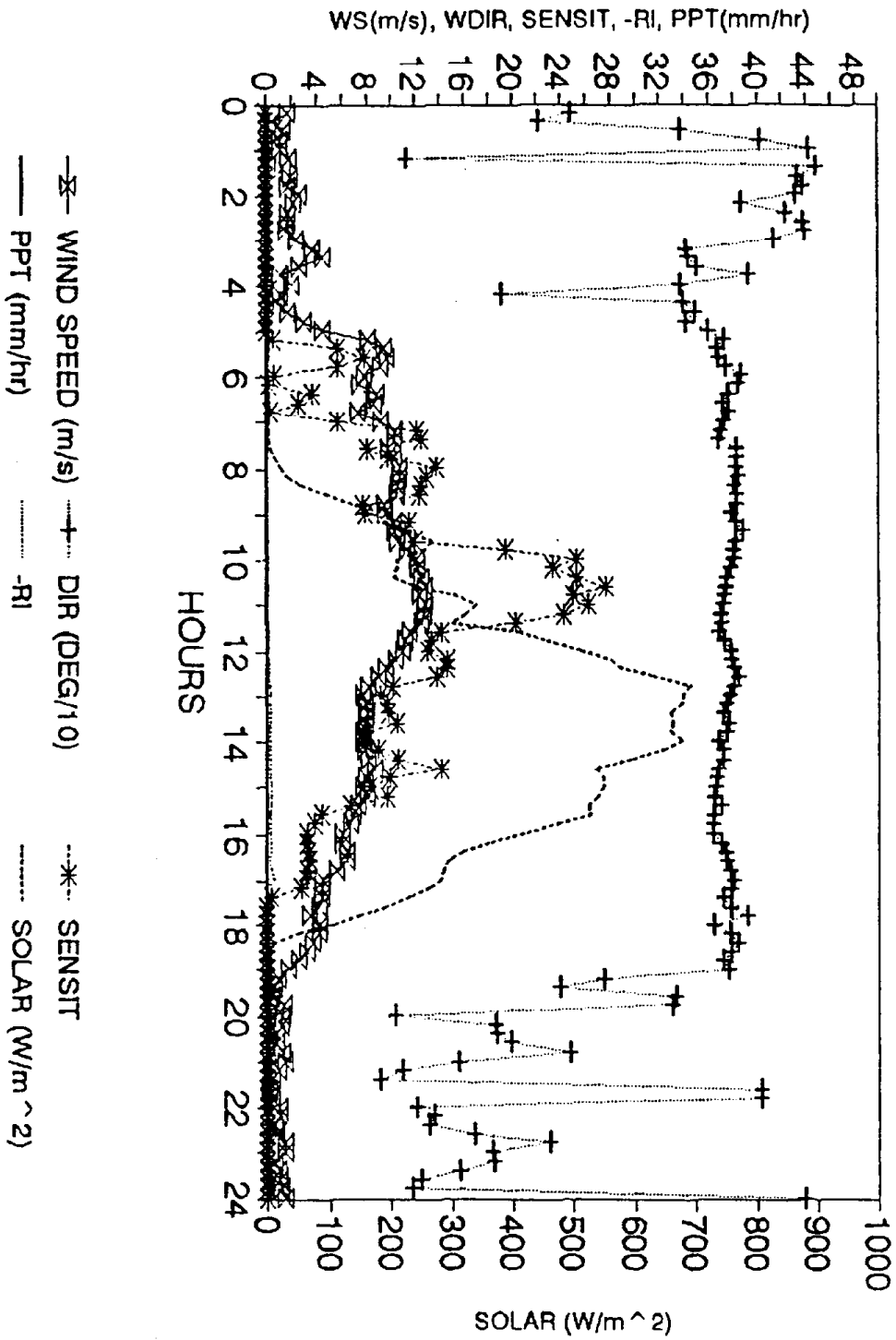


Figure 19. Geomet data for March 11, 1993.

Mass flux

The fluxes collected at six heights (10, 20, 30, 50, 60, and 100 cm above the surface) were interpolated using the formula used by Shao and Raupach (1992) ($c \exp(az + bz^2)$) where a , b , and c are constants) for the same purpose. The fits of the data to the formula gave an average r^2 of 0.96 with standard deviation 0.027. There were no apparent differences of r^2 with location or sampling time. Because fluxes were obtained over a finite time interval, the measurements were represented by

$$Q = \int_0^t q dt \quad (9)$$

The estimate of the 90% confidence interval for Q was $t = 0.05$ (3 degrees of freedom) times the standard error of the least squares fit evaluated at the height of the maximum flux. Because the standard error did not vary with time or location, we estimated the 90% confidence interval for Q to be 9% of the Q value.

The soil mass fluxes were measured over finite periods, so to make the wind data consistent for comparison with the soil flux data, we defined G as follows:

$$G = \int_0^t u_* (u_*^2 - u_{*t}^2) dt \quad (10)$$

The error assigned to each G estimate was related to the errors of both the friction velocity estimate and the threshold friction velocity. For no error in $F(x)$, small fractional errors in threshold friction velocity and friction velocity result in the fractional error of G as:

$$\Delta G/G = [(3-B^2)y + 2Bs]/(1-B^2) \quad (11)$$

where $B = u_{*t}/u_*$, $y = \Delta u_*/u_*$, and $s = \Delta u_{*t}/u_{*t}$. For u_* greater than u_{*t} the error is approximately three times the error of the friction velocity. For friction velocity near the threshold, small errors in both threshold friction velocity and friction velocity are magnified by $1/(1-B^2)$.

Analysis of Results

Soil mass flux

Integrated soil mass fluxes Q were obtained for 12 wind erosion episodes during the March 1993 testing period and one five-hour-long erosion episode during the preliminary test on May 17 and 18, 1991. All of these sets showed an increase of Q from north to south. Data were selected for analysis using the following three criteria:

1. Wind direction was within 10 degrees of the line of the sampling towers.
2. Wind erosion was fully developed at all sampling towers; wind friction velocities were at or above threshold for wind erosion.
3. More than two points of data were required for an erosion episode.

Prior to March 11, the boundary between the fully crusted material and the partially crusted soil was at 75 m. On March 11, 1993, high winds broke the crust back to a distance 503 m north of the zero tower at 1000 local time. That boundary was stable until March 25 when the experiment was terminated by heavy rain. Therefore, 503 m should be added to the distances from the northernmost tower to give the distance of each tower from the crust/broken crust and loose material boundary. From the crust/broken crust boundary to the south, there was a continuous gradation of crustal destruction to the point of no visible crust. The point of no visible crust moved north between March 11 and 25 as the destruction of the partially disaggregated crust steadily proceeded during dust storms. Table IX gives results for the crust integrity and friction velocity for the study.

Seven wind erosion episodes were eliminated using the above selection criteria, including one when wind was from the northwest (March 17, 1993), five when two or more of the locations were below threshold, and the set obtained in 1991 that had only two sampling points. The six selected data sets of Q vs. distance south from the farthest north tower are shown in Figure 20.

Percentage of surface as crust versus date.

Date, March, 1993	zero point	50 m	100 m	150 m	520 m
11, morning	100	100	100	100	100
11, afternoon	33	20	14	3	2
12 through 16	13	10	2	6	
17 and 18	11	7	8	4	6
19 through 25	8	4	4	2	3

Threshold friction velocities in cm/s.

11, morning	60	55	50	50	50
11, afternoon	35.5	31.7	34.6	29.3	18
12 through 16	27		26		
17 and 18	25	25	25		
19 through 25	27	24	24	24	

Table IX. Crust percentage and threshold friction velocities.

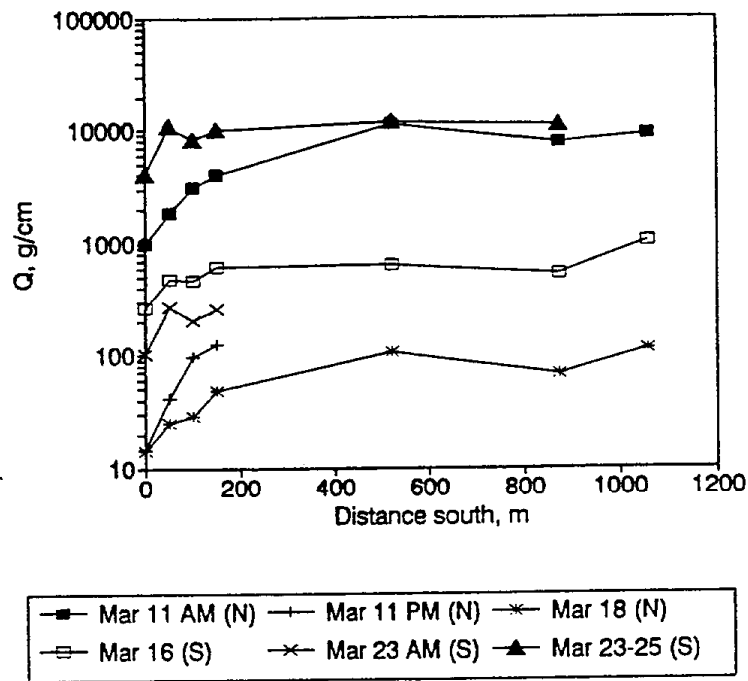


Figure 20. Integrated soil mass fluxes (Q) along the linear transect, Owens Lake Bed fetch effect study, March 1993. N and S denote wind direction.

These data represent north winds that were experienced on March 11, before and after 1200 (a.m. and p.m. in Figure 20), and on March 18. South winds were experienced on March 16, March 23 a.m. and March 23-25. The most obvious feature of the data is the increase of Q from north to south, regardless of the wind direction. The steepest gradients of Q vs. x occurred on March 11, immediately following the breakup of the crust when the surface was in its most aggregated condition. The episodes with southerly winds clearly refute Model 1. The steepest gradients of Q vs. x occurred on March 11 immediately following the breakup of the crust when the surface was in its most aggregated condition. For north winds on March 18, the gradient is smaller and the surface was more homogenous with respect to pulverization. The smallest gradients of Q vs. x occurred for south winds on March 16, 23, and 23-25 when the surface aggregates had been pulverized by several wind erosion episodes and the direction of sand transfer was parallel to the gradient of more-pulverized to less-pulverized. For x greater than 150 m, there is very little gradient of Q with x . Therefore, the data for $0 \text{ m} < x < 150 \text{ m}$ were of primary interest for this analysis.

Aerodynamic roughness heights

We examined the detailed measurements of wind profiles for $0 < x < 150$ m (for data sets satisfying the above selection criteria) for quality of the wind profile data. The ratio of standard error of the friction velocity estimate divided by the friction velocity estimate was used to judge profile quality. Mean values of these ratios for four towers (0, 50, 100, and 150 m locations) for March 11 were 3%, 3%, 1%, and 1% respectively. On March 18 the ratio increased to 36%, 14%, 8%, and 4.6% respectively. On March 23, the mean ratios were 20%, 13%, 33%, and 27% respectively. The data clearly shows a degradation of quality with time probably caused by accumulating bearing friction in the extremely abrasive atmosphere. To use our best data, we emphasized the March 11 observations and the March 18 data for the 50, 100, and 150 m locations. The poorer quality data from March 23 a.m. were used because they were our best representative data for south winds.

Figure 21 shows the estimated aerodynamic roughness heights for $x < 520$ m along with the 90th percentile confidence interval for the 150 m downwind location. Only the upper limit of the confidence interval is shown, the lower limit being zero. From about 0930 to 1100, Z_0 is higher at every measurement location than at 0800 or 1200. For all five locations the aerodynamic roughness height increased during higher wind friction velocities (see next section). Furthermore, although not statistically significant, the data suggest larger Z_0 for downwind locations compared to upwind locations, in agreement with Owen's theory.

The above suggestion is bolstered by the quantity of data in the plot. Although individual point values of Z_0 are not significant, a large number of Z_0 points show a consistent increase with fetch from 0930 to 1100, and this relationship is obliterated after 1200. Any argument that this pattern was caused by stability-based errors in the slope of the wind profile seems improbable, since this pattern corresponded only with the most extreme friction velocities encountered during the entire intensive experiment in March 1993. In addition, meteorological conditions (cloudless sky) implied that solar flux increased monotonically during the morning (not just 0930 to 1100), and the five experimental sites were within 250 meters of each other and had well-calibrated instrumentation.

Figure 21 also shows the decrease of Z_0 occurring after 0500 for all five locations corresponding with the progressive pulverization of the soil crust following the initiation of erosion. Continued sandblasting of the crust during the day reduced the aerodynamic roughness height from its initial value of about 0.1 cm at the beginning of the day. At about 0800, Z_0 was reduced to about 0.04-0.07 cm for all locations. Following the intense sand-blasting of 0930-1100, Z_0 ranged from about 0.01 to 0.03, and there was no significant Z_0 difference between the five locations.

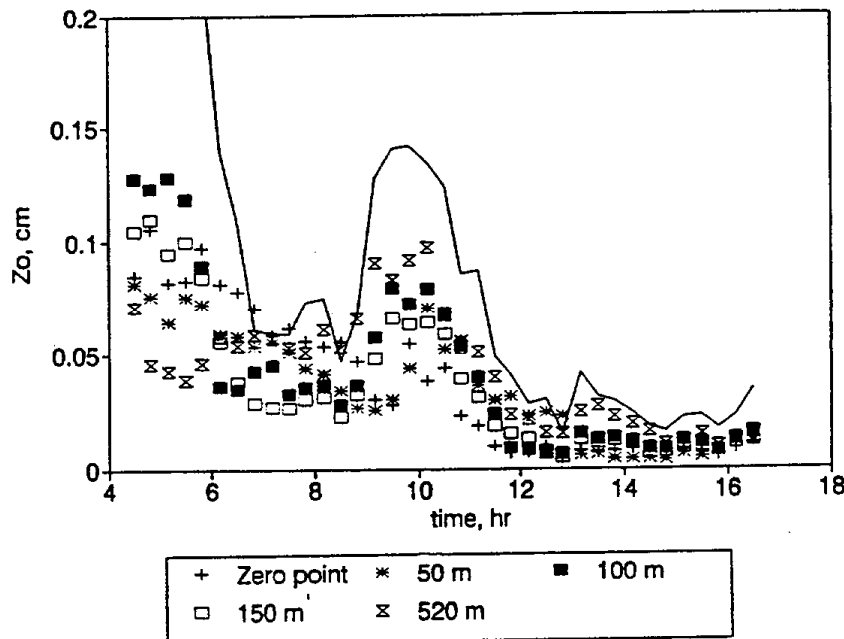


Figure 21. Estimated aerodynamic roughness heights up to 520 m downwind of zero point, Owens Lake Bed fetch effect experiment, March 11, 1993. Solid line indicates 90th percentile upper limit of confidence for the 150 m location.

Figure 22 shows the aerodynamic roughness heights for locations 0 to 150 m downwind, and 90th percentile confidence interval (the lower limit being zero) at 150 m during a north-wind erosion event on March 18, 1993. Following March 11, several erosion events further pulverized surface soil aggregates resulting in aerodynamic roughness heights smaller than 0.01 cm at all the measuring locations. During the erosion period on March 18, Z_0 values were not greatly different for the four locations and no distinct period of increased aerodynamic roughness height was found.

Friction velocities

Figure 23 shows the friction velocities for $x < 150$ m and the 90th percentile confidence intervals for 150 m during the storm of March 11, 1993. At the most intense period of the storm (shortly before 10 a.m. when all the sampling locations showed an increased aerodynamic roughness height) friction velocities at 100 and 150 m downwind appear higher than those at the zero point and at 50 m. To distinguish a 90% significant difference between the friction velocities at the zero-point and 150 m locations, the difference would need to exceed the sum of 90% confidence intervals for both locations. This difference would be about 12% for the pairs (0-100 m, 0-150 m, 50-100 m, and 50-150 m) and 6% for the pair (100-150 m). Indeed, the pairs (0-100 m and 50-100) show such a difference three times before 10 a.m. A significant friction velocity difference

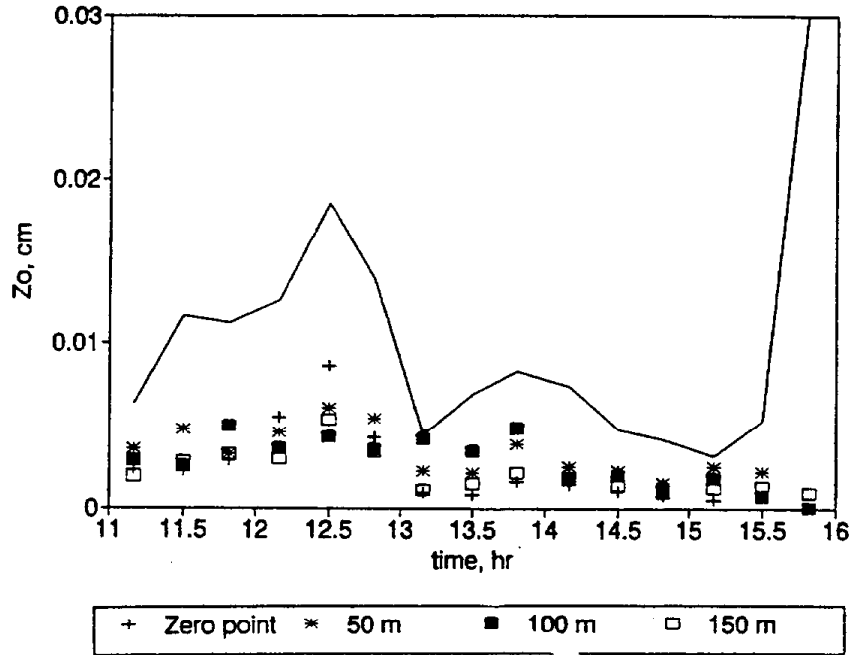


Figure 22. Estimated aerodynamic roughness heights up to 150 m downwind of zero point, Owens Lake Bed fetch effect experiment, March 18, 1993. Solid line indicates 90th percentile upper limit of confidence for the 150 m location.

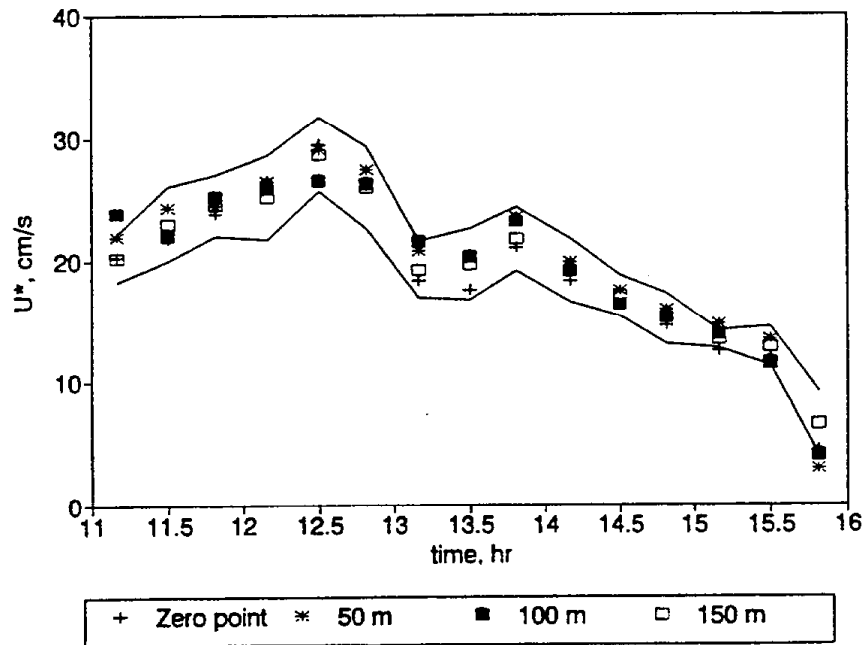


Figure 23. Friction velocities from zero point to 150 m downwind, Owens Lake Bed fetch effect experiment, March 11, 1993. Solid lines indicate the 90th percentile confidence interval for the 150 m location.

coupled with a significant Z_0 increase provides support for Owen's theory of the fetch effect. The friction velocity data do not show a significant difference by location after 1200 local time when wind speeds are lower and aerodynamic roughness heights were uniform for all the measurement locations.

Figure 24 shows the friction velocities for four directly downwind locations for the weak erosion event of March 18, 1993, during which Q increased with fetch.

Figure 25 shows the same four locations on March 23, 1993 for a south wind when Q decreased with fetch. For both the March 18 and 23 cases (except for the u_{*} value at 10.8 for the 150 m location on March 23 which was taken to be an outlier) friction velocity did not significantly differ with downwind fetch although Q increased with fetch on March 18 and decreased with fetch on March 23.

Threshold velocity results

From March 11 after 1600 until March 15, 1993, several wind erosion episodes occurred where friction velocity was just above threshold for one or more of the locations. This gave us the opportunity to make several observations of u_{*t} for $0 \text{ m} < x < 150 \text{ m}$. These friction velocities with 90% confidence intervals (in parenthesis) were 35.5 (1.3), 31.7 (2.9), 34.6 (4.1), and 29.3 (1.8) cm/s for the 0, 50, 100, and 150 m locations, respectively. These values allow only the following inequality at the 90% confidence level:

$$u_{*t}(0 \text{ m}) > u_{*t}(150 \text{ m}) \quad (12)$$

The threshold friction velocities for $x < 520 \text{ m}$ measured from March 11 until March 25 (calculated by least-squares fits of four levels of 20-minute averaged wind speeds) are given in Table IX along with percentage of the surface as unbroken crust. The initial state of homogeneous crust progressed to fairly thoroughly pulverized soil by March 23. The north-south gradient of threshold velocity and percentage of surface as crust was steepest on March 11 and at the smallest on March 23.

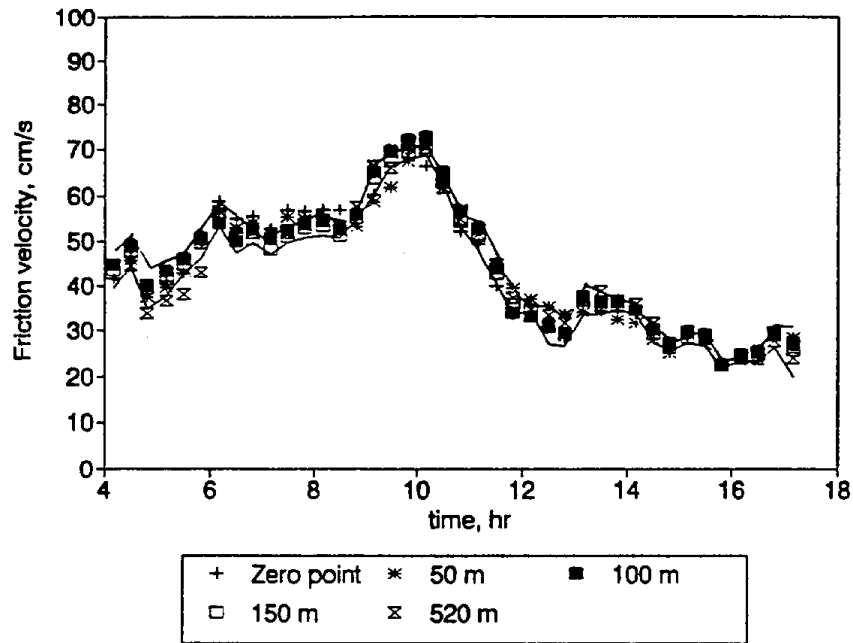


Figure 24. Friction velocities from zero point to 520 m downwind, Owens Lake Bed fetch effect experiment, March 18, 1993. Solid lines indicate the 90th percentile confidence interval for the 150 m location.

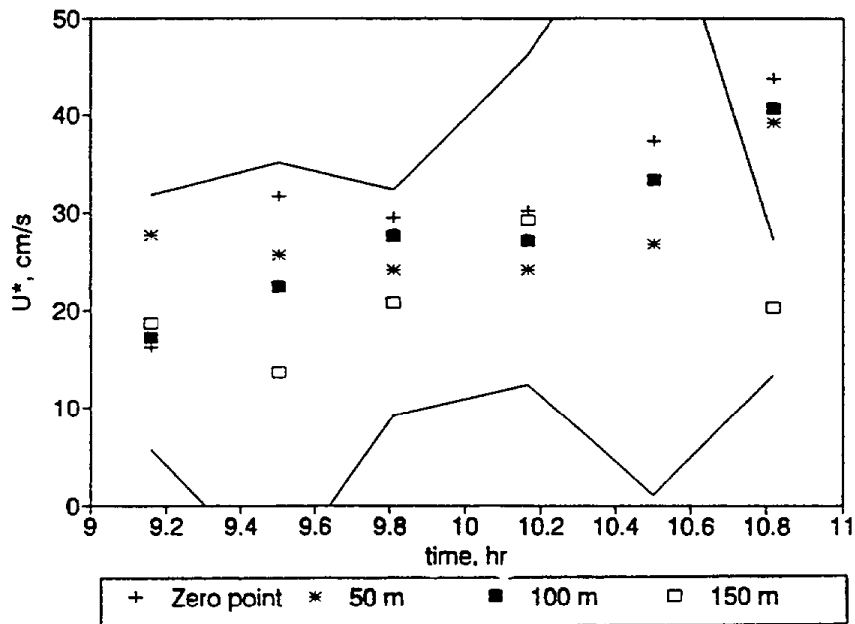


Figure 25. Friction velocities from zero point to 150 m downwind, Owens Lake Bed fetch effect experiment, March 23, 1993 (south wind). Solid lines indicate the 90th percentile confidence interval for the 150 m location.

Figure 26 shows that the measured percentage of surface area as crust fragments correlates well with u_{*t} for the March 1993 Owens (Dry) Lake experiment. The explained variance, r^2 , was 0.93 for 20 degrees of freedom. The regression equation shown in Figure 26 is $u_{*t} = 24.0 + 0.292$ (% of surface of crustal fragments) (cm/s). Standard error of the u_{*t} estimate is 3.2 cm/s. Progressive destruction of the crust with distance suggests a decrease of u_{*t} with fetch distance.

Table X. Relationship Between Friction Velocity u_* and Aerodynamic Roughness Height Z_0 according to the theory of P. R. Owen.

u_* , cm/s	20	40	60	80	100	120	140
Z_0 , cm	0.0043	0.0172	0.0387	0.0687	0.1074	0.1547	0.2105

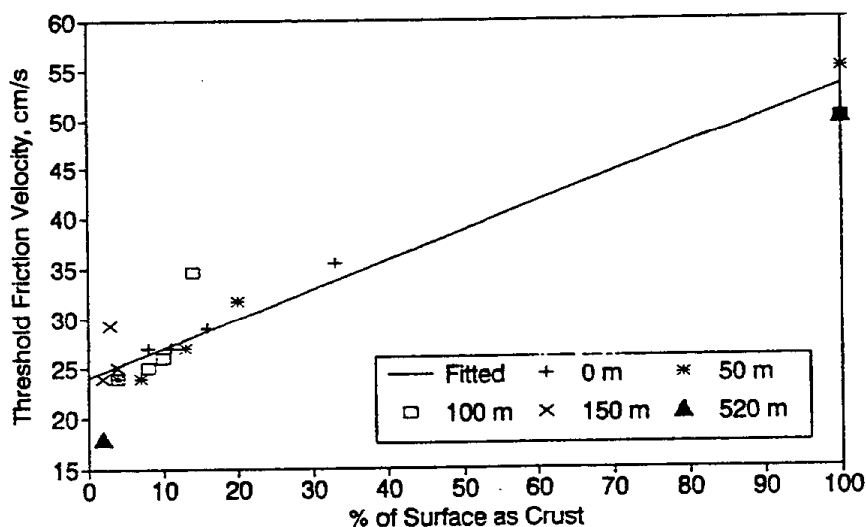


Figure 26. Relation of threshold friction velocity to percent of land surface as crust fragments, Owens Lake Bed fetch effect experiment, March 1993.

Fast response instrumentation in place on March 11 and 18 at the 520 m location illustrate the reduction of u_{*t} above. Figure 27 shows the Sensit response vs. a crude estimate of u_* for two-minute average periods. Sensit response was 100 for no particle impacts and above 100 for detectable particle flux. The two minute u_* values were simply calculated from two-minute average wind speeds and using Equation (5). The use of two-minute averaged estimates of u_{*t} , while insignificant for point-by-point comparisons, does suggest

through the consistency of its overall pattern of more than 250 data points that the threshold friction velocity changed significantly during the course of the March 11, 1993 dust storm. Whereas errors caused by large-scale eddies and/or thermal effects could affect individual points, the overall pattern of the data suggests that there was a significant change of threshold friction velocity.

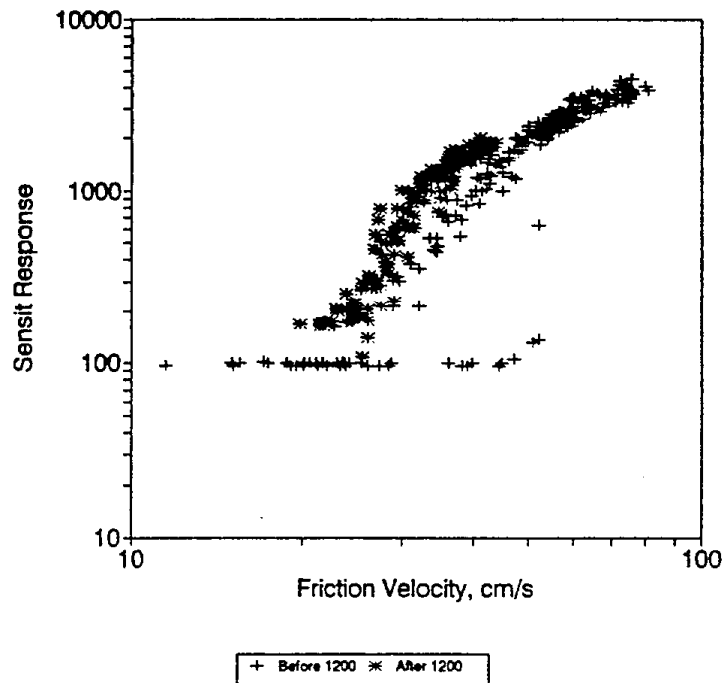


Figure 27. Relation of two-point friction velocity to two-minute Sensit response (saltating particle impact), 520 m downwind of initiation point, March 11, 1993 dust event, Owens Lake Bed South Sand Sheet.

Figure 27 shows that prior to destruction of the crust at 520 m, the approximate u_{*t} was 50 cm/s. Sensit response to no erosion is 100 (background). Shortly after the crust was broken, the apparent u_{*t} (roughly obtained by following the locus of "before 1200" data points to Sensit response = 100) dropped to about 23 cm/s. The reduction of almost 30 cm/s in threshold friction velocity appears to have taken place in just a few minutes. The approximate value of u_{*t} for the "after 1200" points was about 18 cm/s. Another interesting feature of Figure 27 is the apparent flattening of the response for friction velocity greater than 60 cm/s compared to that from 40 to 60 cm/s. This response curve suggests that the mass flux q deviates from the q vs. $u_* (u_*^2 - u_{*t}^2)$ for $u_* > 60$ cm/s. Figure 28 shows Sensit response vs. a crude estimate of u_* for the location 1057 m obtained in the same way as above. Because this location had no detected crust fragments left, it does not show a progression of a higher to a lower u_{*t} resulting from sandblasting of soil aggregates. Indeed, the u_{*t} estimate of approximately 16 cm/s is consistent with fine sand surfaces with no aggregation.

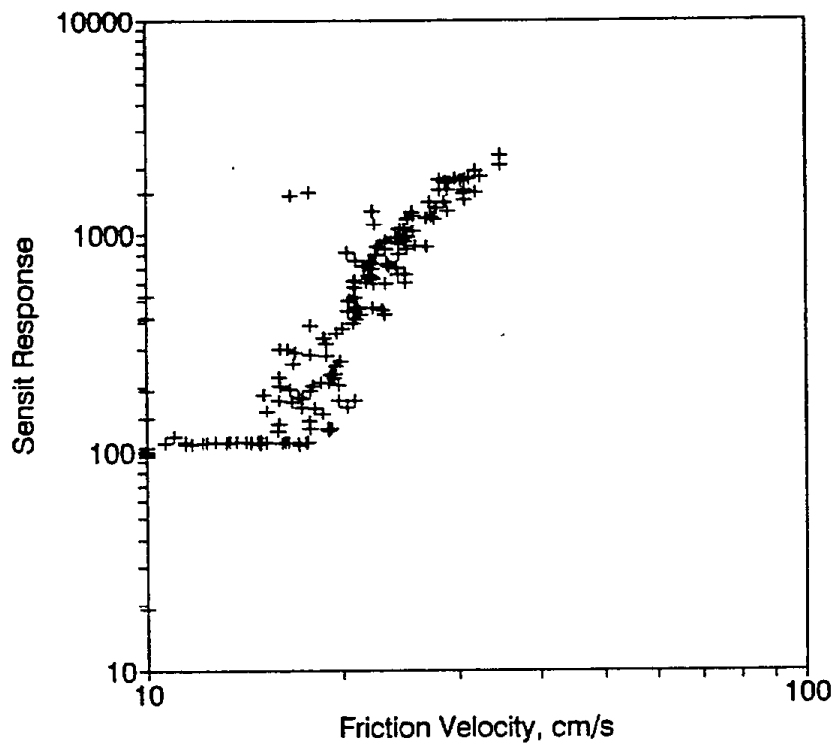


Figure 28. Relation of two-point friction velocity to two-minute Sensit response (saltating particle impact), 1057 m downwind of initiation point, March 11, 1993 dust event, Owens Lake Bed South Sand Sheet

q vs. $u_* (u_*^2 - u_{*t}^2)$

Figure 29 shows integrals in time of q vs. $u_* (u_*^2 - u_{*t}^2)$ (Q vs. G) for the preliminary data set obtained in 1991 (only two points of data) and the data set obtained in March 1993 (on March 17, 1993 wind was from the northwest-off axis). The total number of data pairs of Q vs. G is 36. For G values in which part of the wind friction velocities exceeded 60 cm/s, the points are labeled "g". For the points obtained during north winds and friction velocities less than 60 cm/s, the linear regression is $Q=3.5 \times 10^{-6} G$ with $r^2 = .61$ and a standard error for the coefficient of 0.67×10^{-6} . Referring to Equation (4), this regression constant would correspond to a value of A of 2.8 and $F(x) = 1$. This constant shows reasonable consistency of the data with Equation (4). The greatest source of error for these estimates is the fact that u_{*t} changes continuously but we only measured it for one or two times for each G estimate. To identify possible patterns for the residuals, the locations were labeled in Figure 29 as follows: 1 = 0 m; 2 = 50 m; 3 = 100 m; 4 = 150 m; S1 = 520 m; S3 = 1057 m.

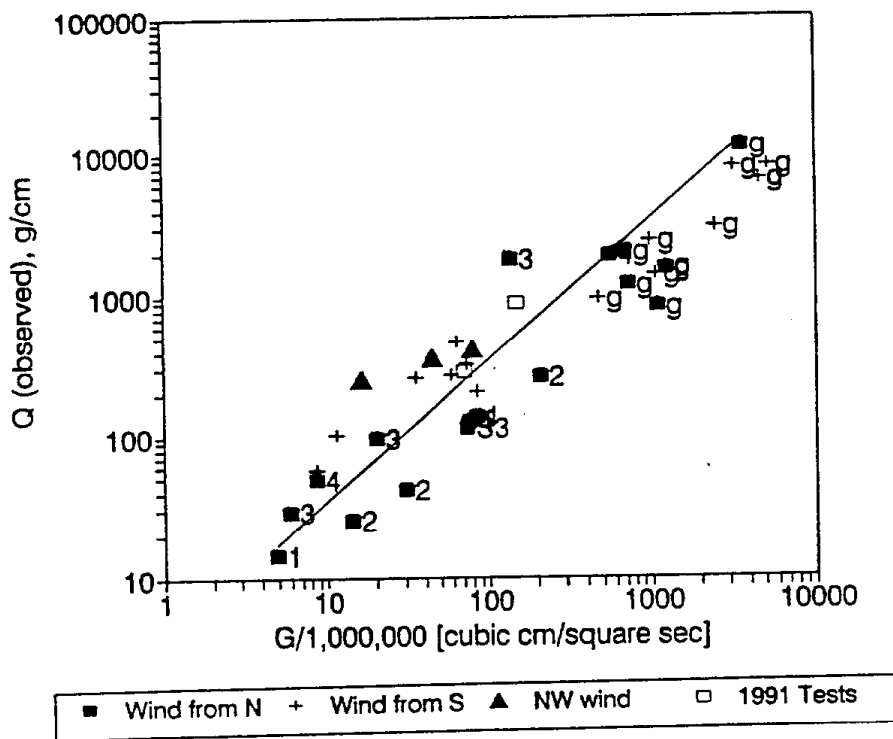


Figure 29. Integrals in time of Q vs. G for March 1993 as well as preliminary data set obtained in 1991.

The distribution of the residuals to the fit for the north wind cases, the zero point and 50 m locations (1 and 2), for friction velocities <60 cm/s, shows the residual is less than zero in 5 of 5 cases. For the 100 m and 150 m locations, the residual is greater than zero in 4 of 5 cases. For the null hypothesis that the residuals are random with equal probability of being positive or negative and do not increase with distance to the south, the (binomial distribution) probability of the observed residuals (9 of 10) is 0.0107 (method of Miller and Freund, 1977). Therefore, the null hypothesis is rejected at the 98% level and in favor of residuals that do increase with distance to the south. We interpret this as a confirmation of the avalanching effect, that is, $F(x)$ is a variable increasing downwind for threshold velocities increasing downwind.

For Q vs. G data points representing winds which exceeded friction velocities of 60 cm/s, Figure 29 shows that G over predicts the observed Q for the regression equation $Q=3.5 \times 10^{-6}G$. This is consistent with our dataset from March 11 at 520 m, showing Sensit response versus friction velocity flattening out for friction velocity greater than 60 cm/s. It appears that the relationship

$$q=A'u_*(u_*^2 - u_{*t}^2) \quad (13)$$

will hold only when u_* does not exceed 60 cm/s.

Finally, we can note from Figure 29 that all but one of the pairs of Q vs. G collected for south winds and friction velocities less than 60 cm/s were greater than the regression equation for north winds with friction velocities less than 60 cm/s. We explain this by noting that airborne sand sized grains are transported beyond their location of origin. Thus, an overshoot would be expected for Equation (4) when the threshold friction velocities are decreasing with fetch, and a smaller decrease of q or Q with distance would be expected than for the increase of q or Q for an equivalent decreasing threshold velocity with distance.

Fetch effect discussion

Evidence of the avalanching effect was seen in the present experiment. However, the following observations led us to favor a model that included (in addition to avalanching) the aerodynamic feedback and soil resistance effects:

1. Aerodynamic roughness height increased during 0930-1100 on March 11, 1993 along with increase of u_* with distance downwind. This increase was consistent with the theory of Owen (1964) which predicts a gradient of friction velocity and q resulting from the saltation induced increase of aerodynamic roughness height.
2. We observed a gradient of threshold friction velocity for all wind erosion episodes. The positive gradient of threshold friction velocity with fetch was probably the dominating cause of the decrease of Q with downwind distance on March 23, 1993.

On March 18, 1993 the negative gradient of threshold friction velocity was probably the dominating cause of the increase of Q with downwind distance. The percentage of sand in the soil correlates with the decreasing threshold friction velocity data.

3. We found a non-random relationship of deviations from the best fit line of Q vs. G with distance downwind. This is interpreted to mean that $F(x)$ in equation (2) is significant and increases with x. Even without the $F(x)$ term, the theory explained 61% of the variance observed.
4. The pure avalanching model failed to explain decrease of Q downwind. This model did not pass either of its two tests for explaining the observed fetch effect in our experiment. It may be important at the leading edge of the erodible deposit, but our field tests were 500 m beyond the leading edge for most events.

The fetch effect is probably dominated by soil resistance and avalanching for wind speeds near threshold and by the aerodynamic feedback mechanism and avalanching for wind speeds greatly in excess of the threshold. The importance of the pre-existing aerodynamic roughness height for the aerodynamic feedback effect was seen in the 1991 data where friction velocities reached levels in excess of 60 cm/s (slightly above threshold for the coarse sandy soil of the Northeast Owens (Dry) Lake site). Even though these friction velocities were close to those for the March 11, 1993 case, no evidence was seen for the aerodynamic feedback mechanism.

Owen's theory is based on a feedback mechanism with respect to distance downwind in which saltation of particles entirely determines the aerodynamic roughness height [$Z_0 = u_*^2 / (\beta g)$ where $\beta = 95$], which then acts to increase friction velocity. Table X shows the increase of the saltation-controlled aerodynamic roughness height. The roughness height of 0.1 for the 1991 Owens (Dry) Lake test surface was already larger than the roughness heights calculated by Owen's formula for friction velocities lower than 100 cm/s. The need for the saltation roughness height to exceed pre-existing roughness height of the natural surface was explained by Raupach (1991). The existence of a smooth upwind surface would be required for the aerodynamic feedback model to dominate. Such was not the case in our experiment in 1991, but on March 11, 1993, the finer surface material pulverized into a smooth surface where saltation could generate a Z_0 larger than that already present. The sediment size distribution of mass for particles between 1 and 2 mm was 23.3% for the 1991 site on the Northeast Sand Sheet and less than 3% for the 11 sediments for the 1993 test sites.

An explanation for the sensitivity for friction velocities close to the threshold is given below. The fractional increase of q may be expressed as a function of the fractional

change of threshold friction velocity and friction velocity by the expression

$$\Delta q/q = [3y - B^2y + 2Bs]/(1 - B^2) \quad (14)$$

where $B = u_{*t}/u_*$, $y = \Delta u_{*t}/u_*$, and $s = \Delta u_*/u_*$. The sensitivity of the increase of q for a change in u_{*t} and u_* is always greatest for friction velocity near the threshold. For example, for $b = 0.95$, the fraction of change of q for a 10% change of threshold friction velocity is 1.95. We see for u_* greater than u_{*t} (small B) that the change of friction velocity dominates.

Except for about two hours, our data did not show any significant changes of aerodynamic roughness height with distance downwind. This observation would imply that the partially destroyed crust provided a relatively homogenous roughness even though the proportion of aggregated material (pieces of crust) to loose sand changed along the fetch. We took this to mean that no internal boundary layers were forming during the March 1993 LODE intensive except for a two-hour period on March 11. During that period when our data suggests that aerodynamic roughness height as well as friction velocity increased with distance (9:30 to 11:30 AM on March 11, 1993), the goodness of fit of the logarithmic profile implies that the ratio of separation distance to tower height (50 m/3 m) was sufficient, and the increase of Z_0 with distance was such, to support our conclusion that these data suggest an increase of Z_0 with distance downwind, and that Z_0 is significantly larger during the peak of the wind storm than during the two hours preceding or following the peak.

The failure of the constancy of Q/G has been verified by independent wind tunnel tests (Rasmussen and Iversen, 1994). The cause of this failure is not fully known at present.

Our data showed that the threshold friction velocity changes with time as well as distance as saltation successively destroys the aggregate structure of the soil. For a complete description of the fetch effect, it is required to know both soil physical state and wind stress and to predict the destruction of soil aggregates by saltation.

Fetch effect conclusions

The data lead us to a conditional acceptance of a model having three mechanisms that cause the wind-erosion fetch effect: avalanching, soil resistance, and aerodynamic feedback. Aerodynamic feedback occurred at one location but not another for similarly strong winds. Differences in pre-existing aerodynamic roughness height reflecting differences in the sediment caused this difference in response. For the conditions present at Owens (Dry) Lake test site in March 1993, progressive disintegration of soil crust by sandblasting from north to south caused a decrease of threshold friction velocity with distance south from the unbroken crust. The gradient of threshold friction velocity contributed to an opposite gradient of soil flux. Finally, the avalanching effect is

important for both small scale (on the order of a few meters) and large scale wind-erosion fetch effects. At the leading edge separating nonerodible material from erodible material, it is a dominating effect. For scales of length greater than 50 to 100 meters, however, it is a residual effect, responsible for a small fraction of the total fetch effect. The dominating fetch effect mechanism at a large scale of length (>100 m) for all but about two hours during the intensive study was the variation of threshold velocity on the surface of the lake bed.

Field observations of friction velocity and soil flux at Owens (Dry) Lake led us to confirm Equation (13), based on the early work of P.R. Owen (1964), for friction velocities that do not exceed 60 cm/s. Our field observations also confirmed measurements made in wind tunnels that for friction velocities greater than 60 cm/s, an asymptotic relationship

$$q = \alpha u_*^n \quad (15)$$

holds, where n is less than 3 and α is a constant.

RESULTS - GENERATION OF PM₁₀ DUSTS

As part of the March 1993 LODE intensive, we made direct measurements of PM₁₀ dusts both along the fetch and from storm to storm at the same time and place as the fetch effect study above. The conditions in which the samples were taken were extremely severe and distinctly dangerous to personnel and equipment, so that special instruments had to be designed for the study.

The Air Quality Group at Davis designed and built a set of nine PM₁₀ Portable Filter Samplers (PFS) for use in the study. These samplers were designed to be portable, wind and dust tolerant, easy to use, and able to provide a PM₁₀ size cut even under high wind speed conditions. Each sampler consists of an insulated carrying case containing the batteries, pump, and programmable controller, a PM₁₀ inlet head with wind baffles, and a cassette for holding and transporting the filter for sampling.

In the March 1993 Owens (Dry) Lake intensive study, six sets of samples were taken during 5 different events, four of which were dust events, and one which provided background data. The result was a total of 44 PM₁₀ measurements. These samples represent the first valid PM₁₀ samples taken on the Owens Lake Bed, and are the first that we know of taken in a region of lake bed dust production. All other samples of PM₁₀ aerosols during dust events on Owens (Dry) Lake were taken using samplers not certified for the wind speeds experienced on the playa, and were taken from the shoreline rather than from the playa itself, in order to provide access for power and personnel. The Portable Filter Sampler design and minimal siting requirement allowed us to directly

sample the plume in its area of genesis, as opposed to previous measurements, which could be taken only when the plume drifted off the lake bed toward Keeler or Olancha.

The spring data were taken on March 10 (background), 11, 17, 18, and 23 along a linear array running north to south at four of the 6 meteorological stations (Figure 30) utilized in the linear fetch effect array. For precision estimates and to gather information useful for the subsequent State Lands Commission (SLC) study, we compared the aerosol data at the north and south ends of the array to that at the center. This gave an indication of the consistency of dust production and concentration in the array. The purpose was to provide an indication of how well one could control PM₁₀ production through the control of saltating particles using sand fences and stabilized dunes (Cahill *et al.*, 1993). The mass concentration ($\mu\text{g}/\text{m}^3$) at each site for each sampling period was derived from the average of the mass concentrations measured at 60 cm and 300 cm at each site. The standard deviations are also included in Table XI. Data are given in Appendix D.

Thus, observations from the tests include:

1. The PM₁₀ mass concentrations through the array were fairly constant for any given storm.
2. Dust production increased as time went on. This appears to be related to the breakdown of the efflorescent crust, destruction of the more permanent crust with subsequent release of salts, silts and other fine blowable materials.

	March 10 02:00 2 hr	March 11 12:00 1 hr	March 11 15:00 2 hr	March 17 15:00 1 hr	March 18 11:41 1.5 hr	March 23 09:01 2 hr
site 1 (N)				3093+/-1352	3568+/-432	13644+/-5099
site 2		1975+/-309	907+/-396	3321+/-790	9276+/-2707	29099+/-7541
site 3	160+/-52	1617+/-926	*	2636+/-930	6389+/-743	30042+/-10576
site 4 (S)	228+/-15	2290+/-877	574+/-261	2840+/-290	6146+/-131	33360+/-6594
(site 2 + site 3) (site 1 + site 4)	0.84	0.76	*	1.00	1.61	1.26

* No data point. Sample could not be obtained due to equipment failure (no flow).

Table XI. PM₁₀ mass concentration in $\mu\text{g}/\text{m}^3$ at each site and sampling period, Owens Lake Bed South Sand Sheet aerosol experiment, March 1993.

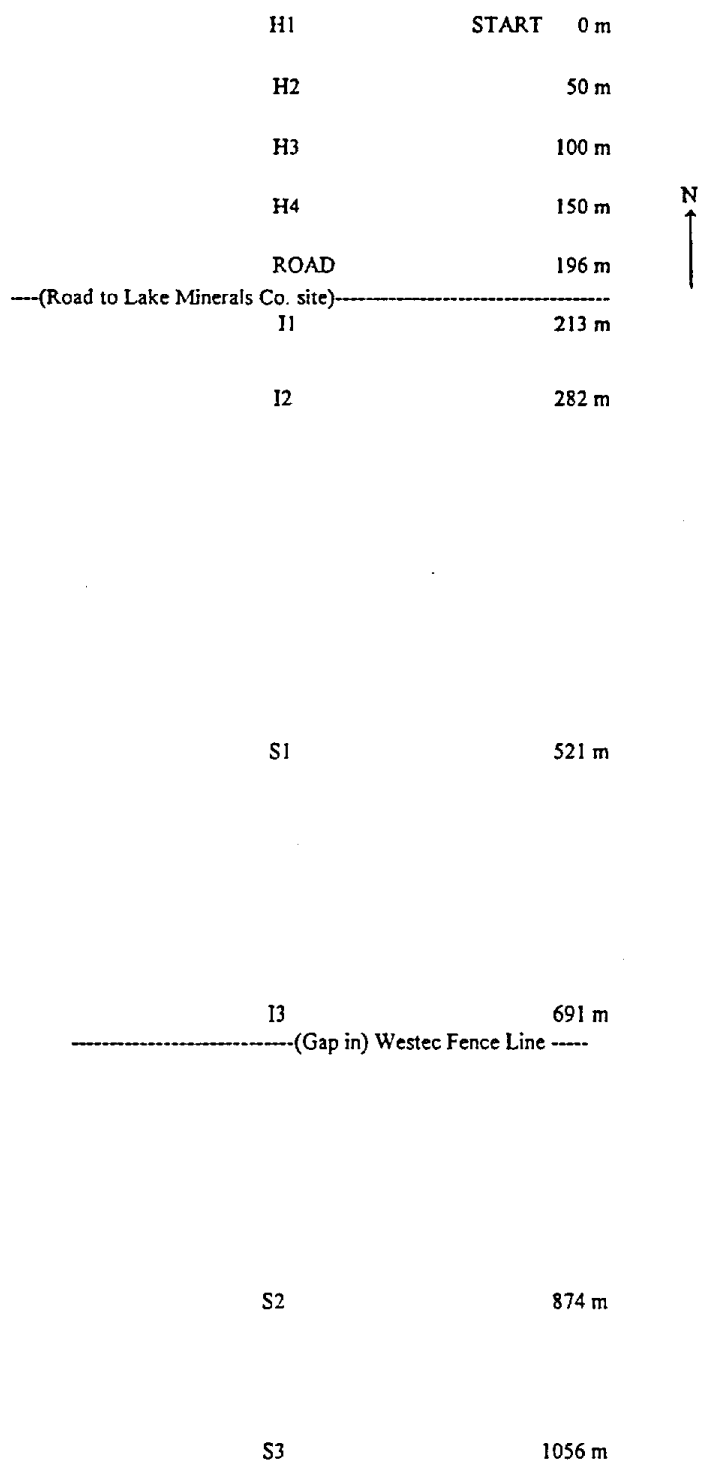


Figure 30. Diagram of NOAA/UCD sampling array by site code, March 1993. See Figure 3 for location and Appendix H for instrumentation at each site. Aerosol samplers at H sites only. Scale: .75 inch = 100 meters

3. Observation photographs indicate plume lofting occurred during most of the dust sampling periods. The consistency of the ground level mass concentration numbers during events in which lofting occurred is indicative of continuous source generation of aerosols, a result that supports the concept of crust destruction generating new or releasing trapped fine aerosols, rather than solely erosion of the efflorescent crust.
4. In Figure 31 for March 10 at 02:00 and March 11 at 12:00, both of which had winds from the north, note that the concentrations at 60 cm are higher than those at 300 cm, and are increasing with downwind distance through the array. This indicates either near laminar air flow through the array from a distant source of PM_{10} , or continuous generation of PM_{10} aerosol at the surface, with rapid mixing resulting in a dilution of the concentrations at elevation. Little dust production occurred on March 10, but on March 11, moderate dust production at the sites occurred during the sampling period.
5. In Figure 31 for March 11 at 15:00, the winds were initially from the north. This resulted in light dust production during the sampling period. One sample was lost due to operator error. The low concentrations at 60 cm, as compared to that at 300 cm, appear indicative of plume transport over the array but little plume generation.
6. In Figure 31 for March 17 at 15:00, winds from the west-northwest resulted in moderate dust production at the sampling array. The array was lined up north to south, so the results must be corrected for wind direction effects.
7. In Figure 31 for March 18 at 11:41, the winds at the site were from the north at the initiation of sampling, but the regional winds were from the south according to the camera logs. The wind flow pattern was complicated, and the array may have been in a localized eddy. The camera logs also indicate that this may have been a very localized storm.
8. In Figure 31 for March 23 at 09:01, the winds were from the south.

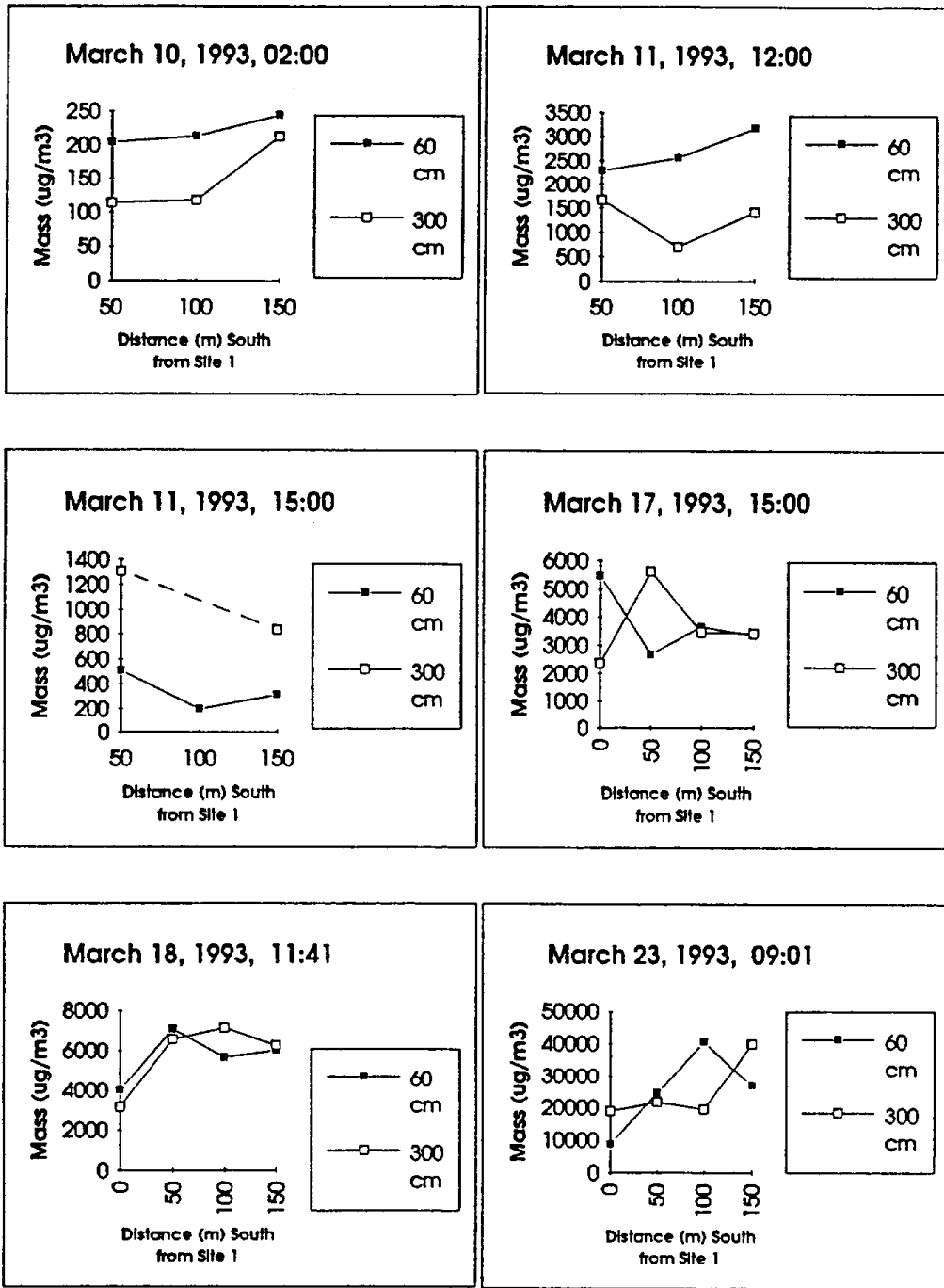


Figure 31. PM₁₀ concentrations at two heights during six events, Owens Lake Bed South Sand Sheet. Wind directions are given in explanatory text on pages 76 and 78.

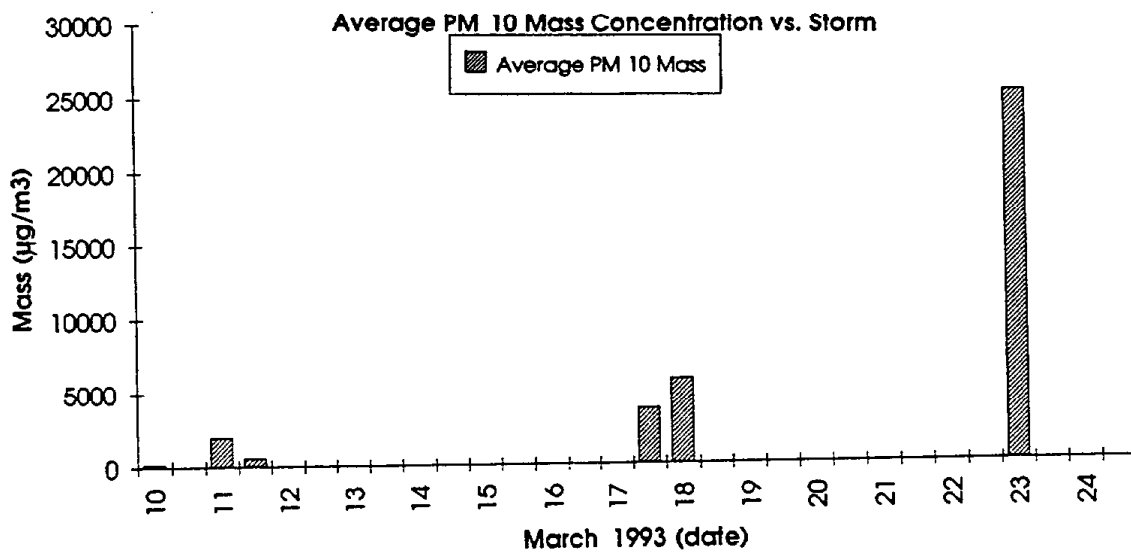


Figure 32. Dust vs. Time

Three points become clear from the PM₁₀ data on the lake bed. First, as shown in Figure 31, the dust concentration was roughly uniform along the array. This was not necessarily anticipated, since during this period, the efflorescent crust was being destroyed. In the early storms, the south end of the array had lost this crust before the north end, yet little gradient was seen in the PM₁₀ dusts. This supports the hypothesis that the efflorescent crust itself was not a major source of PM₁₀ dust. It appears that the later grinding of this crust into a finer powder by the sand motion/saltation process provides the strongest source of PM₁₀ dusts.

The second point is that the amount of dust increased rapidly during the month of March, matching the destruction of the efflorescent and salt crusts (Figure 32). This is a direct confirmation of the role of saltation in generation of PM₁₀ dusts. The levels of dust rose to over 40,000 µg/m³, and shortly thereafter destroyed both the battery powered pumps of the samplers, the large generators for the LODE fetch effect experiment, and the bearings of the anemometers.

The third point to note is the vertical gradients of the PM₁₀ measurements. In 5 of the 6 events, the low level or bottom PM₁₀ sampler had more PM₁₀ dusts than the upper level or a top sampler in Figure 31. This is the expected behavior when the PM₁₀ source is in the immediate vicinity and slightly upwind of the sampler, since this produces a vertical gradient into the relatively cleaner upper air. This is further confirmation that the source was local during these dust storms. The interesting situation of the late afternoon of March 11 is the only counter example. Here, the upper samplers had more dust than the

lower sampler. This is expected when the source is well upwind of the sampler and the area near and below the sampler is not the primary source. Since there is always a removal rate associated with the deposition velocity, the removal sink clearly is dominating the local source in this example. This was a case in which an intense storm started at midday on the South Sand Sheet, and then became general over a large part of the basin by afternoon. Wind shifts occurred, and the wind was falling during this period. Hence, as the storm wound down, and local area ceased to be active, there was an inversion in the vertical dust gradient. Such patterns would be expected in a concentration gradient above a surface that is either (a) emitting or (b) removing a pollutant. The measurements at Owens (Dry) Lake in March 1993 directly confirm this pattern.

Discussion of the PM₁₀ dust results

The following figures are designed to illustrate how the meteorology, crust condition, sand motion, and PM₁₀ data come together in the March intensive. Figure 33 shows the mean wind velocity at the Geomet tower, the percent of efflorescent/salt crust exposed, and the derived friction velocity from the LODE array. The dates are non-linear because they match the sand collection data which was of varying duration, often continuing overnight. Also, on several occasions, more than one sample was being taken at the same time (*viz.*, 3/10 and the first 3/11 both covered the morning of March 11). The data plotted represent the "active period" of the measurement, such as the high wind velocities on the morning of March 11, which decreased in the afternoon. The mean wind velocity was similar for the storms of March 11, 17, 18, and 23. The destruction of the efflorescent crust occurred quickly, in 2 to 3 hours on March 11, and the remaining salt crust was slowly eroded and covered with loose sand/salt debris during the remainder of the study. Note the dramatic drop in friction velocity after the destruction of the crust (Table XII).

Table XII. March 1993 LODE Intensive Data Set

Date	Crust (%)	Friction Velocity (cm/s)	Geomet Wind (m/s)	Sand Capture (gm)	Sand Flux (g/cm ²)	Flux (m ³ /m)	Flux (yd/ft)	PM ₁₀ Dust (ug/m ³)	+/- %	Time	Duration	Dust Ratio	Sand Ratio Log
9	100	53.0	1.6	2	1	0.001	0.0004						
10	100	53.0	1.6					182	5	1400;	2 hrs		
10	14	30.0	6.6	4161	2080.5	1.831	0.875	1961	5	1200;	1 hr	0.94	-0.026
11	14	30.0	6.6	1663	831.5	0.732	0.350	740	20	1500;	2 hrs	0.89	-0.051
11	14	30.0	2.3	43	21.5	0.019	0.009						
12	14	30.0	2.3	106	53	0.047	0.022						
13	14	30.0	2	30	15	0.013	0.006						
14	14	30.0	2.7	5	2.5	0.002	0.001						
15	14	30.0	2.4	15	7.5	0.007	0.003						
16	9	30.0	2.4	763	381.5	0.336	0.160						
17	7	27.0	4.5	317	158.5	0.139	0.067	2972	30	1500;	1 hr	18.7	1.273
17	7	27.0	4.5	392	196	0.172	0.082						
18	7	25.5	4.4	76	38	0.033	0.016	6345	40	1141;	1.5 hr	167.	2.223
19	4	24.7	2.3	0.2	0.1	0.000	0.000						
19	4	24.7	2.3	176	88	0.077	0.037						
20	4	24.7	2.2			0.000	0.000						
21	4	24.7	2.1			0.000	0.000						
23	4	24.7	3.6	144	72	0.063	0.030	26536	40	901;	2 hr	369.	2.567
23+	4	24.7	6	4432	2216	1.950	0.932						
23+	4	24.7	6	3513	1756.5	1.546	0.739						
24	4	24.7	11	1206	603	0.531	0.254						

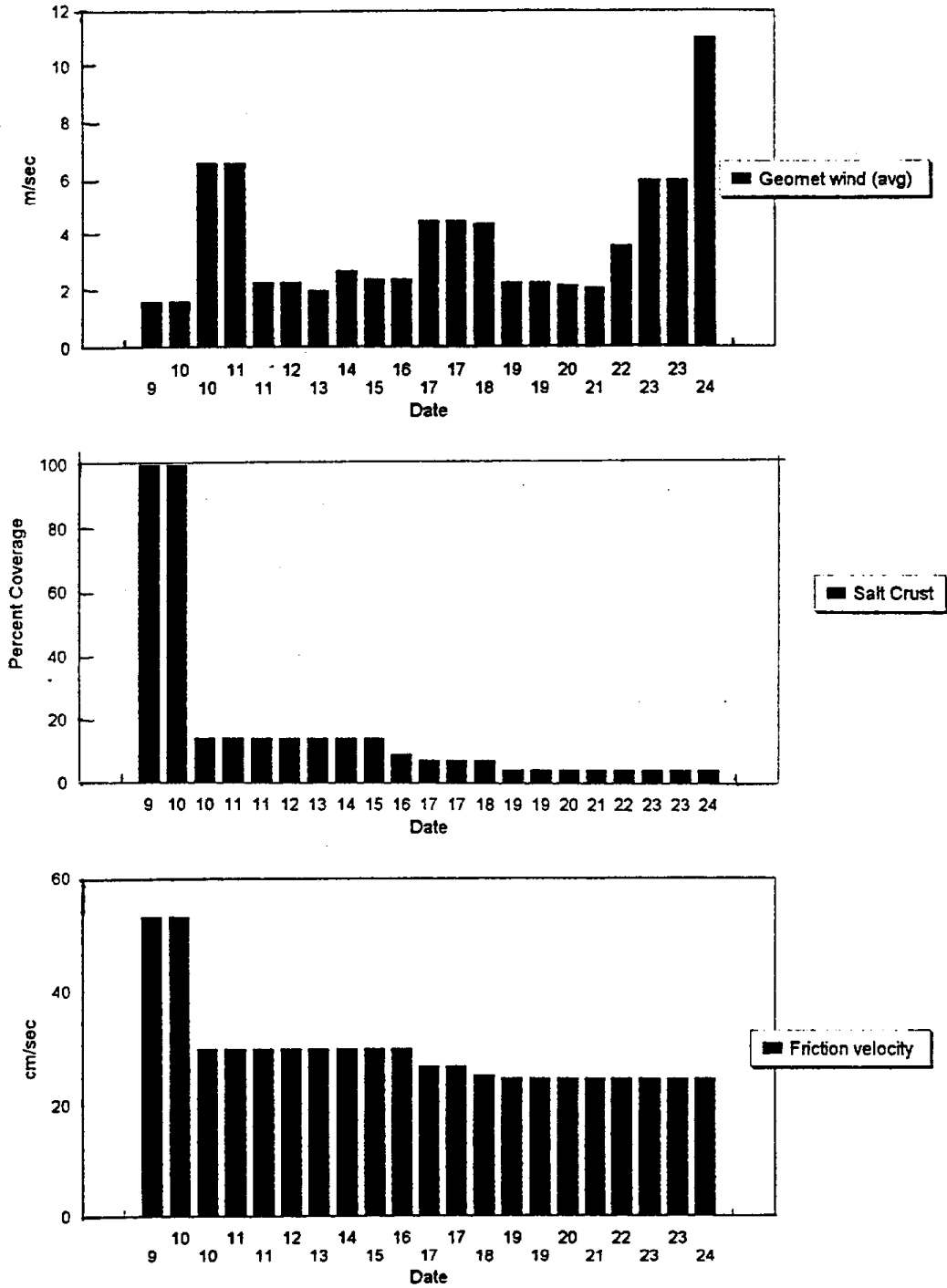


Figure 33. Intercomparison of average wind velocity at Geomet site (top), average percent of surface remaining as crust (center) and average friction velocity (bottom), Owens Lake Bed South Sand Sheet, March 1993.

Figure 34 shows how these conditions influenced sand motion and PM₁₀ dust production. The sand motion data mimic to some degree the meteorology of Figure 33, but the PM₁₀ dust production, averaged along the array and at both the high and low samplers, has a very different behavior, rising steadily throughout the period. Note that the March 23 sample was prior to the massive storm of March 24, and is reflected in the March 22 to March 23 sand flux data. Finally, a ratio is made of the PM₁₀ production to sand motion in Figure 34. From these data we can see that, despite high winds and sand motion on March 11, little dust was generated as the efflorescent crust broke up. But in the next 2 weeks, every storm was more and more efficient in making dust from grinding up the salt and silty components of the lake bed.

Finally, in Figure 35 this is plotted versus the logarithm of the PM₁₀ data, by date, and in part, by percent exposed crust. With an intact crust, PM₁₀ production was low. There are many reasons that the relationship is not exact, since the PM₁₀ is a regional effect while the dust motion is local, yet a good logarithmic regression was achieved. The uncertainties on the final two data points of March 18 and March 23 were as high as +/- 20%, making precise comparisons unlikely. Incidentally, recent tests at Mono Lake by GBUAPCD with their wind tunnel also showed orders of magnitude variations in dust production rates at various sites and times (GBUAPCD, 1993a).

The physical process behind the increasing dust production per unit sand motion is most probably the destruction of weak adhesions between silt and salt by the abrading sand. This suggests the use of an energy parameter in the description of dust production. We propose the term "sand run," a term used in underwater sand transport (Meyer, 1972). We define sand run as sand flux (g/cm²) times wind run (km), and it represents both the mass of sand that crosses an area and the total distance the sand has traveled across the surface. Figure 36 represents the data in this format. It is clear that, until the crust is destroyed, dust production is minimal. After that point, however, the ratio of dust production to sand motion is proportional to the logarithm of sand run, with a very high correlation. The combination of a firm physical foundation (sand run has the units of energy) and a high correlation to dust production makes the concept an attractive one for modeling dust production for Owens (Dry) Lake. Moreover, sand run has a close connection to the parameter Q, used above in the description of the fetch effect.

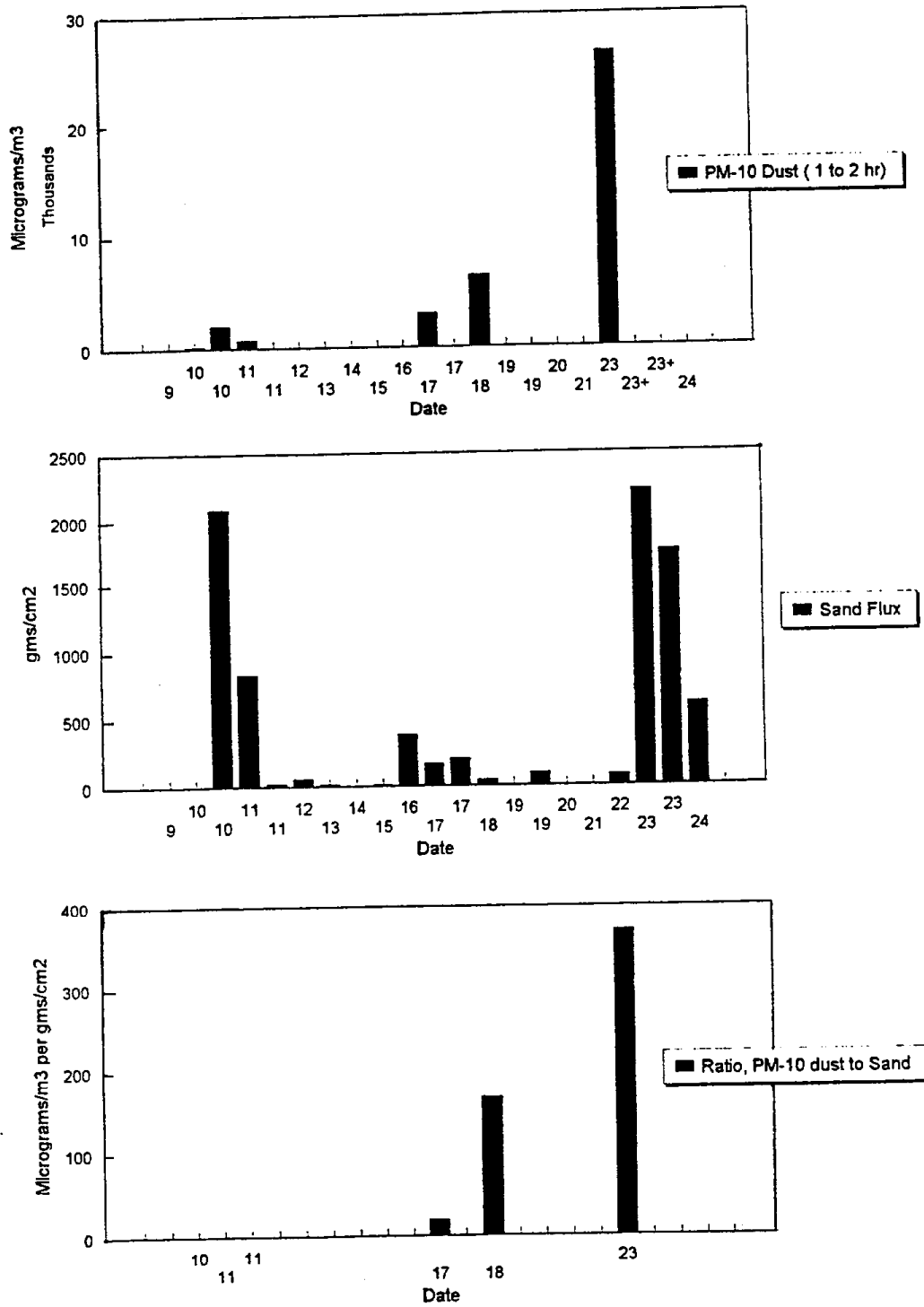


Figure 34. PM₁₀ Dust (top), Sand Flux (center), and ratio of PM₁₀ dust to sand (bottom), Owens Lake Bed South Sand Sheet, March 1993.

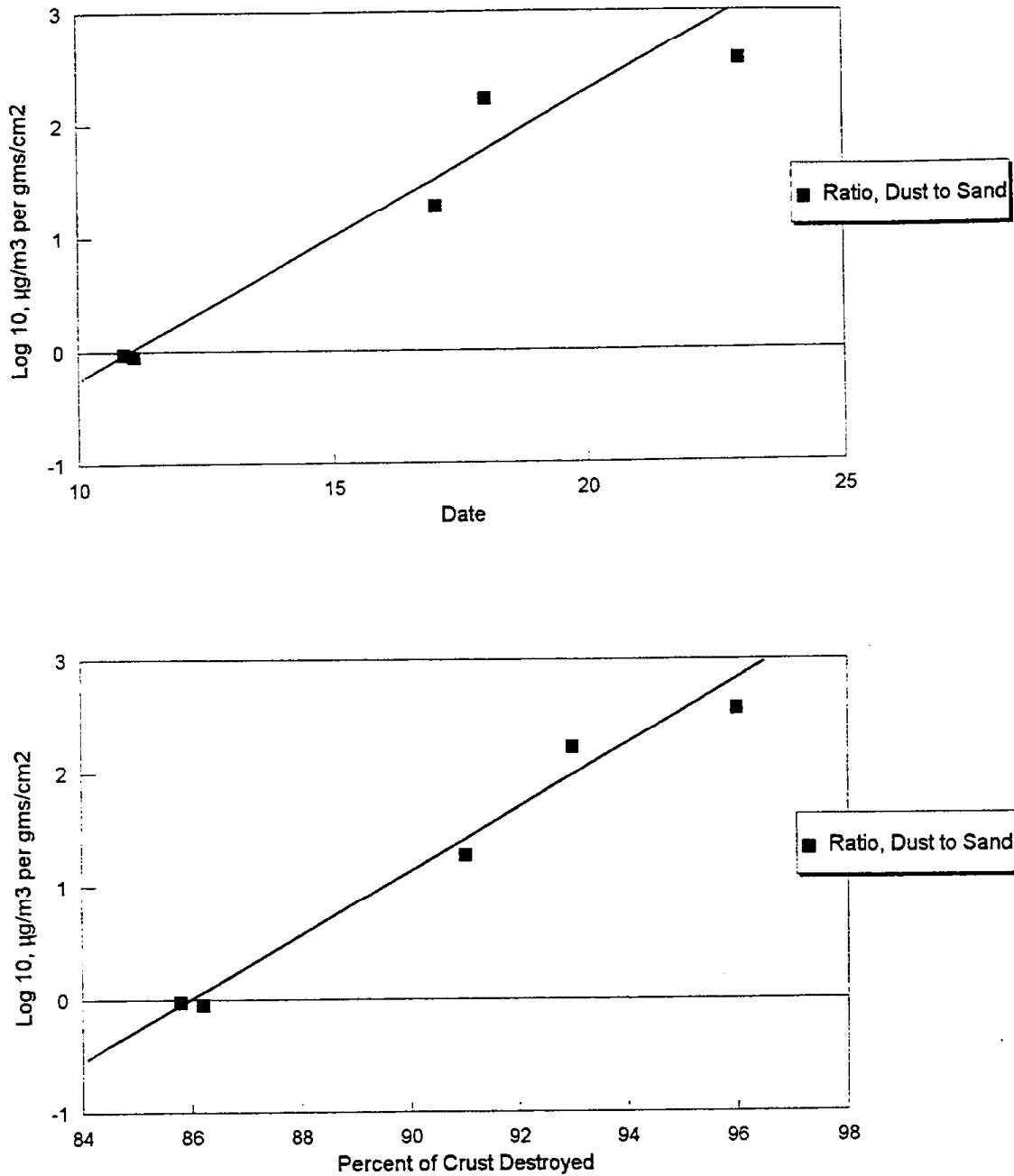


Figure 35. Intercomparison of: Ratio of PM_{10} concentration ($\mu\text{g}/\text{m}^3$) to saltating particle flux (gm/cm^2) vs. date (top) and percent of surface crust destroyed (bottom), Owens Lake Bed South Sand Sheet, March 1993.

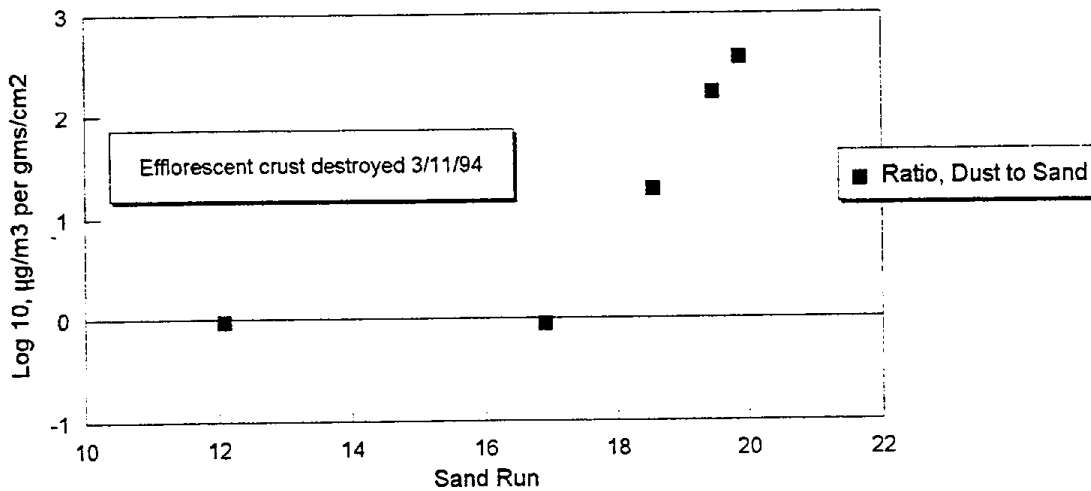


Figure 36. Sand flux (g/cm^2) times wind run (km), representing both the mass of sand that crosses an area and the total distance traveled across the surface.

Conclusions of the PM_{10} Studies

The sand motion and PM_{10} measurements of the March 1993 intensive have provided the first detailed study of the processes that generate the Owens (Dry) Lake dust storms. Clearly, there is no substitute for actually making the measurements on the lake bed during dust storms, despite all the effort such measurements entail.

The conclusion of these comparisons is that the motion of sand across the playa and the subsequent pulverization of lake bed debris are the most important factors in the generation of fine dusts from Owens (Dry) Lake.

These measurements strongly support mitigation proposals that focus on preventing the motion of coarse sand across the playa.